Study on Solar-Wind Hybrid Power System Cooperating with PV Module

March, 2018

Vu Minh Phap

Study on Solar-Wind Hybrid Power System Cooperating with PV Module

Vu Minh Phap

A thesis submitted to

Department of Electrical and Electronic Engineering,

Graduate School of Engineering,

Mie University, Japan

for the degree of

Doctor of Engineering

March, 2018

Abstract

Currently, many countries in the world are finding the suitable solutions to reduce the dependence on fossil fuels such as coal, oil and natural gas because these traditional energy sources have been limited and they cause environmental pollution in the process of usage.

Renewable energy is considered as an important solution that can improve energy security, protects the environment, and develops economy. At the present, the solar power which is a semiconductor technology that converts sunlight directly into electricity is the most promising as a future renewable energy technology, but solar power generation is dependent on sunlight to effectively collect solar energy. Thus, the utilization rate of the power conditioner system (PCS) including DC/DC converter and DC/AC inverter in the photovoltaic (PV) system is very low in the case where the solar array cannot receive the sunlight, especially the night time. The maximum power point tracking (MPPT) is performed by the boost-type DC/DC converter while the power at the output terminals of the solar array is supplied into the utility grid by the grid-tied DC/AC inverter.

We can add the small scale wind power system to the existing solar power generation system to improve the utilization rate of the PCS because the small scale wind turbine utilizes possibly the PCS at night and also can use the remaining capacity of the PCS during the daytime. The grid-connected hybrid power system with the wind generator and the PV array can provide the continuous

maximum power from the wind and solar energy sources by studying the maximum power point (MPP) control technique.

On the other hand, the PCS of the PV system cannot control optimally the small wind turbine in the grid-tied solar-wind hybrid power systems since the output characteristics of the small wind turbine and the PV array are not the same. Therefore, the novel design is proposed in this study by which the small scale wind turbine could be connected to the grid-tied power conditioner of the solar power system by emulating characteristic of the solar panel. The topology of the PV cell emulating system comprises the small scale wind turbine, a battery, and the power converter circuit. The small scale wind turbine charges the battery in the first stage. After that, the power converter circuit detects the current flowing into the PCS and operates it with the help of the control system.

The novel design is composed of technical solutions of the PV cell cooperating system as below:

- The grid-tied PV cell emulating system in stand-alone mode:

When the solar array cannot receive sunlight, only the small scale wind turbine operates the PCS and this operation mode is called in stand-alone mode. In this mode, the solar array is bypassed in order to avoid the situation that it becomes the load. The PV cell emulating system can connect to the DC/DC converter to perform the MPPT control because the power converter circuit emulates the technical characteristic of the actual solar panel and the technical characteristic of the solar panel is modeled by two and three linear equations.

- The grid-tied PV cell cooperating system in connection mode:

When sunlight appears, both the small scale wind power generating system and PV cell can operate the PCS. In this mode, the solar array can be connected to the PV cell cooperating system in series and parallel to generate the power into the utility grid with the support of the PCS.

In this thesis, the simulation and experimental results show that PV cell emulating system in the stand alone mode can connect and transmit the power to the utility grid by the grid-tied power conditioner in case of the PV array cannot receive sunlight and the PV cell cooperating system also can connect to the solar array in the series/parallel connection mode in the case of the solar irradiation becomes weakly in the cloudy and rainy weather. Therefore, the utilization rate of the grid-tied PCS of the solar power system is enhanced.

Acknowledgements

First of all, I would like to express my special thanks of gratitude to Professor Muneaki Ishida, Professor Junji Hirai and Associate Professor Naoki Yamamura for the continuous support of my PhD study and related research, for their patience, motivation, and immense knowledge.

I would like to thank Professor Kazuo Mori and Professor Satoshi Komada for providing the useful feedback and interesting discussion on my research work. I also thank Professor Satoshi Komada for helping to complete the procedures in the last period of my PhD course.

Thank all members of my research group and Energy System Lab, Department of Electrical and Electronic Engineering, Graduate School of Engineering, Mie University for their cooperation in the study work.

My sincere thanks also go to Institute of Energy Science, Vietnam Academy of Science and Technology for giving me the opportunity to study at Mie University, Japan.

Finally, I would like to thank my parents, my wife, my pretty sons, my brothers and my sisters for their love, support, and encouragement.

Contents

List of Figures

List of Tables

Abbreviations

AC	Alternative current
CV	Constant voltage
DC	Direct current
FB	Full bridge
FLC	Fuzzy logic control
IC	Incremental conductance
IEA	International energy agency
LF	Loop filter
LV	Low voltage
MPPT	Maximum power point tracking
MPP	Maximum power point
MV	Medium voltage
NN	Neural networks
PCS	Power conditioner system
PD	Phase detector
PI	Proportional integral
PLL	Phase locked loop
P&O	Perturbation and observation
PSF	Power signal feedback
PV	Photovoltaic
PWM	Pulse width modulation
THD	Total harmonic distortion

TSR	Tip speed ratio
VCO	Voltage controlled oscillator

Chapter 1

Introduction

1.1. Background and purpose

At the present, the solar power systems are quickly developing [1, 2, 3] in many countries to replace the fossil power sources and mitigate the environment pollution. Up to now, the global annual installed solar power capacity is about 80GWp [1], but the solar power generation is dependent on sunlight to effectively collect solar energy. So, it makes lower the utilization rate of the power conditioner system (PCS) in the photovoltaic (PV) system as can be seen in Figure 1.2.

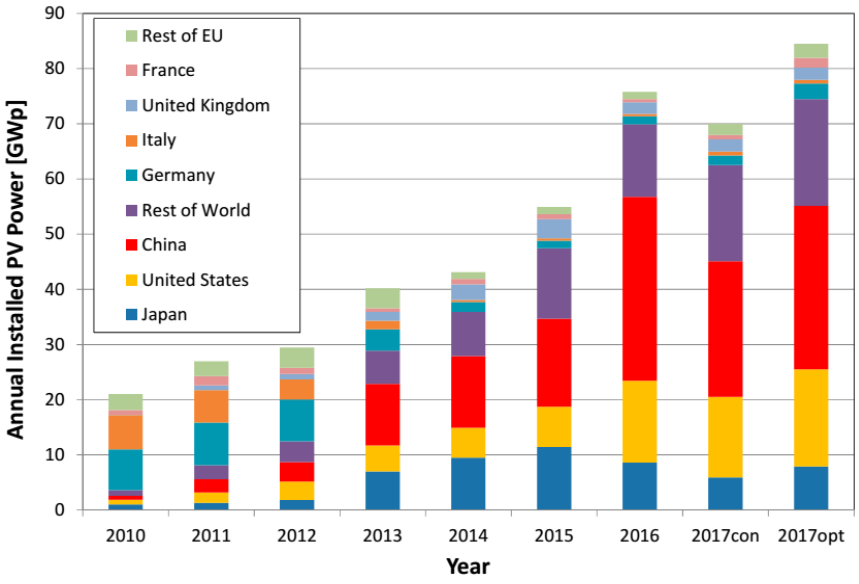

Figure 1.1. Solar power installation from 2010 to 2017 [1]

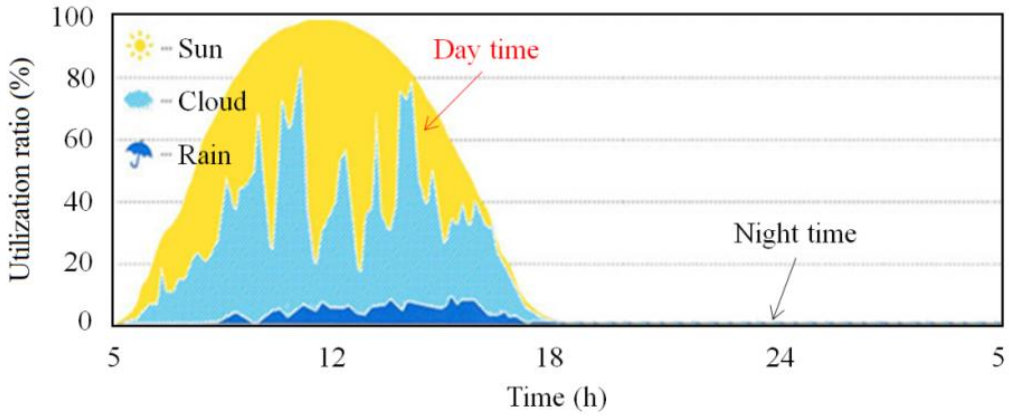

Figure 1.2. Utilization ratio of the PCS in the PV system

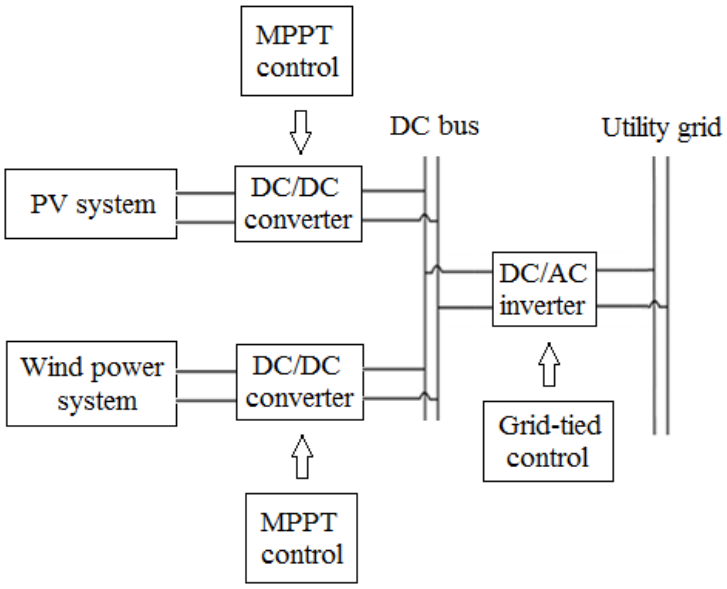

Figure. 1.3. The typical small solar-wind hybrid power system

We can supplement the small scale wind power system to the existing solar power generation system to improve the utilization rate of the PCS because the small scale wind turbine utilizes possibly the PCS at night and also can use the remaining capacity of the PCS during the daytime. The typical grid-connected hybrid power system with the wind generator and the PV array as shown in Figure 1.3 can provide the continuous maximum power from the wind and solar energy sources by studying the maximum power point tracking (MPPT) control technique. The MPPT control methods [4, 5, 6, 7] for solar power generation mainly include the conventional methods such as the perturbation and observation method (P&O), the fixed duty cycle method, constant voltage (CV), the

incremental conductance (IC), and the novel intelligent methods such as optimum gradient method, fuzzy logic control (FLC), neural networks (NN). Previous research papers [4, 6] have analyzed the traditional maximum wind power control types such as namely tip speed ratio (TSR) control, power signal feedback (PSF) control and hill-climb searching (HCS) control as well as the novel method such as neural networks (NN). In general, the conventional MPPT control methods of solar power and wind power are successfully demonstrated in actual systems with easier application and better price, but lower accuracy in comparison with the novel intelligent control methods.

On the other hand, the PCS of the PV system cannot control optimally the small wind turbine in the grid-tied solar-wind hybrid power systems since the output characteristics of the small wind turbine and the PV array are not the same. Therefore, we can use solution that the small scale wind turbine connects to the grid-tied power conditioner of the solar power system by emulating characteristic of the solar panel.

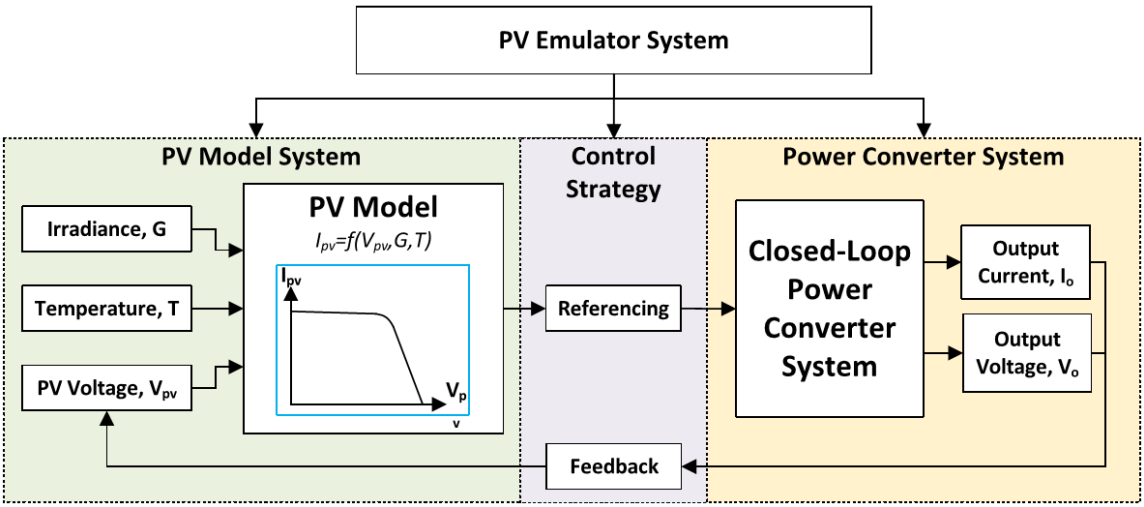

Figure. 1.4. Configuration of the PV cell emulating system [8]

The PV cell emulating system is studied by many researchers in the world and most of their research purpose is to manufacture the PV cell emulating system as a power source for the experimental test of the solar power system [8]. In general, the configuration of the PV cell emulating system includes three parts as can be

seen in Figure 1.4.

Firstly, the PV model system is used to make the I-V characteristic of the solar panel signal. The PV model types and the method which performs the PV model are displayed in Figure 1.5. After that, the control methods as presented in Figure 1.6 establishes the operating point of the PV cell emulating system to connect the PV model with the power converter system.

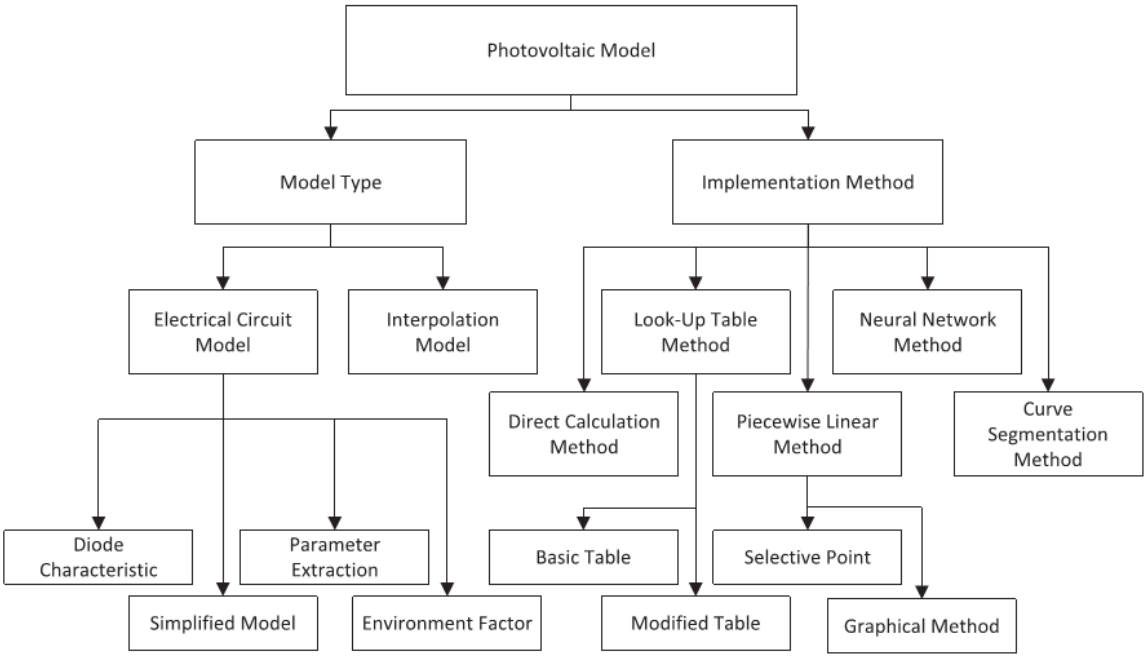

Figure. 1.5. PV model type & implementation method [8]

Finally, the function of the power converter system is to convert the I-V characteristic of the PV module into the useful I-V characteristic for generating power because the PV model only supplies the signal and cannot generate power. Figure 1.7 shows the types of power converter which are used in the application of the PV cell emulating system.

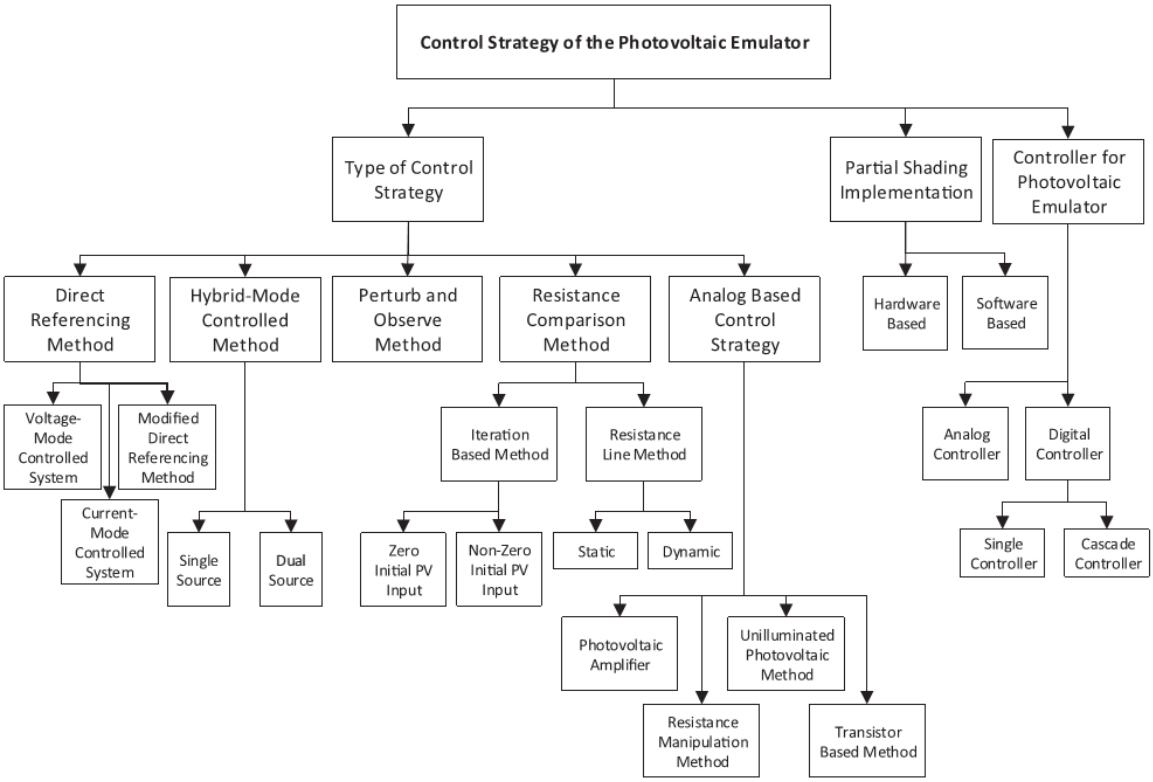

Figure 1.6. Control method of the PV cell emulating system [8]

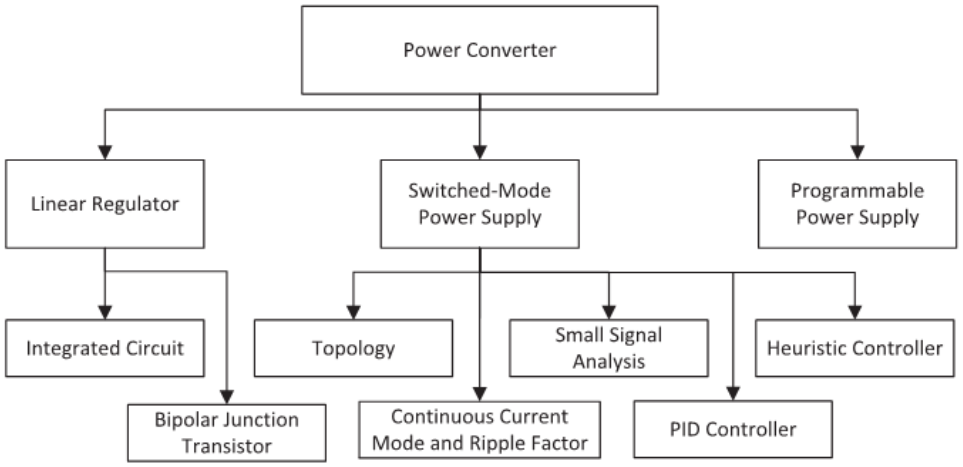

Figure 1.7. Types of power converter in the PV cell emulating system [8]

In this study, the proposed novel technical design solutions of the PV cell emulating system which can connect to the PCS in the solar power system are the grid-tied PV cell emulating system in the stand-alone mode and the grid-tied PV cell cooperating system in connection mode as can be seen in Figure 1.8 and Figure 1.9.

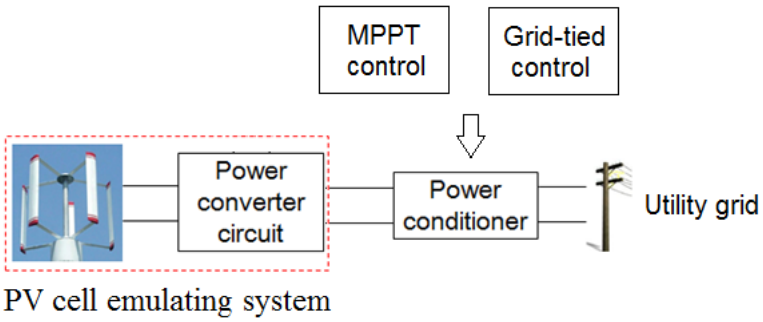

Figure 1.8. Proposed grid-tied PV cell emulating system in stand-alone mode

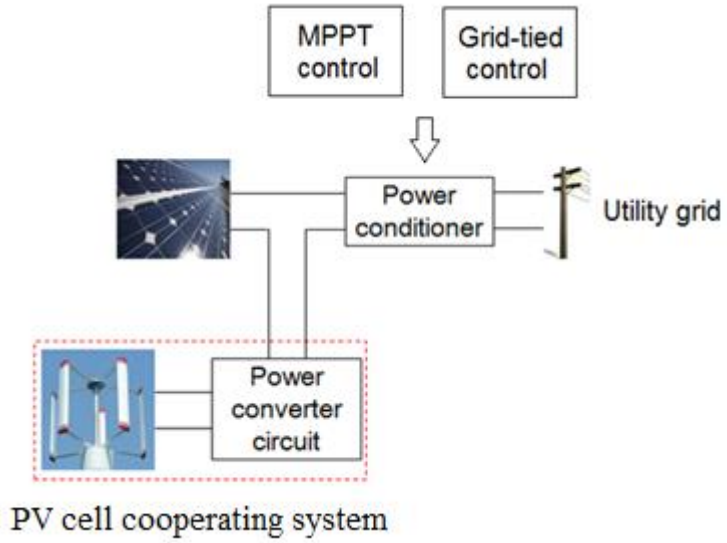

a. Series connection mode

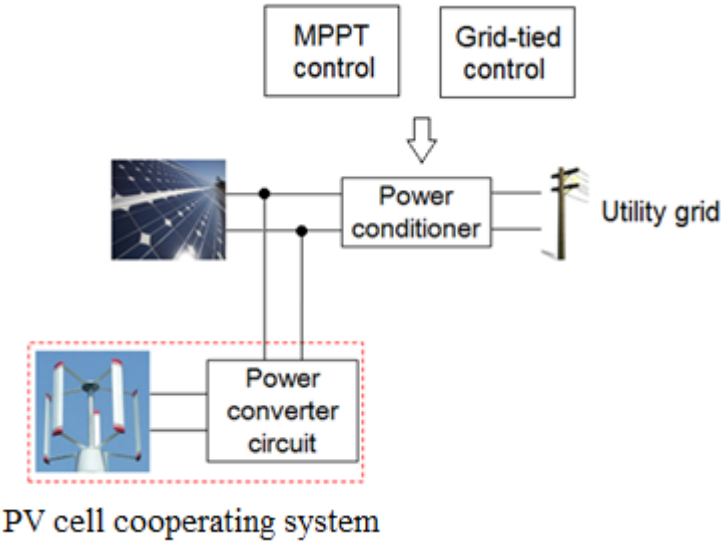

b. Parallel connection mode

Figure 1.9. Proposed grid-tied PV cell cooperating system in connection mode

- The grid-tied PV cell emulating system in the stand-alone mode:

When the solar array cannot receive sunlight, only the small scale wind turbine operates the PCS and this operation mode is called in the stand-alone mode. In this mode, the solar array is bypassed in order to avoid the situation that it becomes the load. The PV cell emulating system can connect to the DC/DC converter to perform the MPPT control because the power converter circuit emulates the technical characteristic of the actual solar panel and the technical characteristic of the solar panel is modeled by two and three linear equations.

- The grid-tied PV cell cooperating system in connection mode:

When sunlight appears, both the small scale wind power generating system and PV cell can operate the PCS. In this mode, the solar array can be connected to the PV cell cooperating system in series and parallel to generate the power into the utility grid with the support of the PCS.

1.2. Composition of the thesis

There are 6 chapters in this thesis:

Chapter 1 introduces general background, purpose, and the contribution of the thesis.

In chapter 2, the configuration and the operation of the solar power system are analyzed. Moreover, the MPPT control system and the grid-tied control system in the PCS are also described in detail.

In chapter 3, the operation, linear equations, and the control system of the grid-tied PV cell emulating system in stand alone mode are introduced. The simulation and experimental test results verify the control method of the grid-tied PV cell emulating system in the stand-alone mode.

In chapter 4, the configuration, the I - V characteristic, and the control system of the grid-tied PV cell cooperating system in series connection mode are described. Next, the operation modes of the system are analyzed by the simulation results. Finally, the effectiveness of the proposed hybrid power system is

confirmed by the results of experimental investigation.

In chapter 5, the operation, the I - V characteristic, and the control system of the grid-tied PV cell cooperating system in parallel connection mode are analyzed. The simulation results are used to verify the operation modes of the system.

In chapter 6, the summary of this thesis and the future works are presented.

1.3. Contributions

In this thesis, I have proposed the novel design of the PV cell emulating system using the small scale wind turbine in order to improve the work efficiency of the PCS in the grid-tied solar power system.

The research results show that the PV cell emulating system in the stand alone mode can connect and transmit the power to the utility grid by using the grid-tied PCS in the case of the PV array cannot receive sunlight. Besides, the PV cell cooperating system also can connect to the solar array in the series and parallel connection mode in the case of the solar irradiation becomes weakly in the cloudy and rainy weather. Hence, the utilization rate of the PCS is increased because the PV cell cooperating system can use the remainder of the capacity of the PCS by day regardless of altering solar irradiation as well as in the case where the solar array cannot receive the sunlight, especially the night time.

There are some main materials of this thesis have been presented as below:

Vu Minh Phap, N. Yamamura, M. Ishida, J. Hirai, and K. Nakatani, “Development of Novel Connection Control Method for Small Scale Solar -Wind Hybrid Power Plant,” *International Journal of Engineering Research*, vol. 5, no. 8, pp. 730-734, 2016.

Vu Minh Phap, N. Yamamura, M. Ishida, J. Hirai, K. Yubai and Nguyen Thuy Nga, “Modeling and Experimental Test of Grid-Tied Photovoltaic Cell Emulating System in the Stand-alone Mode,” *Journal of Electrical Systems*, vol. 13, no. 2, pp. 387-397, 2017.

Vu Minh Phap, N. Yamamura, M. Ishida, K. Nakatani, and Nguyen Thuy Nga,

"Experimental Study on Photovoltaic Cell Emulating System in Series Connection Mode," *Journal of Electrical Systems*. (Accepted)

Vu Minh Phap, N. Yamamura, M. Ishida, J. Hirai, and N. T. Nga, "Design of Novel Grid-tied Solar - Wind Hybrid Power Plant Using Photovoltaic Cell Emulating System," *Proceeding in IEEE 4th International Conference on Sustainable Energy Technologies (ICSET)*, Hanoi, Vietnam, 2016, pp. 168-171.

Vu Minh Phap, N. Yamamura, M. Ishida, and N. T. Nga, "Impact of Solar Irradiation on PV Cell Emulating System in Series Connection Mode," *Proceeding in IEEE International Conference of High Voltage and Power System (ICHVEPS)*, Bali, Indonesia, 2017, pp. 282-285.

Kirian Guiller, Vu Minh Phap, N. Yamamura, M. Ishida, J. Hirai, "Study on new control system design of PV cell emulating system in the stand alone mode," *Proceeding in International Conference on Engineering, Science, and Application (ICESA)*, Tokyo, Japan, 2017, vol.1, no.1, pp. 153-161.

Vu Minh Phap, N. Yamamura, M. Ishida, I. Mizoguchi, T. Yamashita and N. T. Nga, "Efficiency Enhancement of PV Cell Emulating System in Connection Mode," *Proceeding in IEEE International Conference on Industrial Technology (ICIT)*, Lyon, France, 2018.

Chapter 2

Solar Power System Fundamentals

2.1. Basics of PV cell

2.1.1. Electrical circuit model

Semiconductor materials which are operated by the photoelectric effect [9] form PV cells. When sunlight comes to the PV cell, the solar photons break the bonds of valence electrons and move the electron up to higher energy in the conduction band of semiconductor [9] as displayed in Figure 2.1. The movement of these electrons in the external circuit can transmit the electricity.

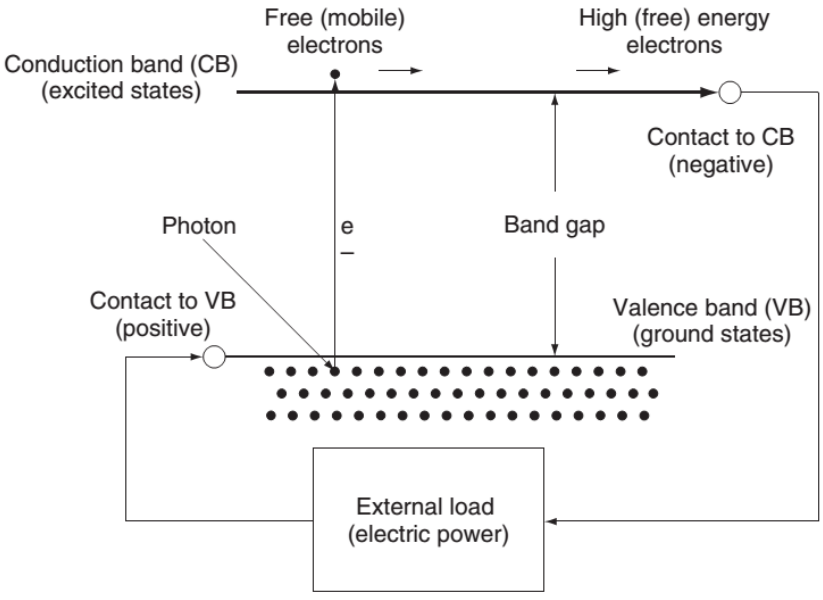

Figure 2.1. Operation principle of PV cell [9]

As a result, the solar module which is composed of many connected PV cells can generate the direct current (DC) after absorbing the sunlight. The PV cell is modeled by the equivalent electrical circuit as shown in Figure 2.1:

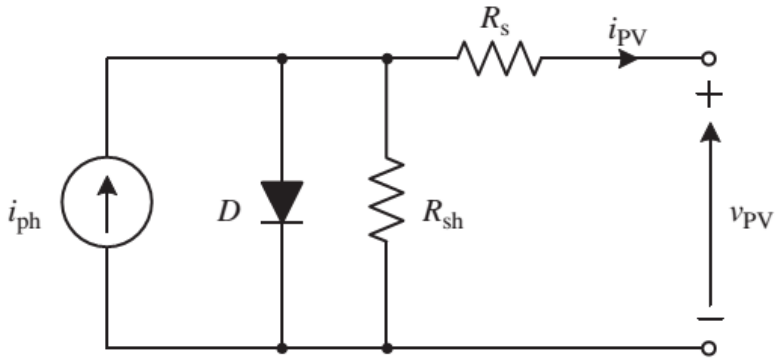

Figure 2.2. The electrical model of PV cell

The equation [10] that describes a PV cell is:

$$i_{pv} = i_L - i_0\left(e^{\frac{q(v_{pv}+i_{pv}R_s)}{nKT}} - 1\right) - \frac{v_{pv}+i_{pv}R_s}{R_{sh}} \tag{2.1}$$

where the parameters are listed in table 2.1 as below

Table 2.1. PV cell parameters

Variable	**Parameter**
v_{pv}	output voltage of PV cell (V)
i_{pv}	output current of PV cell (A)
R_s	Cell series parasitic resistance (Ω)
R_{sh}	Cell shunt parasitic resistance (Ω)
q	Electronic charge: 1.6×10^{-19} (Coulombs)
K	Boltzmann constant: 1.38×10^{-23} (J/K)
T	Absolute temperature in unit Kelvin
i_0	Cell reverse saturation current: 10^{-12} (A/cm^2)
i_{ph}	Cell photocurrent
n	Ideality factor of diode

2.1.2. I-V characteristic

Operation of the current and voltage a solar panel under different conditions of solar irradiation and temperature is presented by I–V characteristic curve in Figure 2.3.

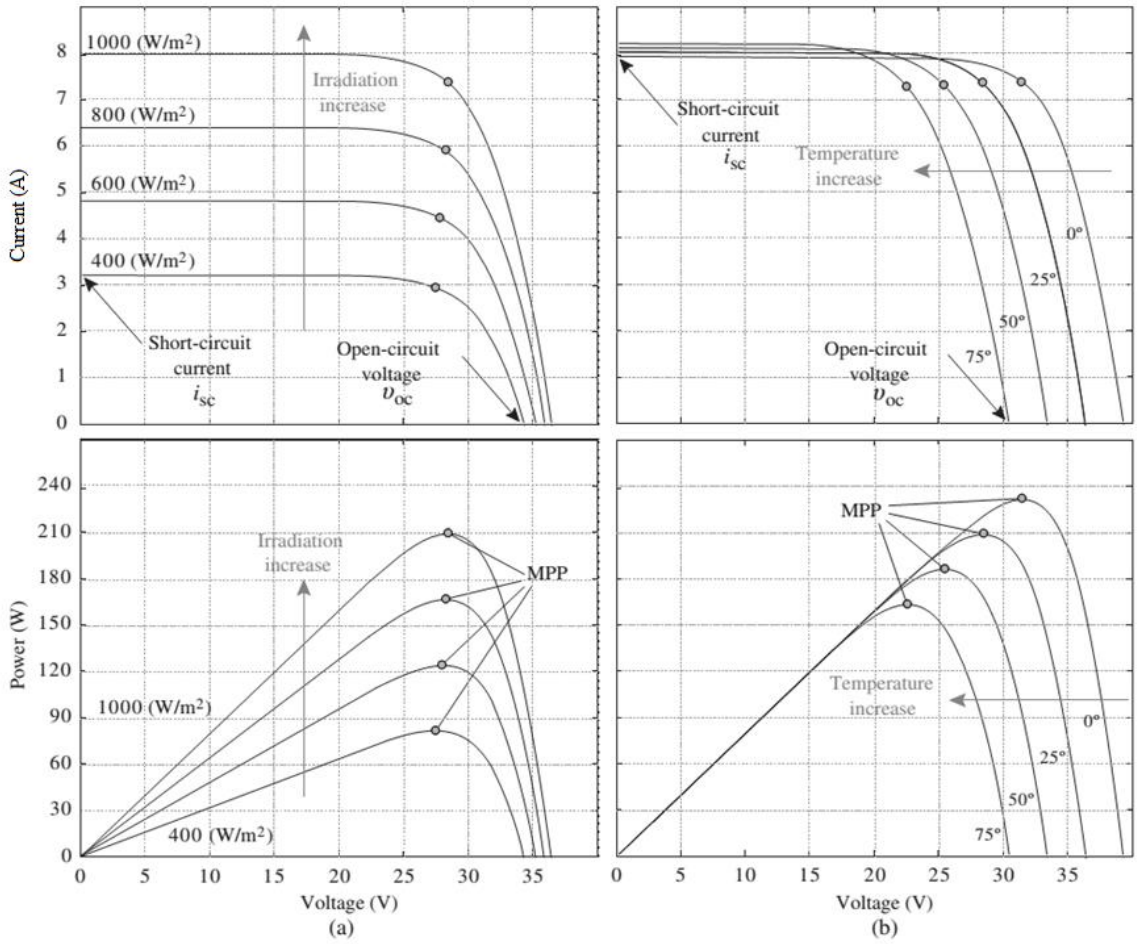

Figure 2.3. I-V characteristic of solar panel [11]

The output voltage of the solar panel changes slightly while the output current is strongly influenced [11] by the various values of solar irradiation. In contrast, the output current of the solar panel alters slightly while the output voltage is significantly affected by the changing of the temperature.

In the I–V characteristic curve, there is a special combination point of current and voltage of the solar panel, by which the power achieves the maximum value. The point at which the solar panel can supply maximum electrical power is the

maximum power point (MPP). This maximum power point value changes in the I–V characteristic curve of the solar panel in accordance with the impact of the solar irradiation and temperature at different times.

When the solar panel connects with a passive load, the I–V curve of the load will intersect the I–V characteristic curve of the solar panel and determine the power transmitted by the solar module, but it is not the MPP value in the I–V characteristic curve of the solar panel. To resolve this technical problem, a DC–DC or DC–AC power converter can be used to adjust the load curve characteristic and intersect the solar panel I–V characteristic curve at the MPP, this content will be discussed in next parts.

2.2. Solar power system

2.2.1. Stand alone PV system

Stand alone PV system is the power source that works independently and this system does not connect to the utility grid. Figure 2.4 illustrates the configuration of a stand alone PV system system consisting of one or more PV modules, charge controller, battery, DC-DC or DC-AC power converter and loads.

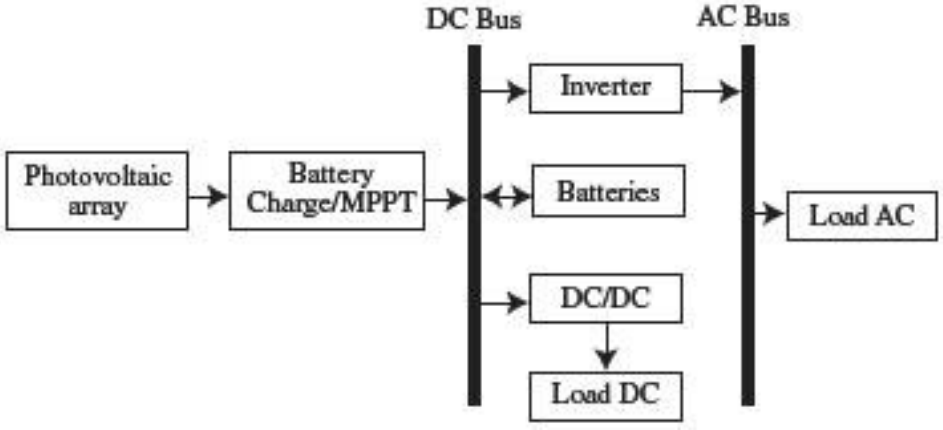

Figure 2.4. Diagram of the stand alone PV system [12]

The solar system generates electricity to charge batteries with the help of the charge controller during the day for utilization in the rainy day and night time. The

DC electricity from the battery can supply to the DC load or it is converted to AC power for AC appliances by using DC-AC inverter. The stand alone PV systems are mostly used for demands in rural area, remote area such as islands or villages on the mountain. The size of the sand alone PV system depends on the demand requirement.

2.2.2. Grid-tied solar power system

A grid-tied solar power system is an electricity generating solar power system that is connected to the utility grid. The size of this system from small residential and commercial rooftop systems to large utility-scale solar power stations.

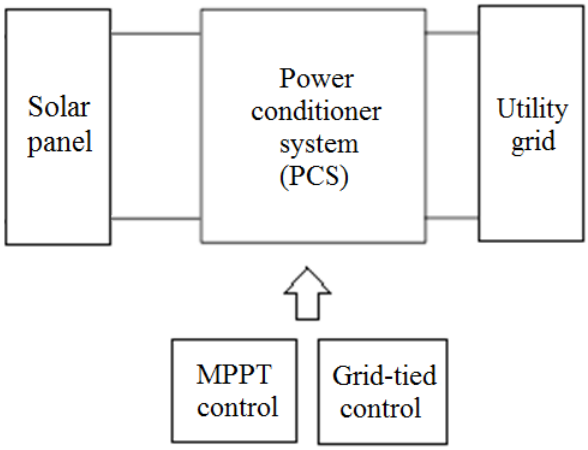

Figure 2.5. Small grid-tied solar power system

Figure 2.5 displays the configuration of the small scale grid-tied solar power system [13] with the PCS, including the DC/DC converter and the grid-tied DC/AC inverter. The solar panel generates the DC power to the PCS, in which the maximum power point tracking (MPPT) is performed by the boost-type DC/DC converter while the power at the output terminals of the solar array is supplied into the utility grid by the grid-tied DC/AC inverter. At any time of the day, a customer's solar system may produce more or less electricity than they need for their home or business. When the system's production exceeds the customer demand, the excess energy generation automatically goes through the electric meter into the utility grid, running the meter backwards to credit the customer

account with the support of Net-metering policy [14]. At other times of the day, the customer's electric demand may be higher than the renewable energy system is producing, and the customer relies on additional power needs from the utility grid. Switching between solar system's power and the utility grid power is instantaneous and customers never notice any interruption in the flow of power.

Figure 2.6 shows a typical configuration of a large scale grid-tied solar system. The solar modules are connected in series to form strings, and in parallel to form an array connected to the grid-tied DC/AC inverter. The DC/AC inverter performs the MPPT of the solar array by controlling the DC-link voltage to maximum power point voltage, and synchronizing the AC grid currents with the grid voltage for active and reactive power control [11]. Then, the DC/AC inverter is connected to the grid via an inductive grid filter and a transformer to increase the voltage from low voltage (LV) to medium voltage (MV) of a few thousand volts (LV/MV) to decrease losses in supplying electricity to the utility grid.

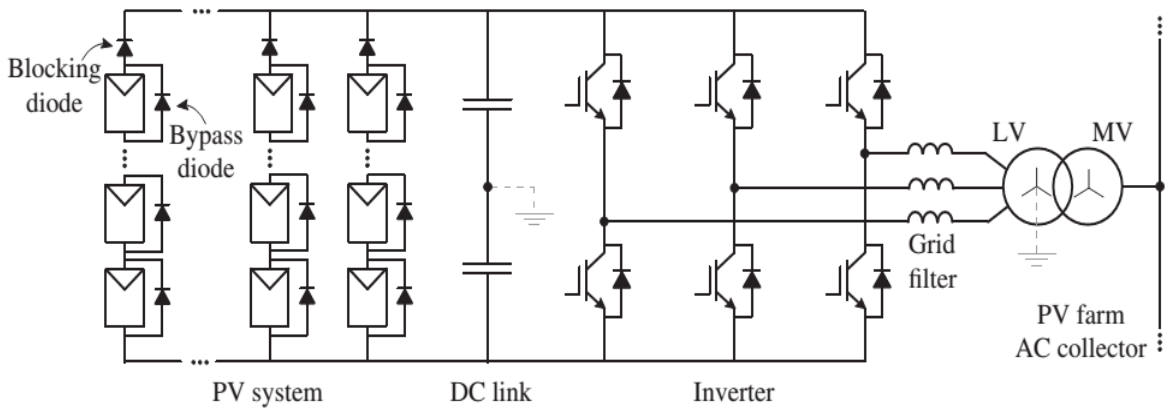

Figure 2.6. Large scale grid-tied solar power system [11]

In addition, with the support of a feed-in tariff policy [15], eligible solar farm investors are paid a cost-based price for the electricity from solar farms transmitting to the utility grid.

2.2.3. Hybrid power system

Hybrid power systems [16, 17, 18, 19] are used to combine the PV system with

other power generating energy sources such as wind power, hydro power, fuel cell diesel generator, etc. Other renewable power sources and diesel gensets can constantly fill in the gap between the present load and the actual generated power by the PV system because the operation of the PV system is strongly impacted by the sunlight.

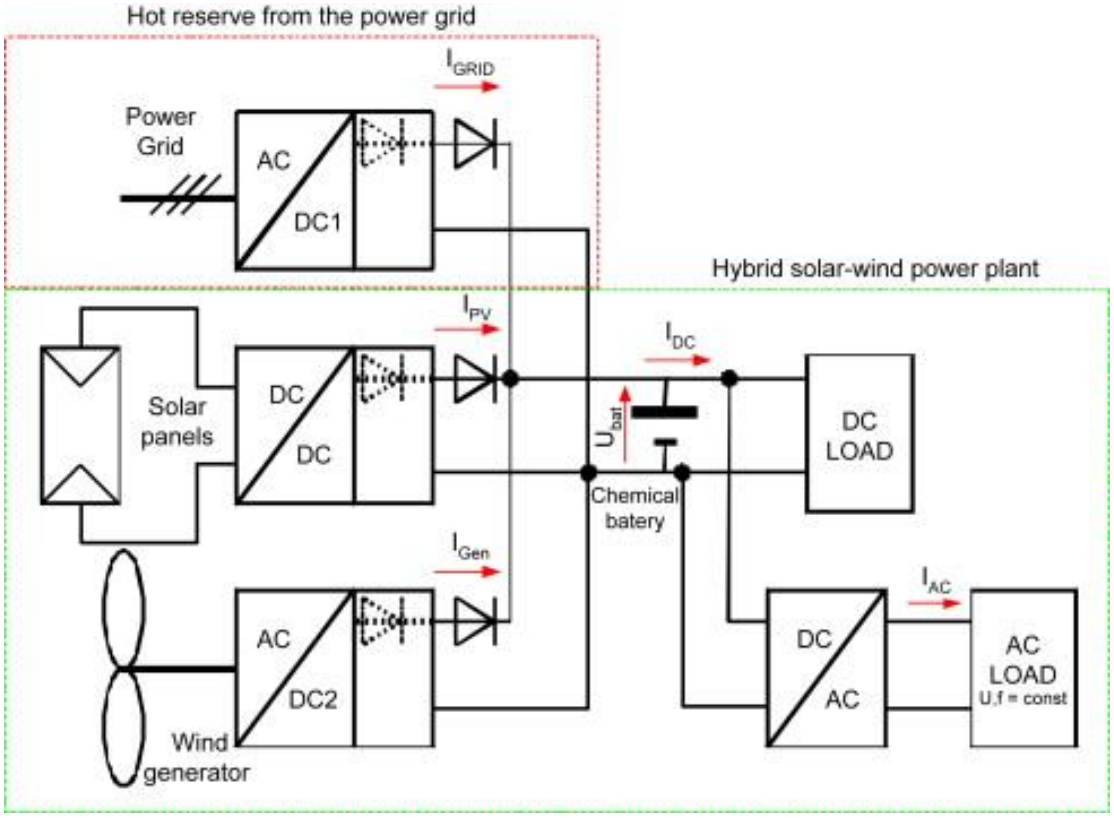

Figure 2.7. Hybrid solar-wind power system [16]

Configuration of a hybrid power system includes renewable energy sources, battery storage, power conditioning equipment, diesel generators and/or power grid as shown in Figure 2.7. Hybrid power systems can be connected to the power grid, but they can also work independently feeding separated receivers, from one or several homes/farms, small industrial plants to large local communities, in the mining sector and on remote areas.

2.3. Power conditioner system

2.3.1. DC/DC converter

The main function of the DC/DC converter in the PCS is to convert the power from solar modules to the highest power by using maximum power point tracking (MPPT) method. There are some typical types of DC/DC converter such as boost converter, buck converter, buck-boost converter, and bi-direction converter can be used in the solar power systems.

a. Boost converter

Boost converter [20, 21, 22] is used to increase the input voltage and the output voltage is always larger than the input voltage. When the switch is on, the diode is reversed biased, and it is isolating the output stage. The input generates energy to the inductor. When the switch is off, the output stage receives energy from the inductor and from the input.

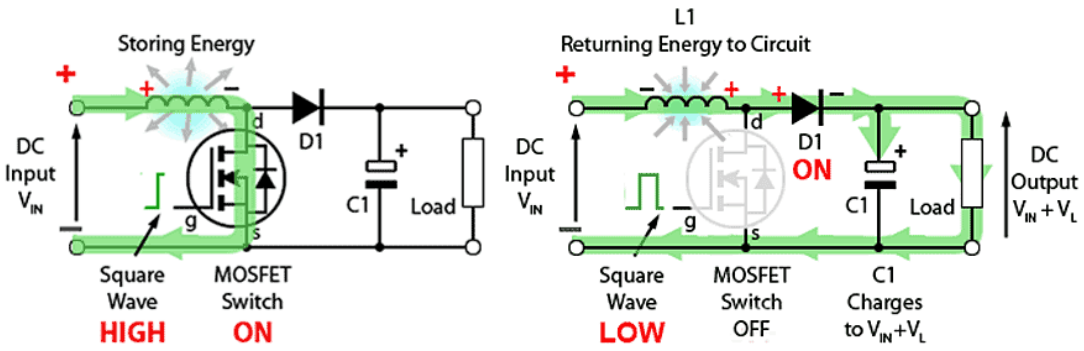

Figure 2.8. Boost converter [23]

The relationship among input voltage V_{in}, output voltage V_{out} and duty cycle D of switch in boost converter in the steady-state is shown in the equation as below:

$$\frac{V_{out}}{V_{in}} = \frac{1}{1-D} \tag{2.2}$$

b. Buck converter

The function of Buck converter [20, 24, 25] is to lower the input voltage and

the output voltage is smaller than the input voltage. When the switch is on, the diode is reversed biased, it is supplying the load with current and this initially current is also stored in the inductor. When the switch is off, the energy stored in the inductor is released back to the output stage as shown in Figure 2.9.

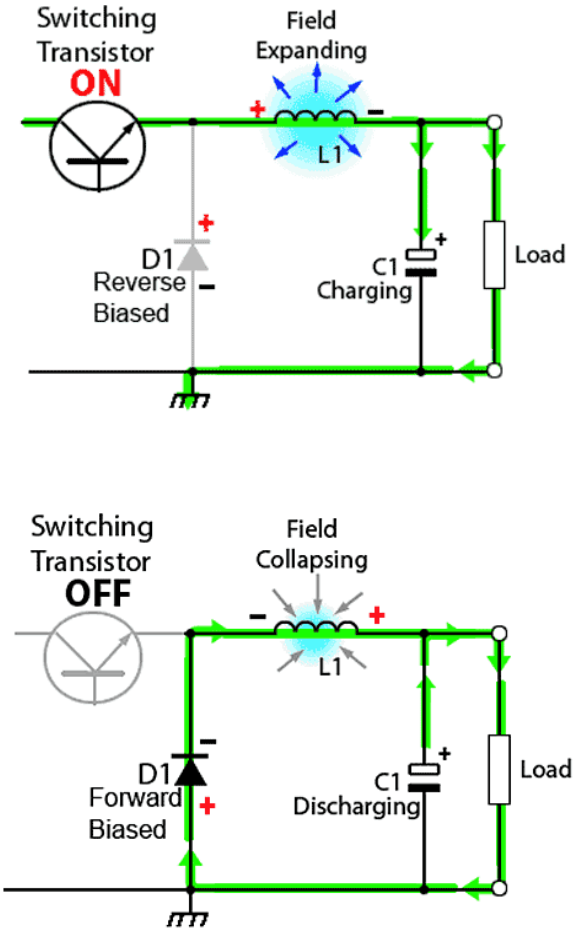

Figure 2.9. Buck converter [23]

Equation 2.3 presents the relationship of input voltage V_{in}, output voltage V_{out} and duty cycle D of switch in buck converter in a steady-state .

$$\frac{V_{out}}{V_{in}} = D \tag{2.3}$$

c. Buck-boost converter

Buck-boost converter [20, 26, 27] is used to control DC power supplies and the output voltage can be regulated to be higher or lower than the input voltage. In

other words, the buck-boost converter combines the operation modes of either the buck converter and the boost converter. In Figure 2.10, when the switch 1 are on and off while switch 2 is off, this converter works in buck mode. In contrast, when the switch 1 is on while switch 2 are on and off, this converter operates in boost mode.

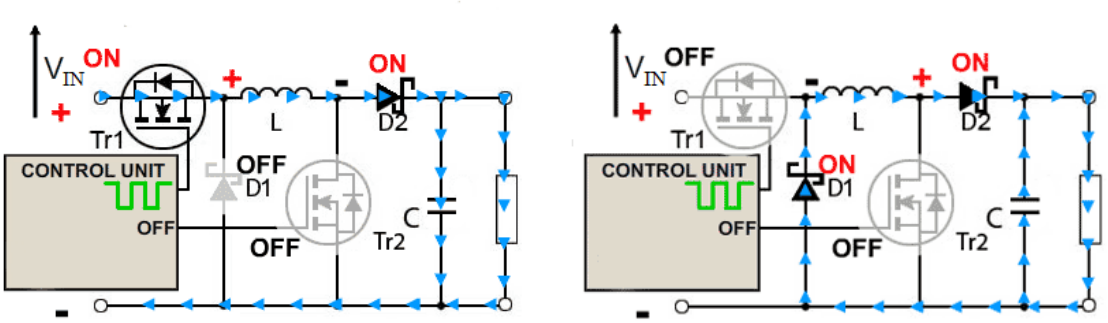

i. Operation in Buck mode

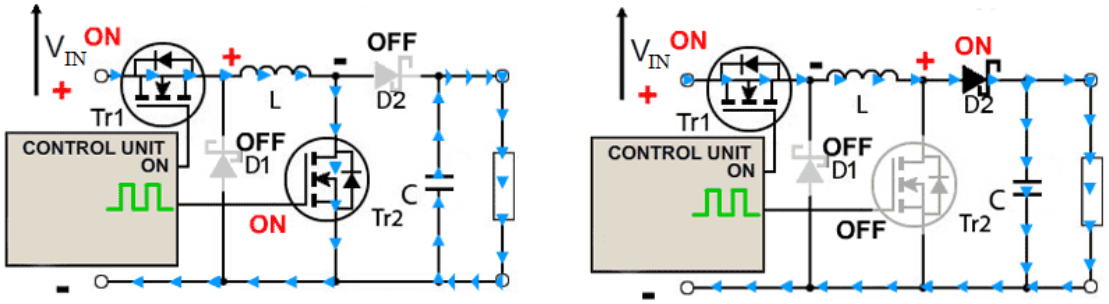

ii. Operation in Boost mode

Figure 2.10. Buck-boost converter [23]

In a steady-state condition, the relationship of input voltage V_{in}, output voltage V_{out} and duty cycle D of switch in buck - boost converter is:

$$\frac{V_{out}}{V_{in}} = \frac{D}{1-D} \tag{2.4}$$

d. Bidirectional converter

A bidirectional converter [28, 29, 30] can transmit current in both directions, but can support the voltage in only one direction. There are two-quadrant switches

in the bidirectional converter, by which energy can move in both directions.

In boost mode, bidirectional converter operates in accordance with the principle of a typical boost converter. In this mode, the switch S2 behaves as a diode by sending zero to its gate.

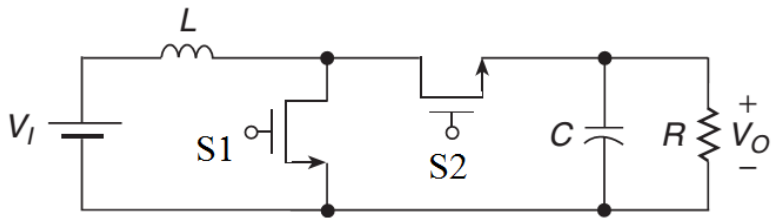

Figure 2.11. Bidirectional converter in boost mode

2.3.2. MPPT control system

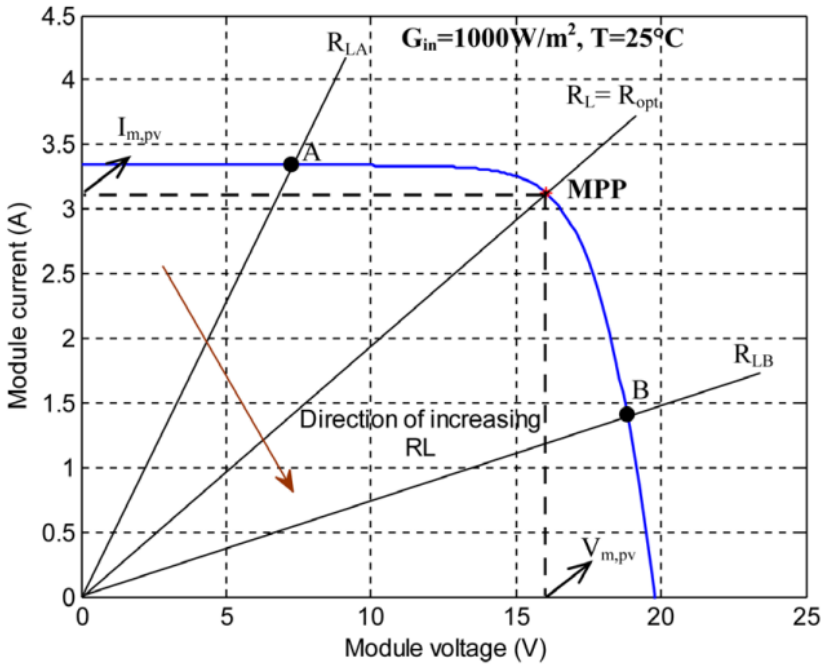

Figure 2.12. Operating point of a PV module with different resistive load [31]

When a solar array is directly connected to a load, the system's operating point will be at the intersection (A or B) of the I–V curve of the PV array and load line is shown in Figure 2.12 [31]. In general, this operating point is not at the MPP so the solar array must usually be oversized to ensure that the load's power requirements

can be supplied. However, this will increase the system cost and energy losses.

In order to solve this problem, a DC–DC or DC–AC power converter can control the load curve characteristic and intersect the PV curve at the MPP. The control techniques for the power converter are maximum power point tracking (MPPT) methods.

a. Impedance matching

A DC/DC converter which interface between load and module, serve the purpose of transferring maximum power from PV module to the load. According to the impedance matching principle [32, 33], the power output of a circuit is maximum when the source impedance matches with the load impedance.

When PV is connected directly to a load, the working point of PV will be determined by load characteristic. Load resistance is defined as follows:

$$R_{load} = \frac{V_{out}}{I_{out}} \tag{2.5}$$

where V_{out} is output voltage, I_{out} is output current

The maximum load of solar panel is:

$$R_{MPP} = \frac{V_{MPP}}{I_{MPP}} \tag{2.6}$$

where V_{MPP} is maximum voltage, I_{MPP} is maximum current

When the value of the largest load matches the value of R_{max}, the transmission power from PV to load will be the largest capacity. So, MPPT will match the impedance of the load with the largest load impedance of solar panel with the help of the DC-DC converter.

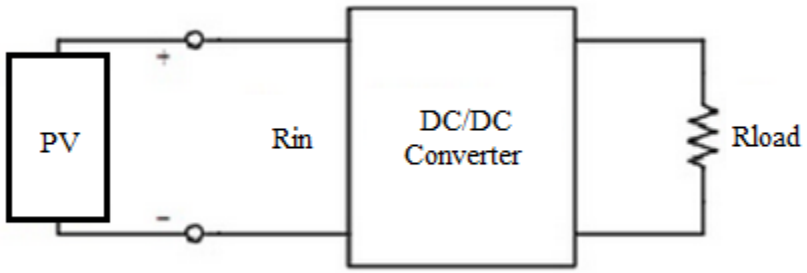

Figure 2.13. PV system with DC/DC converter

With Boost converter according to Equation (2.2) as mentioned above:

$$\frac{V_{out}}{V_{in}} = \frac{1}{1-D}$$

where V_{out} is output voltage, V_{in} is input voltage, D is duty cycle

To assume

$$P_{in} = P_{out} \tag{2.7}$$

where P_{out} is output power, P_{in} is input power

Then:

$$\frac{I_{in}}{I_{out}} = \frac{V_{out}}{V_{in}} \tag{2.8}$$

where I_0 is output current, I_i is input current

$$I_{in} = \frac{I_{out}}{1-D} \tag{2.9}$$

So:

$$R_{in} = \frac{V_{in}}{I_{in}} = (1-D)^2 \frac{V_{out}}{I_{out}} = (1-D)^2 R_{load} \tag{2.10}$$

Thus, the value of R_{in} is adjusted in accordance with R_{MPP} by modifying the value of D. R_{in} varies from R_{load} to 0 as D varies from 0 to 1 correspondingly.

b. Perturb and Observe (P&O) algorithm

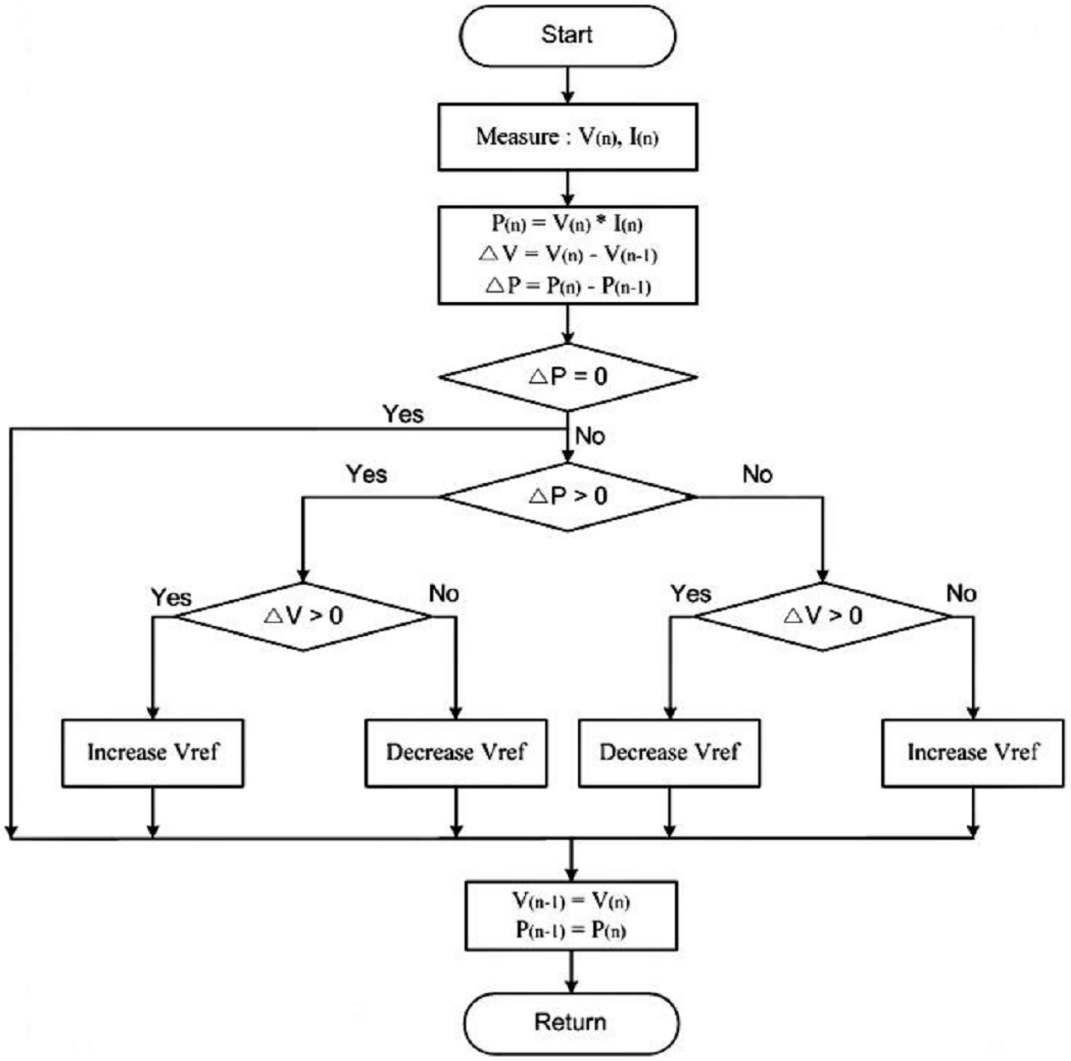

$V_{ref} = V_{ref}(n-1) \pm \triangle V$

Figure 2.14. Flowchart of P&O algorithm

There are many MPPT methods [5, 6, 7, 24, 34] but the Perturb and Observe (P&O) algorithm [35] is selected for the PV system in this study because it is the most commonly used in practice and the implementation is easy. Perturb and Observe (P&O) consisting of a continuous reference voltage search process to reach the MPP. The search is performed by perturbing the reference voltage and then measuring the system response (observing) to determine the direction of the next perturbation. The reference voltage perturbations are performed in the direction in which the power should increase.

The perturbation in the reference voltage is always of the same magnitude

while the sign is determined by the power variation. If the power has increased from the last sample, the sign of the perturbation is maintained. If the power has decreased, the sign is reversed.

c. MPPT control structure with DC/DC converter in boost mode

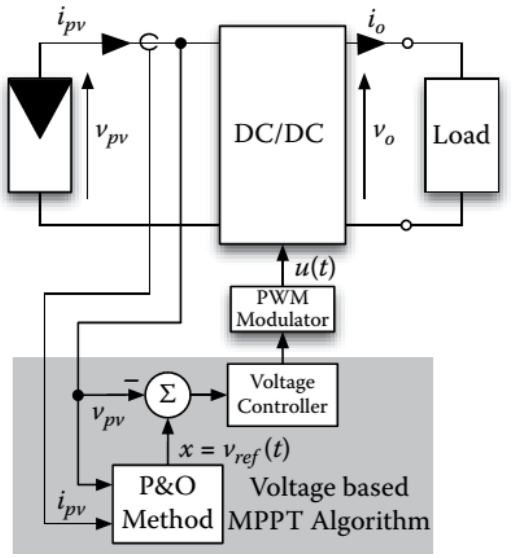

Figure 2.15. Diagram of the MPPT control system [35]

Figure 2.15 shows a block diagram of a classic control system used to perform MPPT in the solar system with a DC/DC converter in boost mode. The PV system current i_{PV} and voltage v_{PV} measurements are required for the P&O MPPT algorithm which generates the reference voltage V_{ref}. MPPT technique will compare the PV array voltage v_{PV} with a constant reference voltage V_{ref}, which corresponds to the maximum power point voltage.

A linear proportional-integral (PI) controller is used to reduce the error between reference voltage V_{ref} and the PV system voltage v_{PV} by varying the duty cycle of the DC/DC converter, which is modulated using carrier-based PWM. The gate signal controls the switch of the DC/DC converter.

2.3.3. DC/AC inverter

In the PCS, the DC/AC inverter will convert direct current (DC) into an alternating current (AC) and transmit the power from the solar array to the utility grid with the

support of grid-tied control system.

There are many types of grid-tied DC/AC inverter, but the H-bridge or full-bridge (FB) inverter is widely used in actual systems because this topology is very versatile, low-cost, can be used for both DC–DC and DC–AC conversion and also be executed in full-bridge form (with two switching legs) or in half-bridge form (with one switching leg) [11, 36]. Some typical H-bridge inverter topologies are presented in Figure 2.16, Figure 2.17 and Figure 2.18.

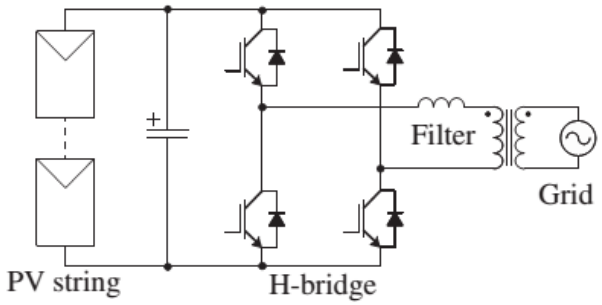

Figure 2.16. H-bridge topology with low-frequency isolation transformer [11]

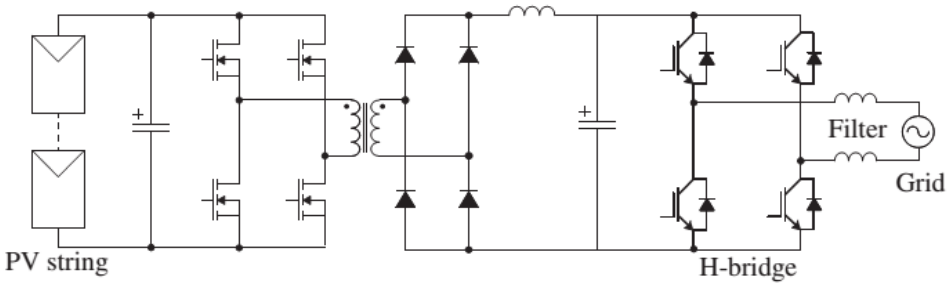

Figure 2.17. H-bridge topology with high-frequency isolation transformer in DC–DC stage [11]

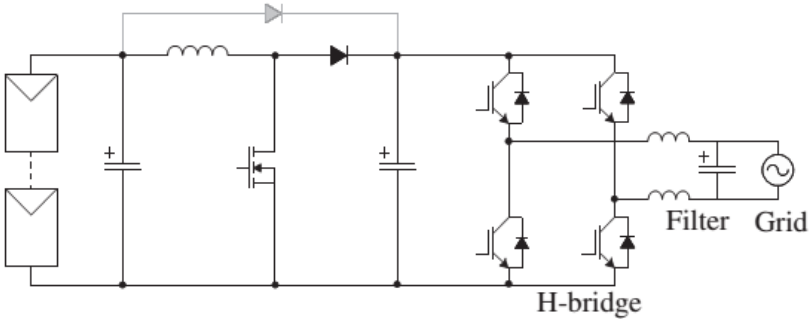

Figure 2.18. H-bridge topology with DC/DC boost converter [11]

2.3.4. Grid-tied control system

a. Introduction

The control system of a typical grid-connected solar power system is illustrated in Figure 2.19. The solar array is connected to the DC-DC converter in boost mode, which is used to perform the MPPT. The electrical energy from the solar array is injected into the grid by using the DC/AC inverter. A low-pass filter allows only the fundamental and some minor voltage harmonics to appear at the connection point with the utility grid [37].

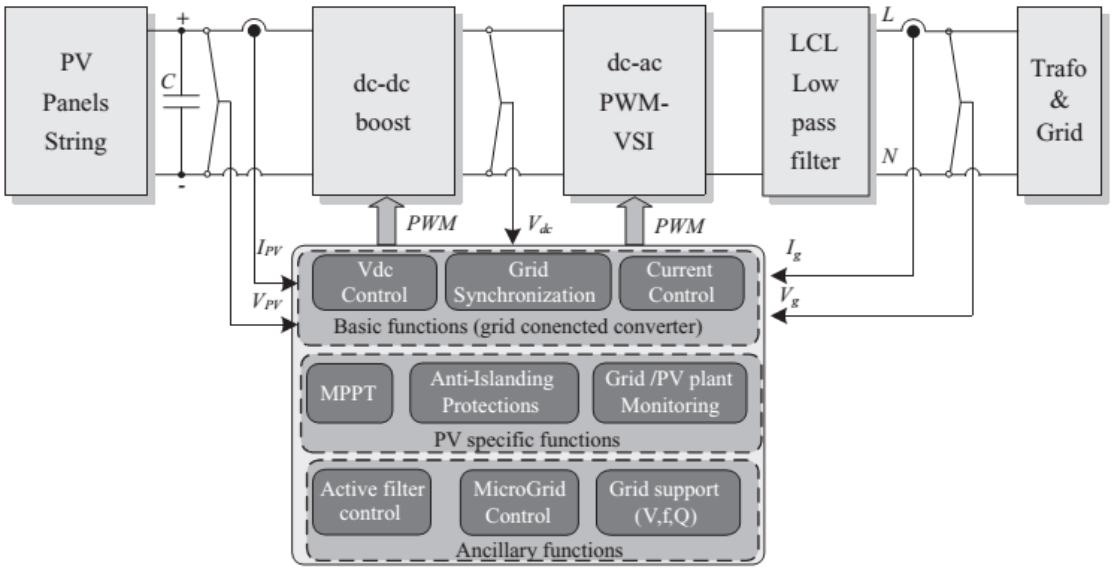

Figure 2.19. Control system of grid-tied solar power system [36]

The output current of the DC/AC inverter is regulated to synchronize with the grid voltage to supply the active power into the utility grid by the support of the hysteresis band method and the Phase Locked Loop (PLL) method in the grid-tied control system of the DC/AC inverter.

Figure 2.20 shows the equivalent circuit of a single phase grid-tied DC/AC inverter while Fig 2.21 displays the phasor diagram of grid voltage, output voltage and output current of the DC/AC inverter. The magnitude of the inverter output voltage (V_{inv}) should be larger than the grid voltage (V_{grid}) to allow the inverter output current (I_{out}) to be transmitted to the utility grid [38, 39]. In addition, the

inverter output voltage (V_{inv}) has to conduct the grid voltage (V_{grid}) with the angle α in order to get the inverter output current (I_{out}) in phase with the grid voltage in order to obtain the unity power factor.

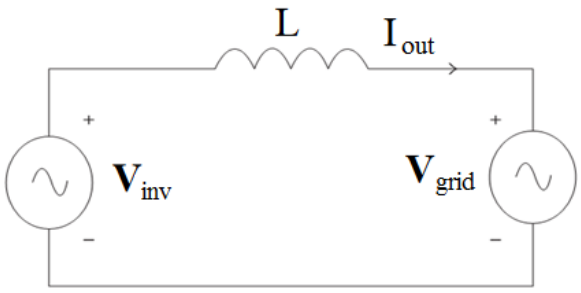

Figure 2.20. Equivalent circuit of the grid-tied DC/AC inverter [38]

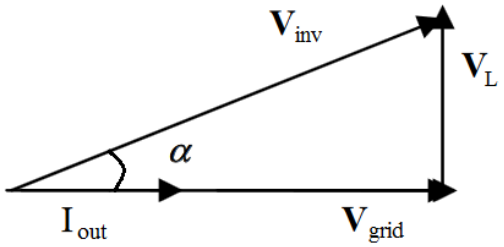

Figure 2.21. Phasor diagram

b. Grid-tied control system

The grid-tied control system is composed of the Phase Locked Loop (PLL) method [40, 41, 42] to generate a synchronizing signal which is in phase synchronized with the grid voltage and the hysteresis band method [37, 43, 44, 45] by which the instantaneous output current I_{out} of the DC/AC inverter can follow the reference current as shown in Figure 2.22.

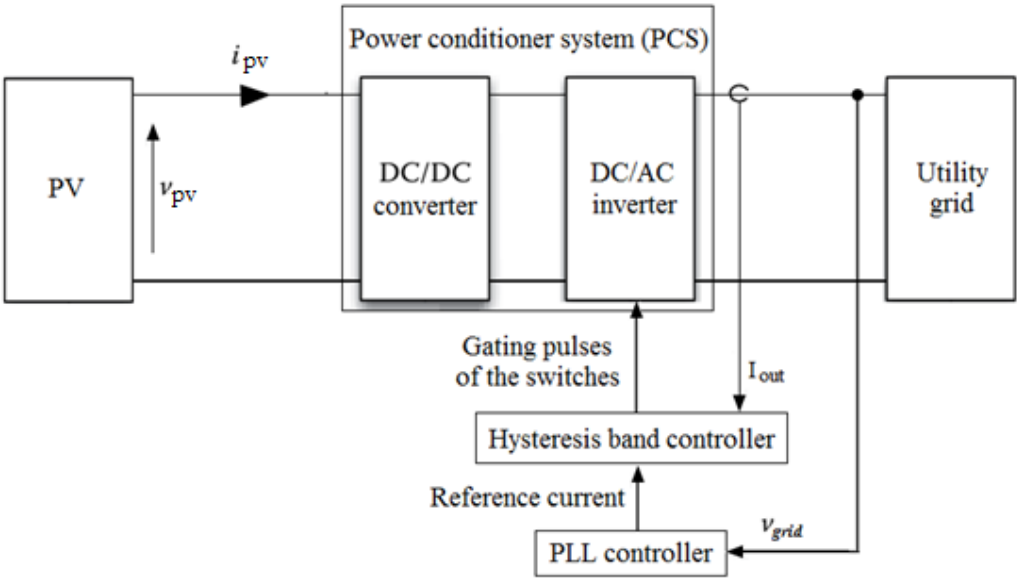

Figure 2.22. Diagram of the grid-tied control system

Firstly, the grid voltage Vgrid comes through the PLL system as the input signal. A PLL (Phase Locked Loop), including three general blocks – a phase detector (PD), a loop filter (LF) and a voltage-controlled oscillator (VCO), works as a filter regardless of the presence of noise, disturbances or harmonics. In which, the VCO produces a sinusoidal signal whose phase angle is proportional to the integral of the input of the VCO [41].

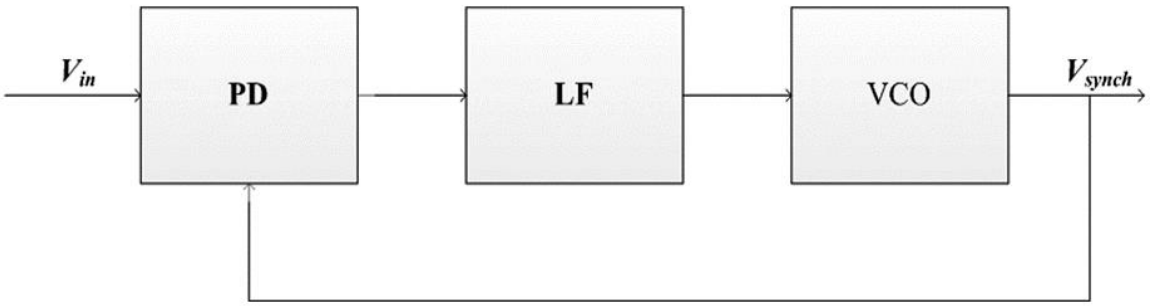

Figure 2.23. Diagram of a single phase PLL

The output of the PLL system is a sinusoid with unity amplitude and in phase with the fundamental component of the grid voltage V_{grid}. This sinusoid is then multiplied by $\sqrt{2}$ x $P_{mpp}/V_{grid(rms)}$ to create the reference current as can be seen in Figure 2.24, where P_{mpp} is the maximum power of the PV cell emulating system

and $V_{grid(rms)}$ is root mean square grid voltage. The hysteresis band method forms a narrow band around the instantaneous reference current.

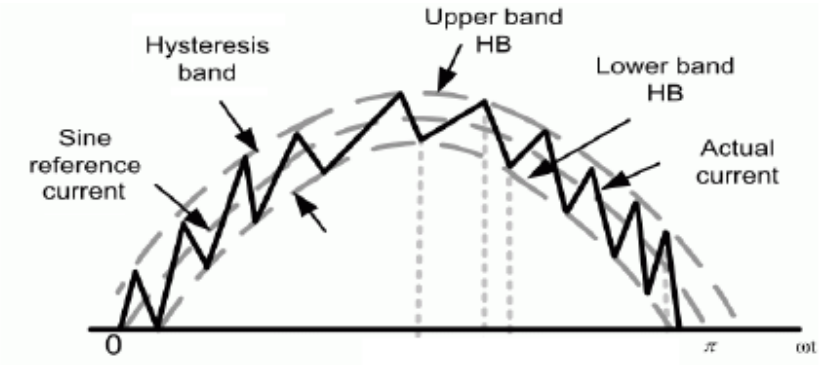

Figure 2.24. Hysteresis band form

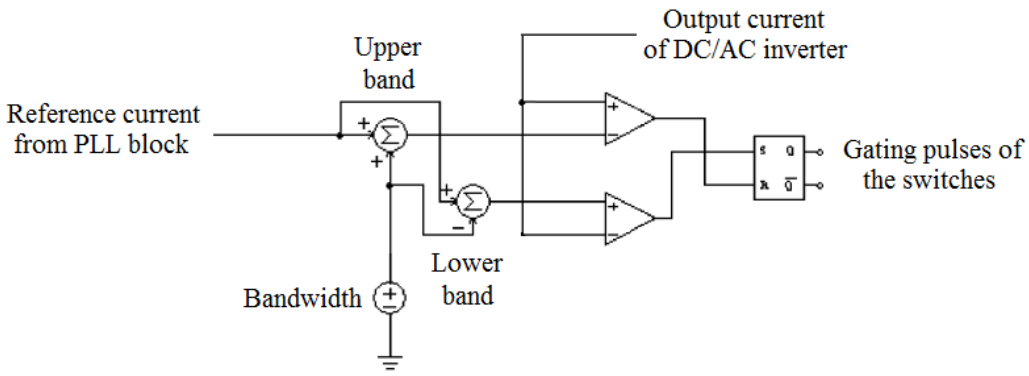

Figure 2.25. Hysteresis band control block diagram

The switches of the DC/AC inverter are adjusted [37] by comparison of the values of the upper limit and the lower limit of this narrow band with the output current I_{out} of the DC/AC inverter.

A large switching frequency and small current harmonic distortion can be created by a very narrow band and the width of this narrow band equals to 5% [37] of the peak value of the nominal inverter current. Finally, the gating pulses of the switches are produced by the flip-flop.

2.4. Conclusion

The configuration and the operation of the solar power system were analyzed in Chapter 2. Besides, the MPPT control system and the grid-tied control system in the PCS were also described in this chapter.

Chapter 3

PV Cell Emulating System in Stand Alone Mode

3.1. System configuration

Figure 3.1 displays the grid-tied solar power system with the PCS, including the DC/DC converter and the grid-tied DC/AC inverter. The maximum power point tracking (MPPT) is performed by the boost-type DC/DC converter while the power at the output terminals of the solar array is supplied into the utility grid by the grid-tied DC/AC inverter.

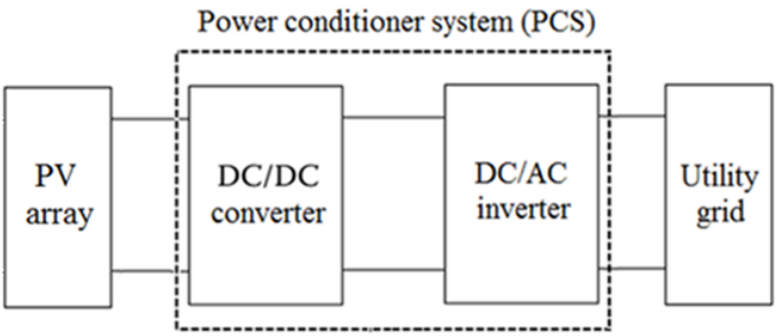

Figure 3.1. Grid-tied solar power system

The topology of the PV cell emulating system as illustrated in Figure 3 comprises the small scale wind turbine, a battery, and the power converter circuit. The small scale wind turbine charges the battery in the first stage. After that, the

power converter circuit detects the current flowing into the PCS and operates it with the help of the control system.

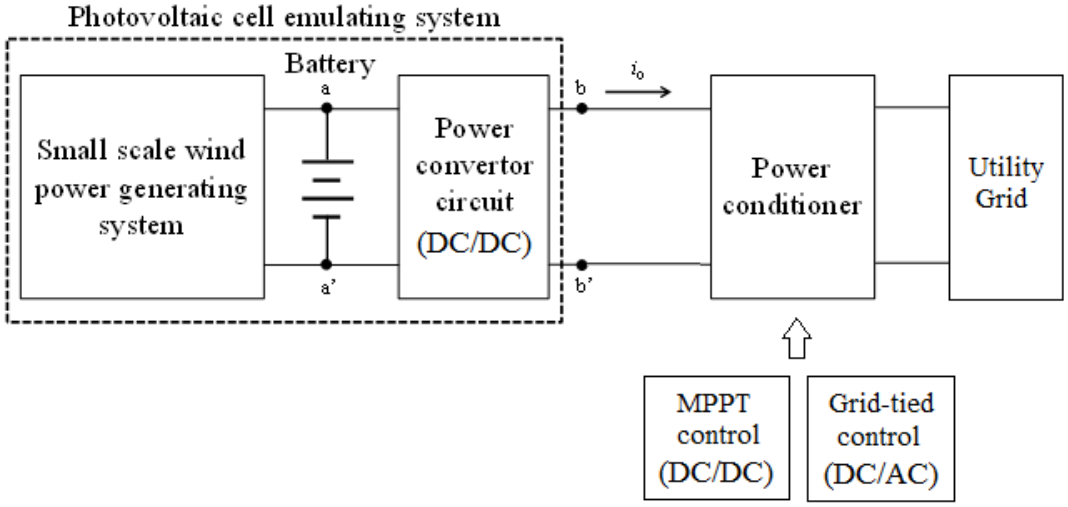

Figure 3.2. PV cell emulating system in the stand-alone mode

When the solar array cannot receive sunlight, only the small scale wind turbine operates the PCS and this operation mode as shown in Figure 3.2 is called in the stand-alone mode. In this mode, the solar array is bypassed in order to avoid the situation that it becomes the load.

3.2. Model equation of Stand-alone mode

In the stand-alone mode, the PV cell emulating system can connect to the DC/DC converter to perform the MPPT control because the power converter circuit emulates the technical characteristic of the actual solar panel as displayed in Figure 3.3. The technical characteristic of the solar panel is modeled by two linear equations in Figure 3.4. The maximum power point current I_{max} is determined by dividing generated power from the small scale wind turbine by the maximum power point voltage V_{max} while the maximum power point voltage V_{max} is calculated considering the operating voltage of the PCS. The open voltage and the short current are computed by multiplying correlative constant factors by the maximum power point voltage and the maximum power point current respectively.

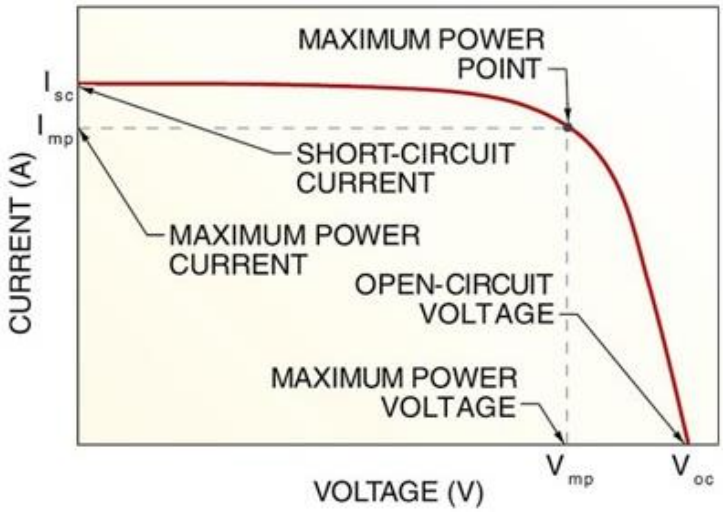

Figure 3.3. Technical characteristic of an actual PV cell

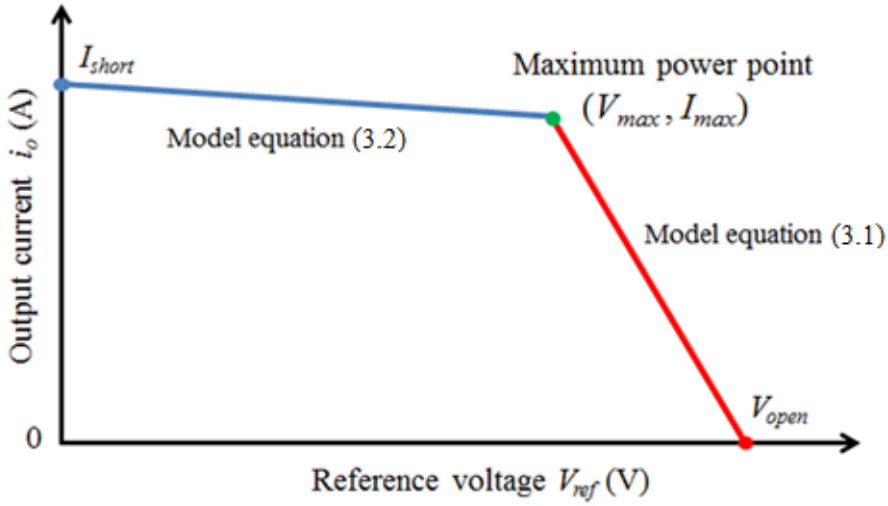

Figure 3.4. Model equation of solar panel technical characteristic

The technical characteristic of the solar panel is determined by two linear model equations (3.1) and (3.2) as follows:

$$V_{ref} = -\frac{V_{open} - V_{max}}{I_{max}} i_o + V_{open} \tag{3.1}$$

$$V_{ref} = -\frac{V_{max}}{I_{short} - I_{max}} i_o + \frac{V_{max} I_{short}}{I_{short} - I_{max}} \tag{3.2}$$

with V_{max} and I_{max} are the maximum power point voltage and the maximum power

point current respectively; V_{open} is the open voltage; I_{short} is the short current; V_{ref} calculated by the linear model equations is the reference voltage to PI controller; i_o is the output current of the PV cell emulating system.

The author uses an example of linear model equations in Figure 3.5 with the parameters as listed in table 3.1.

Table 3.1. Parameter for example of linear model equations

Parameter	Value
Maximum power point voltage V_{max}	85 V
Maximum power point current I_{max}	4 A
Open voltage V_{open}	102 V
Short current I_{short}	4.4 A

3.3. Power converter circuit in the stand-alone mode

The small scale wind turbine charges the battery at the first stage and then the small wind turbine is disconnected from the battery when the battery is fully charged. Thus, the grid-tied PCS is operated by the power converter circuit and the battery.

The topology of power converter circuit in the stand-alone mode is presented in Figure 3.5. In this mode, a bi-directional chopper circuit in boost mode is used as the power converter circuit in order to increase the battery voltage up to the operating voltage of the grid-tied PCS. First of all, the output current i_o flowing into the grid-tied PCS is detected by the current sensor. Secondly, the used model equation is determined to calculate the reference voltage v* by comparing the output current value with the current value of the intersection of the model equations with the help of the comparator. A PI controller is used to reduce the error between the output voltage v_o and the reference voltage v* by varying the duty factor. Finally, the switches of the bi-directional chopper circuit are regulated by the output gate signal. The output filter with the inductor L2 and the capacitor C2 suppresses the ripple at the output terminal while the inrush current flowing

into the capacitor C2 and the internal capacitor of the grid-tied PCS is impeded by the resistor R.

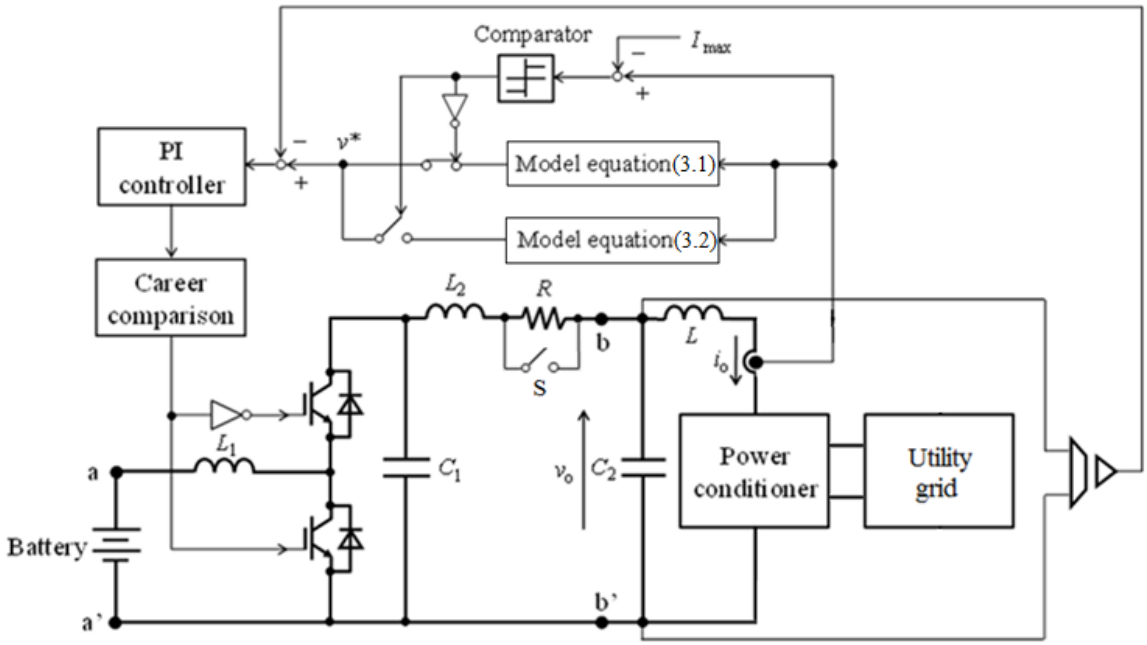

Figure 3.5. Power converter circuit in the stand-alone mode

3.4. Modeling in PSIM program

3.4.1. MPPT control for DC/DC converter

The diagram of the MPPT control system of the PV cell emulating system with a DC/DC converter in boost mode is presented in Figure 3.6. The MPPT algorithm with the Perturb and Observe (P&O) method is used to measure the output current i_0, the output voltage v_0 of the PV cell emulating system and generate the reference voltage V'_{ref} which is similar to the output voltage at the maximum power point.

The proportional-integral (PI) controller compares the output voltage v_0 with the constant reference voltage V'_{ref} and minimizes the voltage error between the reference voltage V'_{ref} and the output voltage v_0. The switches of the DC/DC converter in boost mode are controlled by the output gate signal from the PWM modulator.

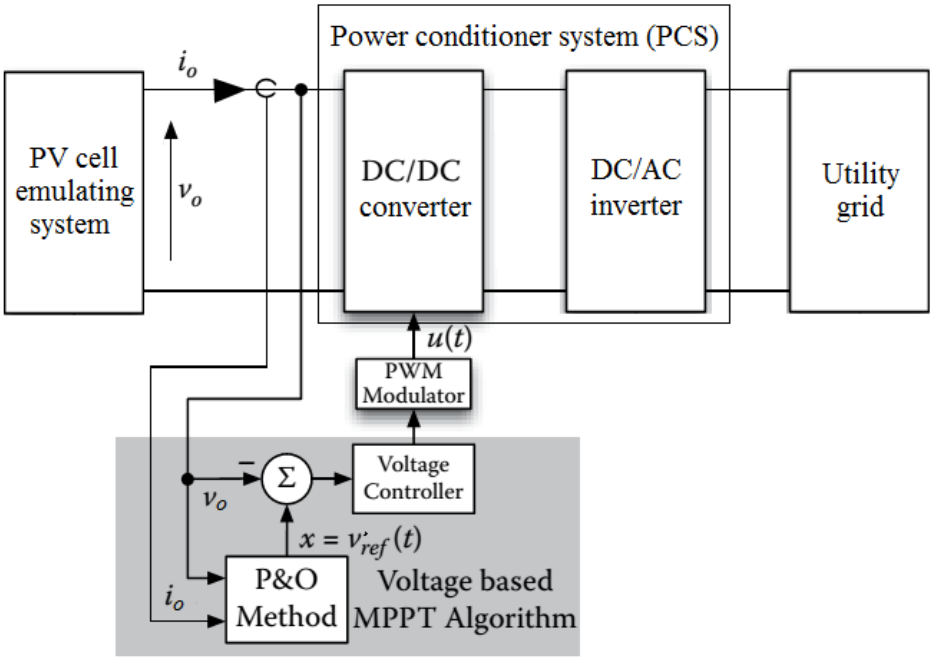

Figure 3.6. Diagram of the MPPT control system

3.4.2. Grid-tied control for DC/AC inverter

The DC/AC inverter supplies the active power from the PV cell emulating system into the utility grid with the support of the grid-tied control system. The output current I_{out} of the DC/AC inverter must be synchronized with the grid voltage v_{grid} and so the switches of the grid-tied DC/AC inverter can be controlled to inject the active power into the utility grid.

The grid-tied control system is composed of the Phase Locked Loop (PLL) method to generate a synchronizing signal which is in phase synchronized with the grid voltage and the hysteresis band method by which the instantaneous output current I_{out} of the DC/AC inverter can follow the reference current as shown in Figure 3.7.

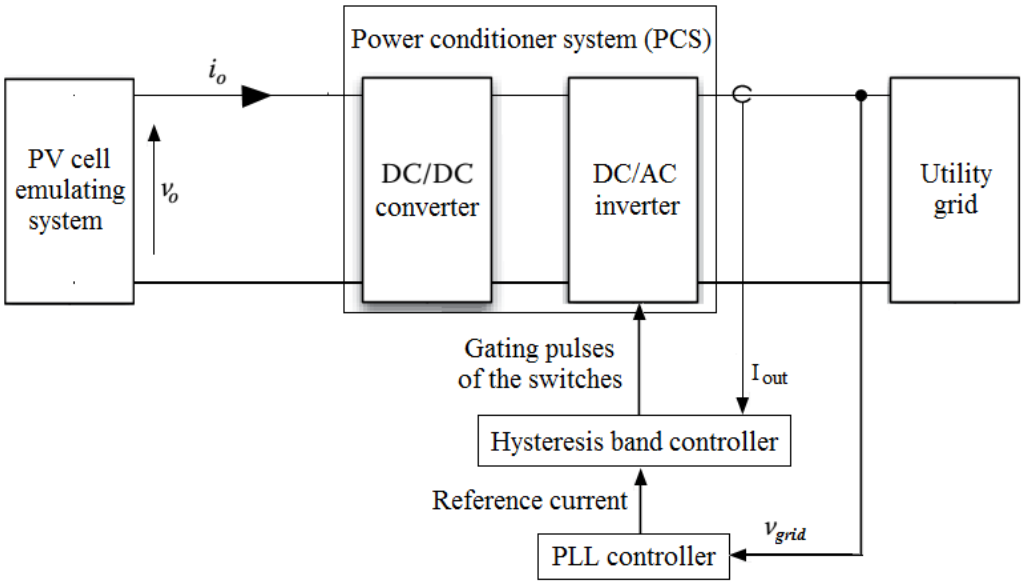

Figure 3.7. Diagram of the grid-tied control system

3.4.3. Simulation result

Figure 3.8 shows the circuit of the grid-tied PV cell emulating system in the stand-alone mode. A DC/AC power inverter is required to convert the DC voltage from the PV cell emulating system into AC voltage. The single phase grid voltage is of 110Vrms (root mean square) and the output voltage of the PV cell emulating system is around 85 V. The DC voltage is increased to around 200V by the DC/DC bi-direction converter in boost mode before inverting the DC voltage to AC voltage of 155Vp (peak voltage) which is equivalent to 110Vrms. The PV cell emulating system is connected to the utility grid by a DC/AC full-bridge inverter with an L-type filter.

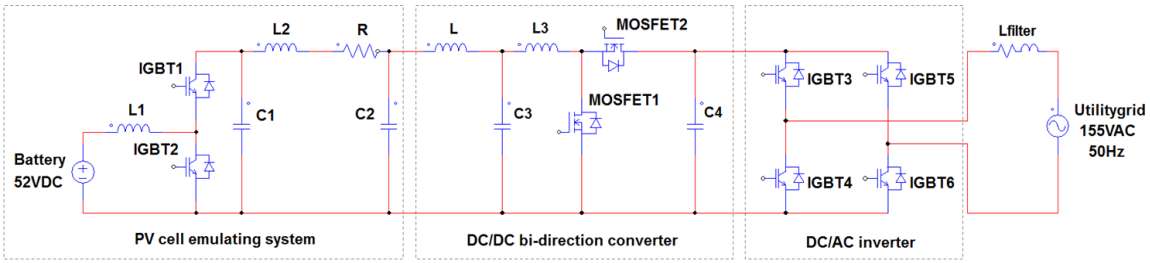

Figure 3.8. Circuit of grid-tied PV cell emulating system in the stand-alone mode

Table 3.2. Parameter of the system

Parameter	Value
Voltage of battery	52 V
Inductor L1, L2	10 mH, 2 mH
Capacitor C1, C2	13.2 µF, 15 µF
Capacitor C3, C4	400 µF, 300 µF
Inductor L, L3	1 mH, 2 mH
Peak grid voltage	155 V
Grid frequency	50 Hz

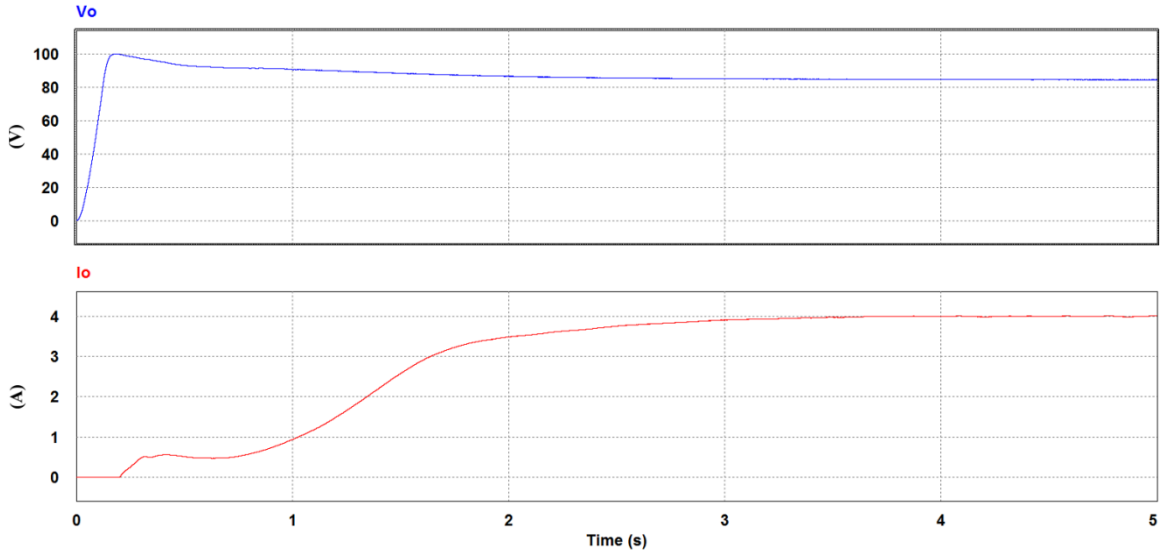

Figure 3.9. Simulation result of output voltage and output current of PV cell emulating system in the stand-alone mode

Figure 3.9 presents the simulation result of the output voltage V_o and the output current I_o of the PV cell emulating system. The internal capacitor of the grid-tied power conditioner is charged in about initial 0.2 seconds and then grid-tied power conditioner performs the MPPT control to obtain the maximum power. The simulation results match with maximum power point characteristics (MPP voltage of 85V, MPP current of 4A) of the linear model equations (3.1) and (3.2). The output power of the PV cell emulating system is illustrated in Figure 3.10 and the output power can reach the maximum power in the

steady-state condition.

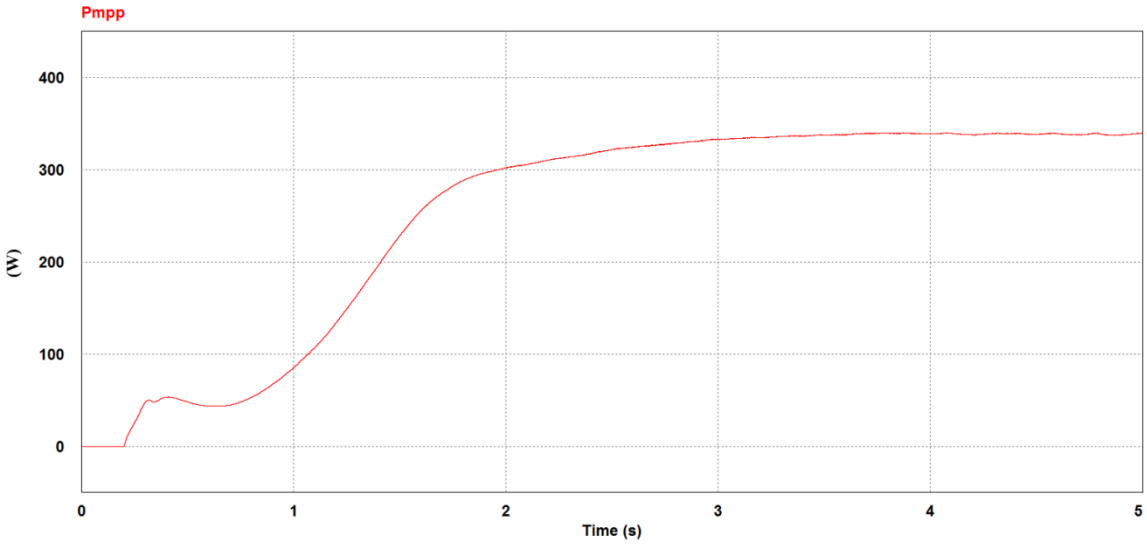

Figure 3.10. Output power of the PV cell emulating system in the stand-alone mode

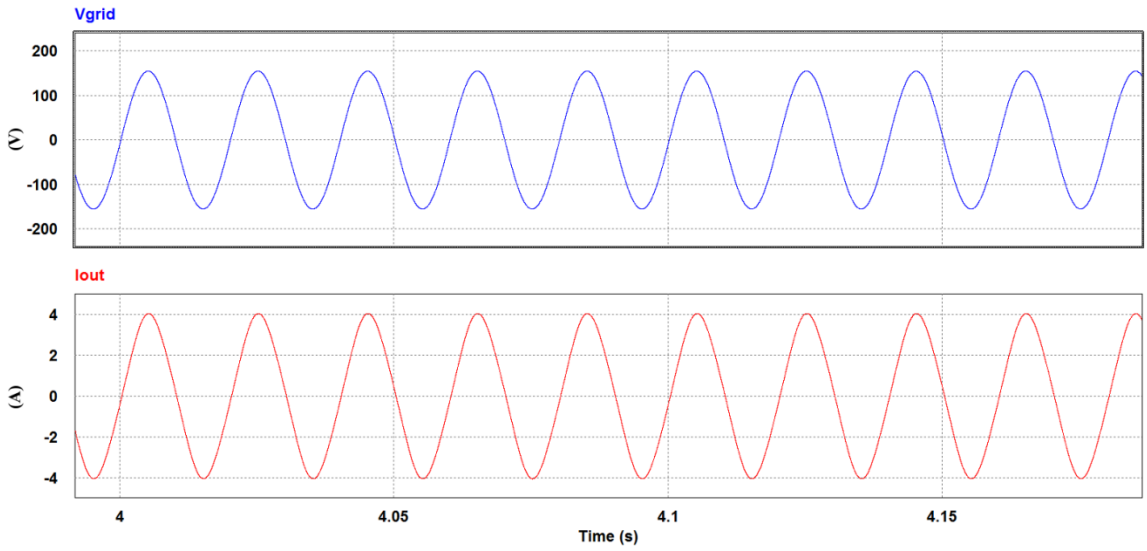

Figure 3.11. AC grid integration result of the PV cell emulating system

Figure 3.11 shows the AC grid integration result of the PV cell emulating system in the stand-alone mode. The output current I_{out} of the DC/AC inverter is sinusoidal and in phase with the grid voltage V_{grid}. Hence, the PV cell emulating system can connect and inject the active power into the utility grid with the support of the grid-tied control method. The total harmonic distortion (THD) of the output current I_{out} of the DC/AC inverter is presented in Figure 3.12 and the THD value of

the output current is small because of depending on the width of a very narrow band in the hysteresis band method.

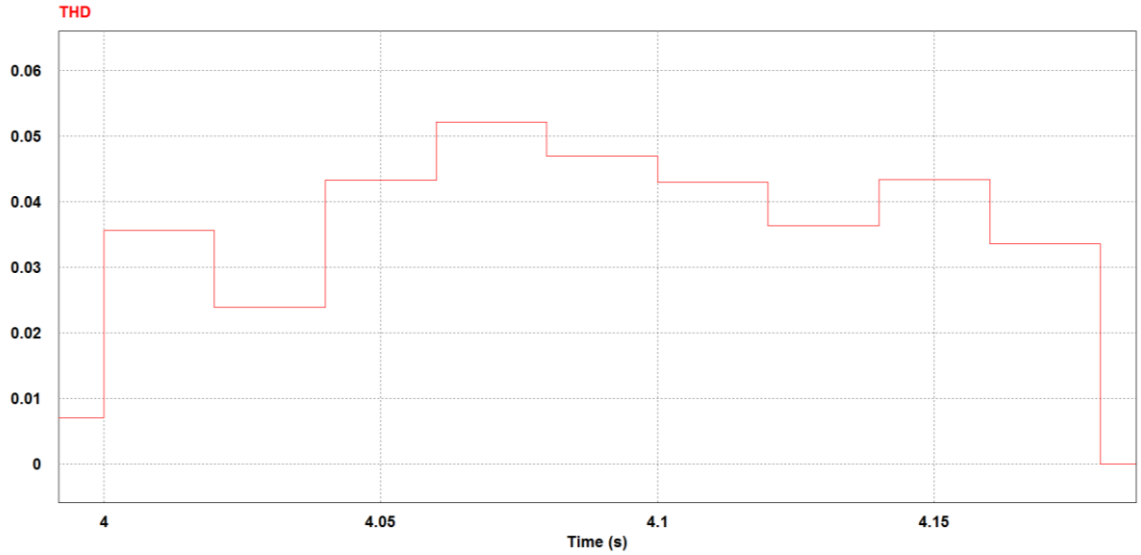

Figure 3.12. THD of the output current of the DC/AC inverter

3.4.4. Experimental test

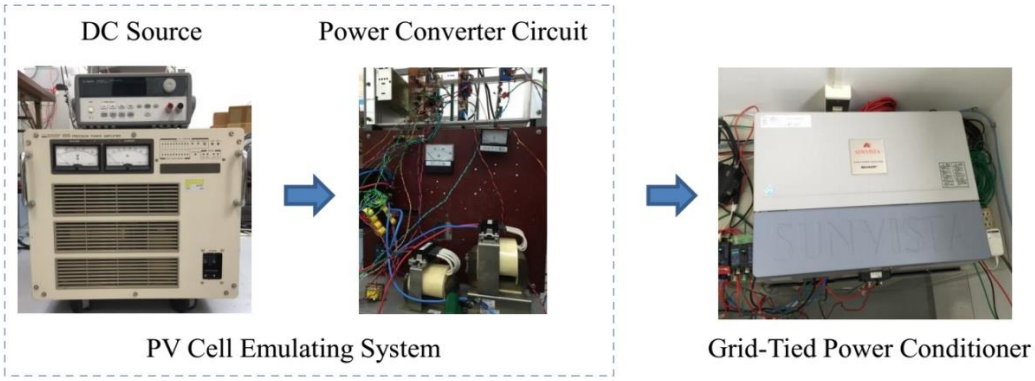

Figure 3.13. Overall of experiment system

The experimental system of the grid-tied PV cell emulating system in the stand-alone mode is displayed in Figure 3.13. The DC source system, including a DC power supply device and a power amplifier device, is used to supply DC voltage of about 52 V. In this study, a boost type bi-directional chopper circuit is made as the power converter circuit and this bi-directional chopper circuit increases the DC source voltage up to operating voltage range from 80V to 320V of the grid-tied power conditioner SUNVISTA JH-S402. The grid-tied PCS

performs the MPPT control and supplies the electrical energy at the output terminals of the DC source system into the utility grid. The Graphtec GL900 8 channel Data Acquisition Data logger is used to measure the output voltage and the output current values of this system.

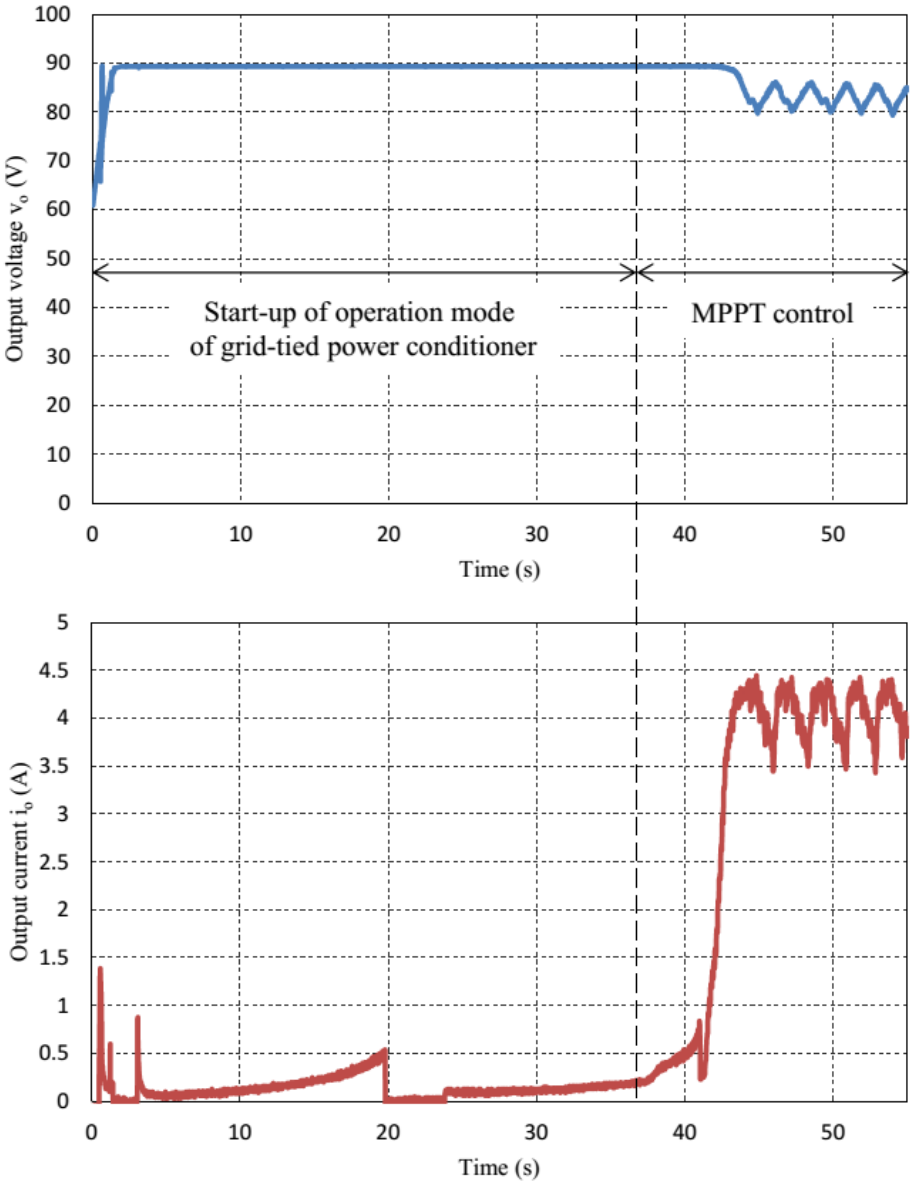

Figure 3.14. Experimental results of the output voltage and the output current of the PV cell emulating system in the stand-alone mode

Figure 3.14 shows the experimental results of output voltage v_0 and output current i_0 of the grid-tied PV cell emulating system in the stand-alone mode. These

results verify that the PV cell emulating system in the stand-alone mode can operate the grid-tied PCS of the solar power by actual test. Firstly, the grid-tied power conditioner charges the internal capacitor in about initial 37 seconds, then it performs the MPPT control to achieve maximum power. The output voltage and output current values of the PV cell emulating system are operated near the maximum power point (MPP voltage of 85V, MPP current of 4A) in the linear model equations (1) and (2) with the parameters in Table 3.1. Thus, the utilization rate of the power conditioner of grid-tied solar power system increases in the case where the solar array cannot receive the sunlight, especially the night time.

3.5. New model of Stand-alone mode using 3 equations

3.5.1. Introduction

The two model equations are connected at the maximum power point in previous study. When operating in the steady state, the maximum power point will continuously permute between 2 reference equations. Therefore, the output current of the PV cell emulating system can strongly fluctuate and it leads to reduce the quality of the output power. We propose a new model with 3 equations including 4 parameters (Figure 3.15) to solve the disadvantage of the old model as the operating point will be moving on a linear equation and not fluctuating around the intersection of linear equations. The parameters of the new model are:

The maximum power point P_{max} (V_{max}, I_{max}),

The open circuit voltage (V_{oc}, 0),

The short circuit current (0, I_{sc})

And a voltage width V_h (which will determine the width of the center equation).

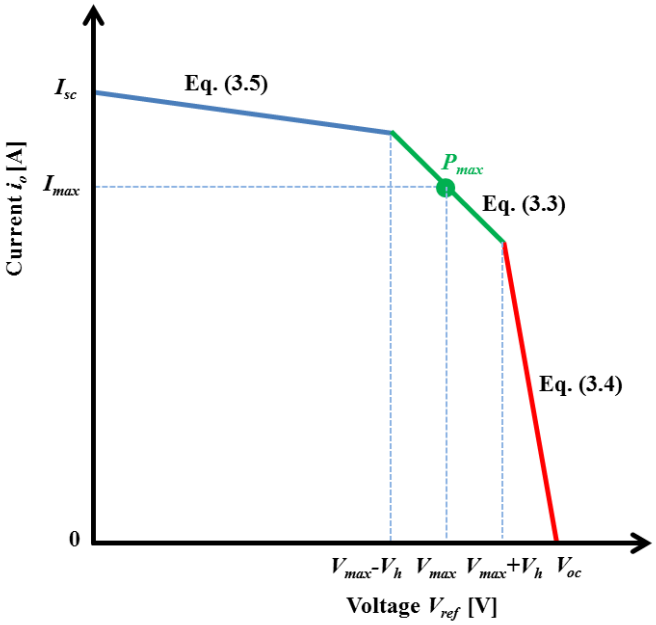

Figure 3.15. 3 model equations of the PV cell technical characteristic

After resolving the system, we have the following equations:

$$V_{ref} = -\frac{V_{\max}^{\ 2}}{P_{\max}} i_o + \frac{V_{\max}^{\ 2}}{P_{\max}} i_{\max} + V_{\max} \tag{3.3}$$

$$V_{ref} = \frac{V_{\max} + V_h - V_{oc}}{-\frac{P_{\max}}{V_{\max}^{\ 2}} V_h + i_{\max}} i_o + V_{oc} \tag{3.4}$$

$$V_{ref} = \frac{V_{\max} - V_h}{\frac{P_{\max}}{V_{\max}^{\ 2}} V_h + i_{\max} - i_{sc}} (i_o - i_{sc}) \tag{3.5}$$

Table 3.3. Parameter of the 3 linear model equations

Parameter	Value
Maximum power point voltage V_{max}	85 V
Maximum power point current I_{max}	4 A
Open voltage V_{oc}	102 V
Short current I_{short}	4.4 A
Voltage width V_h	7 V

In this paper, an example of 3 linear model equations is used in Figure 3.15 with the parameters in Table 3.3.

3.5.2. Power converter circuit

First of all, the small scale wind power generating system is connected to the battery and charges it. When the battery is completely charged, it disconnects from the small scale wind turbine and connects to the power converter which will convert the power suitable for the power conditioner.

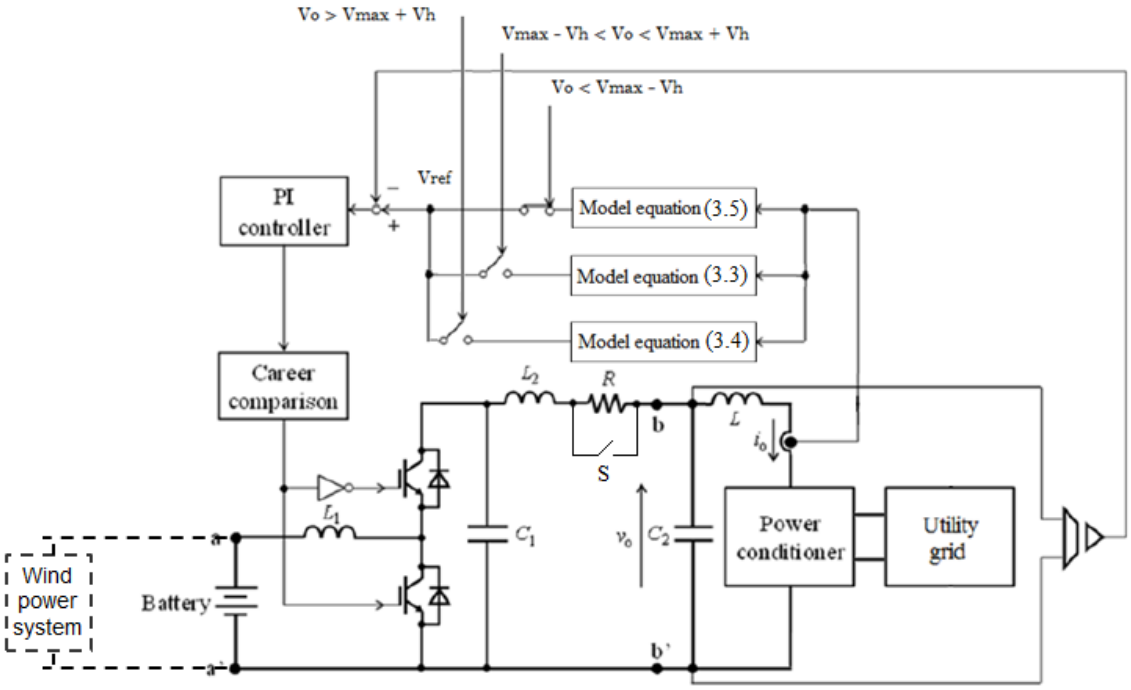

Figure 3.16. New control system with 3 model equations

Figure 3.16 presents the configuration of the power converter circuit in the stand alone mode. A bi-directional chopper circuit is used, as a boost chopper, for increasing the battery voltage to the operating voltage of the power conditioner. The current I_o coming into the power conditioner and the voltage V_o are measured for the control system.

The PV emulator control block determines the used model equation to calculate the voltage reference V_{ref} by comparing the output voltage value with $V_{max\text{-}Vh}$ or V_{max+Vh}. Then, a PI controlled PWM compares the reference voltage with the output voltage V_o for determining the duty factor. The power is then

converted by the two switches and smoothed by the inductor L2 and the capacitor C2.

3.5.3. Study result

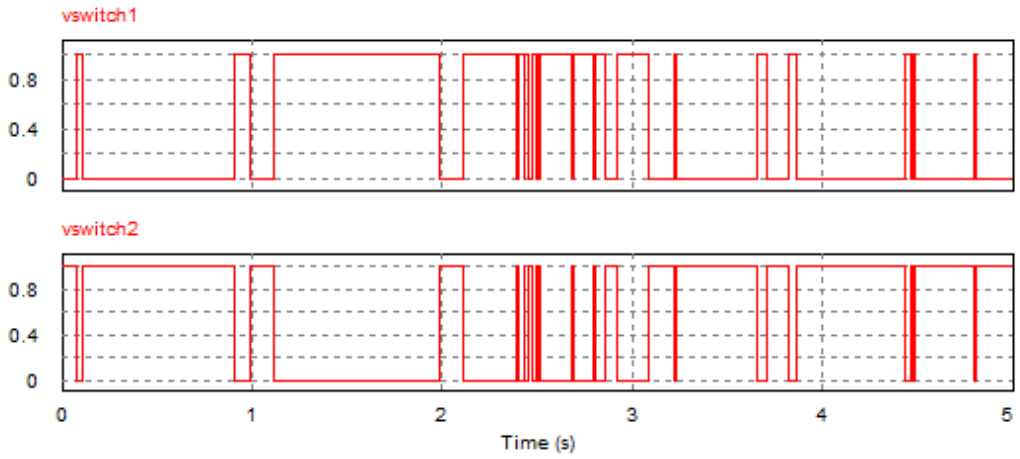

Figure 3.17. State switches of old 2 model equations

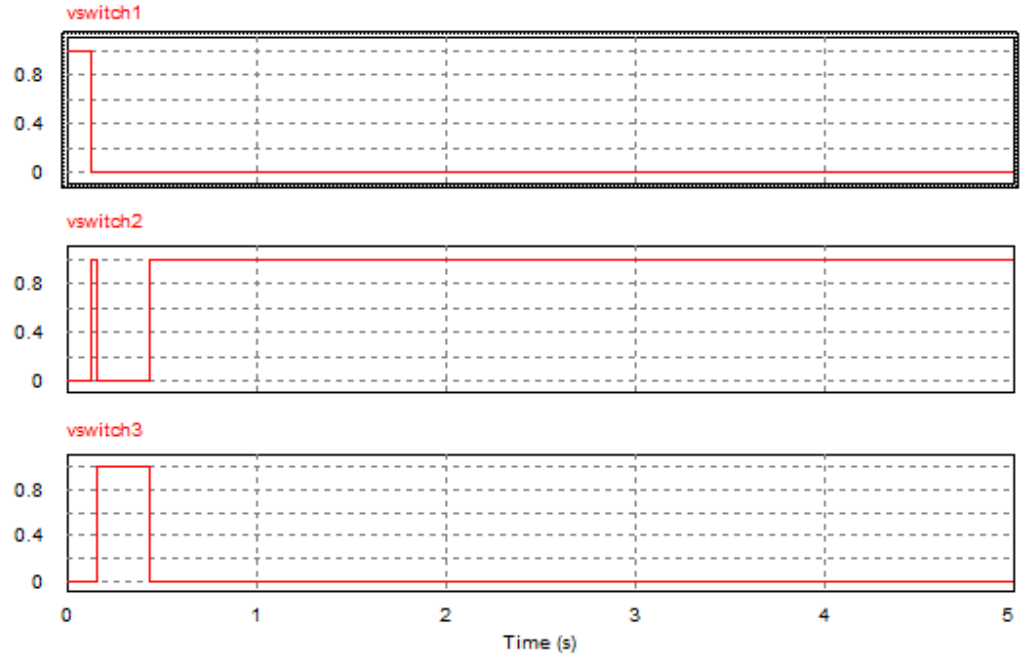

Figure 3.18. State switches of new 3 model equations

In the old topology, the two switches of the power converter circuit were permuting continuously in Figure 3.17 but we can see with the new model, the state of the switches are more stable as can be seen in Figure 3.18.

To validate this new model, we need to compare the value of the output characteristics of the PV cell emulating system in both configurations.

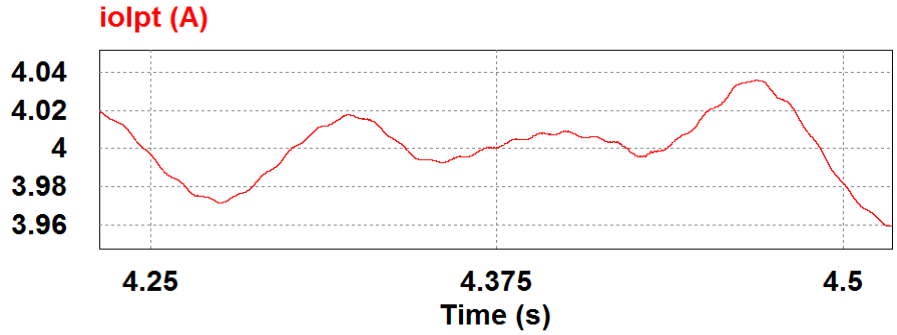

Figure 3.19. Fluctuations of the output current for the old 2 model equations

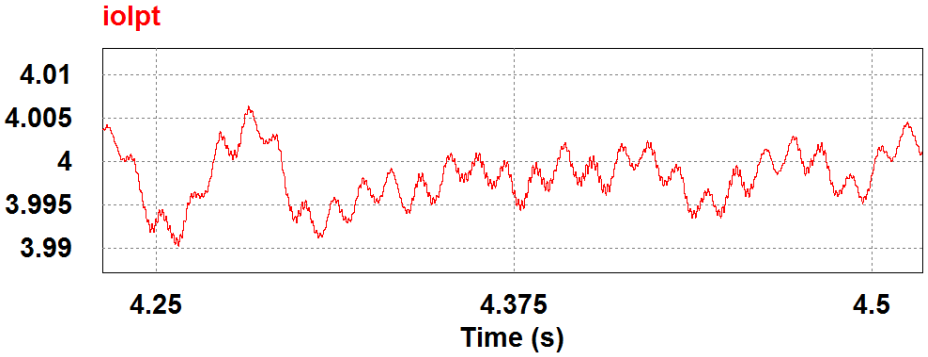

Figure 3.20. Fluctuations of the output current for the new 3 model equations

Figure 3.19 and Figure 3.20 show that the value of the current of the new model equation is more stable than the value of the old model equation. Through the calculation of the different gap, we find that there is a fluctuation of the output current of about 7.5%I_{max} for the old model equation and only 1.5%I_{max} for the new model equation. That's mean the new model is about 5 times more steady than the old one.

Hence, the quality of the output power is increased by using the new model equations and the PV cell emulating system also can connect to the PCS.

3.6. Conclusion

This chapter presented the configuration and operation of the grid-tied PV cell emulating system in the stand-alone mode using 2 and 3 linear model equations. The research results confirmed that the utilization rate of the PCS of grid-tied solar

power system was improved in the case where the solar array did not receive the sunlight, especially the night time.

Chapter 4

PV Cell Cooperating System in Series Connection Mode

4.1. Configuration of PV cell cooperating system

Figure 4.1 presents the configuration of the grid-tied PV cell cooperating system in series connection mode which comprised of the small scale wind turbine, a battery and the power converter circuit. In this mode, the small scale wind turbine is able to connect with the solar panel in series with the help of the battery and the power converter circuit. The PCS is used to convert DC power to AC power with maximum power point tracking (MPPT) technique and generate the power to the utility grid by the boost type DC/DC converter and the grid-tied DC/AC inverter.

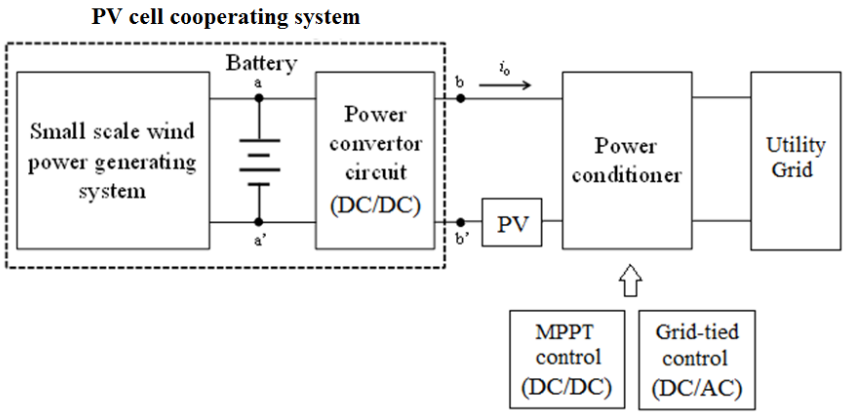

Figure 4.1. Configuration of PV cell cooperating system in series connection mode

First of all, the battery is fully charged by the small scale wind turbine and then disconnected from the small scale wind turbine. In the next step, the current flowing into the PCS is detected by the power converter circuit.

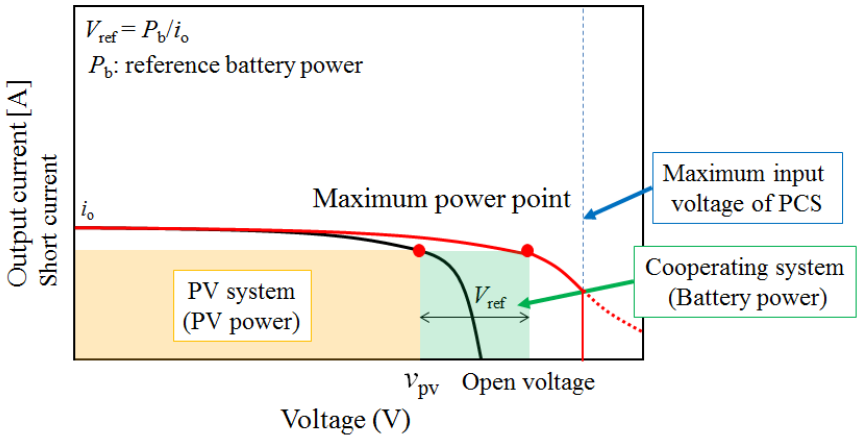

Figure 4.2. I-V characteristic in series connection mode

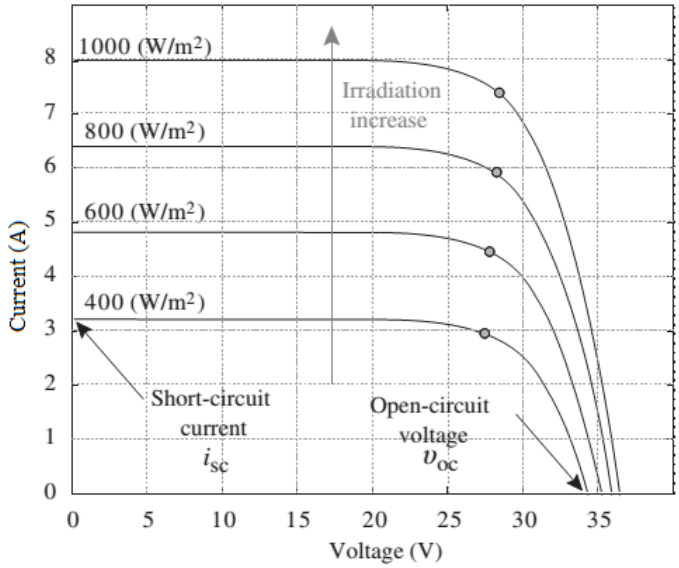

Figure 4.3. I - V curve of PV under the various levers of solar irradiation [11]

Figure 4.2 shows the current - voltage characteristic in the series connection mode of the solar panel and the PV cell cooperating system. The output current value of the cooperating system matches the maximum power point current value of the solar panel in this mode since the solar panel connects with the PV cell cooperating system in series. Thus, the input power of the PCS can be controlled to

become the maximum power. Moreover, the input voltage and the input power of the PCS are enhanced to correspond the total of output voltages and the output powers of the PV cell emulating system and the solar panel, respectively.

When solar irradiation is changed, the output voltage v_{pv} of PV array varies slightly for different levels of solar irradiation, as it can be seen in Figure 4.3. In contrast, the output current i_o of the PV array is very linearly dependent on the solar irradiation. Thus, the reference voltage value V_{ref} in Figure 4.4 is adjusted in accordance with the changing values of the PV array output current i_o and the constant value of the reference battery output power P_b.

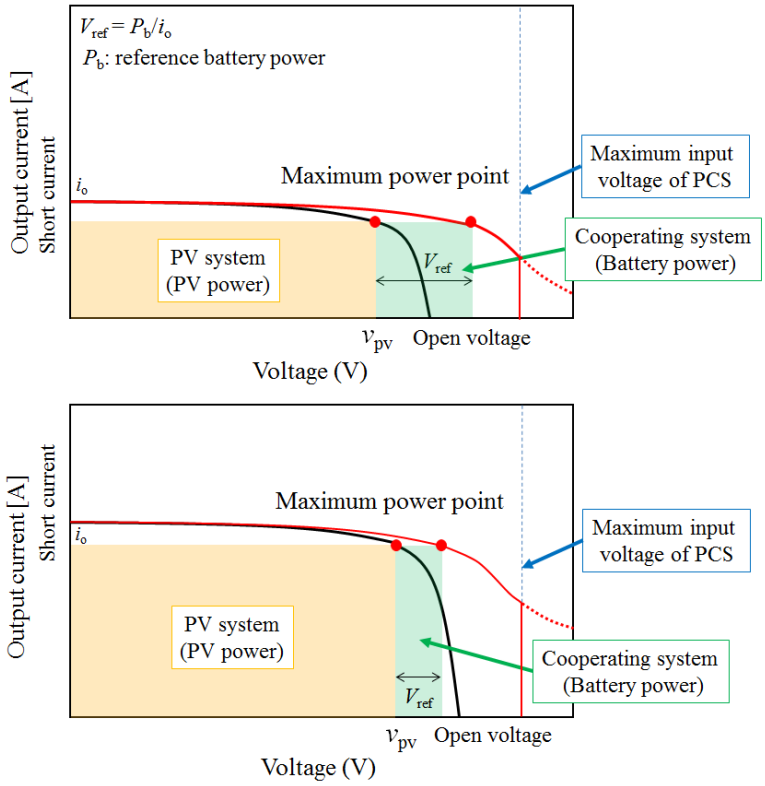

Figure 4.4. I - V characteristic in series connection mode under different levels of solar irradiation

4.2. Control method of the system

4.2.1. Control system of the PV cell cooperating system

Figure 4.5 describes the control method of the PV cell cooperating system in series

connection mode. In this research, the bi-directional chopper circuit is used as the power converter circuit to decrease the battery voltage because the input voltage value of the PCS is limited and the total of the output voltages of the PV array and the power converter circuit supplied to the input terminal of the PCS can not exceed the rated voltage of the PCS. The input filter with the inductor L1 and the capacitor C1 suppresses the ripple at the input terminal. The control system structure of the PV cell emulating system comprises a voltage control loop and a current control loop. In the first stage, the reference voltage value V_{ref} is calculated as follows:

$$V_{ref} = \frac{P_b}{i_0} \tag{4.1}$$

where, P_b is reference battery output power and i_o is the output current of the solar array.

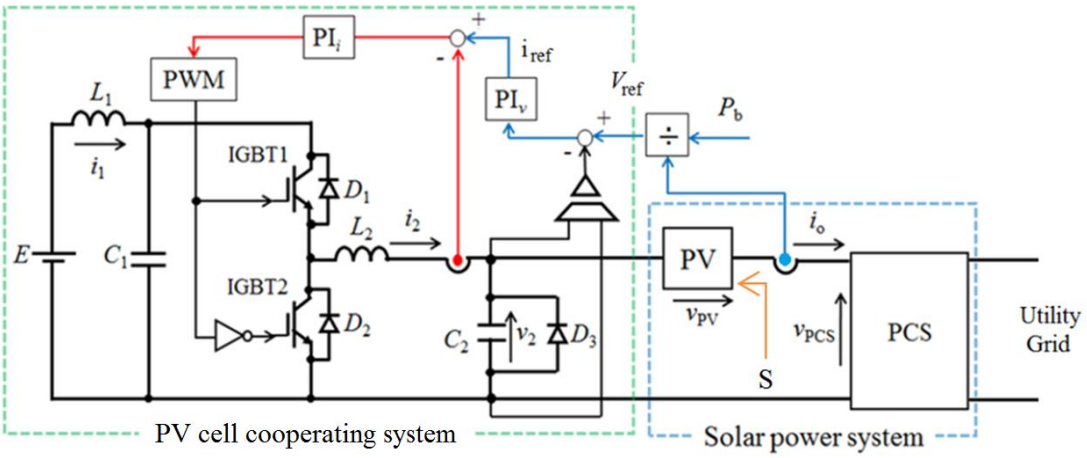

Figure 4.5. Power converter circuit with control design

After that, the PV cell cooperating system output voltage v_2 is regulated to match the reference voltage value V_{ref} by the voltage control loop. The cooperating system output current i_2 is controlled to be the similar value with the output current i_o of the PV array by the current control loop because they are connected in series as shown in Equation (4.2).

$$i_0 = i_2 \tag{4.2}$$

where, i_0 is the MPP output current of the solar array and i_2 is the output current of the PV cell emulating system.

In the real operation condition, the output current value i_o of the PV array and the output current value i_2 of the PV cell cooperating system are dependent on the changing of the solar irradiation value S. Finally, the switches of the bi-directional chopper circuit are regulated by the output gate signal from Pulse Width Modulation (PWM) system.

4.2.2. MPPT control system

In the function of the PCS, the maximum power point tracking (MPPT) as illustrated in Figure 4.6 is performed by the boost type DC/DC converter. The Perturb and Observe (P&O) method is used as the MPPT algorithm in this study to generate the reference voltage V'_{ref} because the implementation is simple and it is widely utilized in the actual PCS equipments. The P&O method perturbs the voltage at the operating point and then observes the increasing power of the system to determine the direction of the next perturbation. By which, the operating point is moved to the maximum power point and oscillates around it in the steady state.

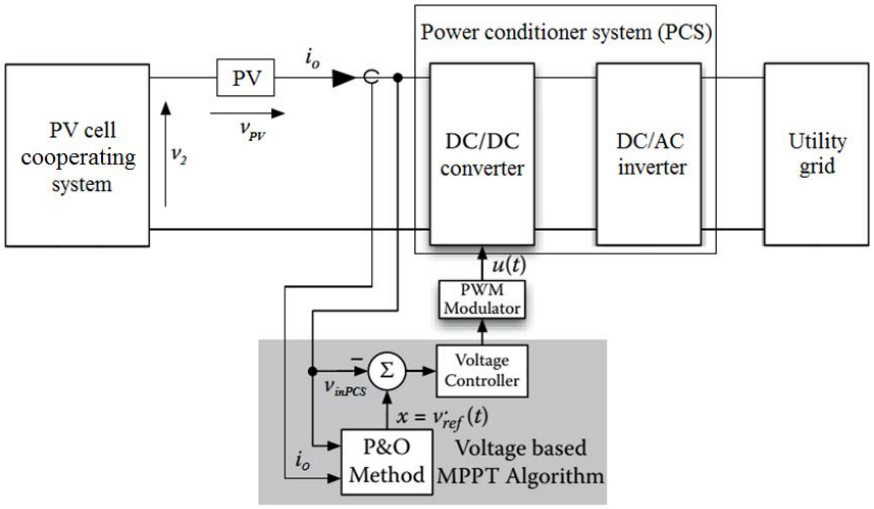

Figure 4.6. Diagram of the MPPT control system

The proportional-integral (PI) controller compares the input voltage v_{inPCS} of the PCS with the constant reference voltage V'_{ref} and minimizes the voltage error between the reference voltage V'_{ref} and the input voltage v_{inPCS}. The switches of the DC/DC converter in boost mode are controlled by the output gate signal from the PWM modulator.

The input voltage v_{inPCS} of the PCS is considered to be similar with the reference voltage V'_{ref} which corresponds to the voltage at the maximum power point and can be computed by the equation as below:

$$v_{inPCS} = v_2 + v_{PV} \tag{4.3}$$

where, v_2 is the output voltage of the PV cell cooperating system and v_{PV} is the output voltage of the PV array.

4.2.3. Grid-tied control system

The output current I_{out} of the DC/AC inverter in Figure 4.7 can be synchronized with the grid voltage v_{grid} to supply the active power into the utility grid by the support of the Phase Locked Loop (PLL) method and the hysteresis band method in the grid-tied control system of the DC/AC inverter.

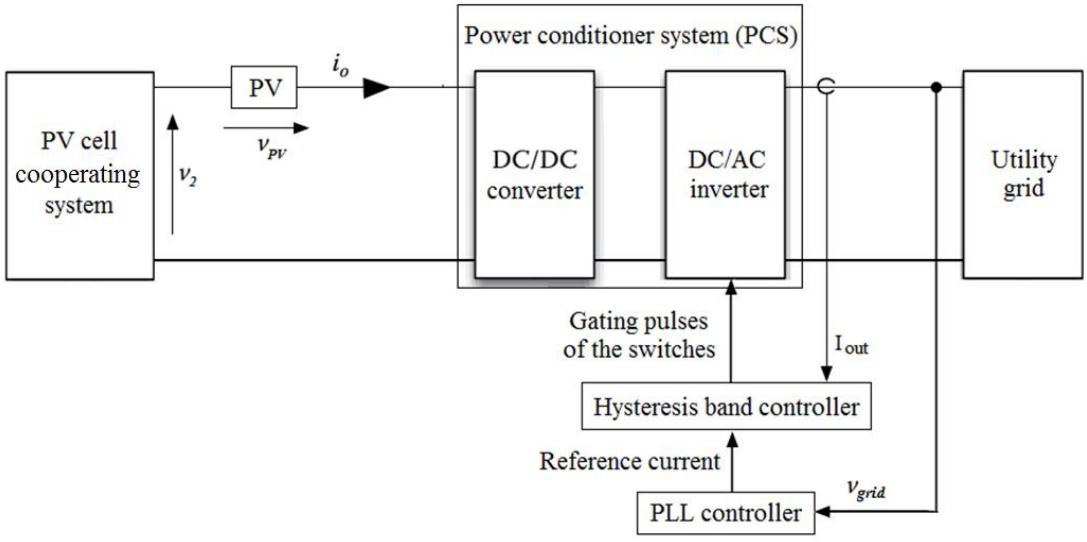

Figure 4.7. Diagram of the grid-tied control system

4.3. Simulation results

The control method of the grid-tied PV cell cooperating system in series connection mode is confirmed by using PSIM electronic circuit simulation software with the simulation circuit structure as shown in Figure 4.8 and the system parameters for the simulation are listed in Table 4.1.

Table 4.1. Parameter of the system

Power of solar array in solar radiation of 600 W/m^2	490 W
Power of battery	50 W
Inductor L1, L2	5 mH, 20 mH
Capacitor C1, C2	13.2 µF, 15 µF
Capacitor C3, C4	500 µF, 300 µF
Inductor L3	2 mH
RMS grid voltage	230 V
Grid frequency	50 Hz

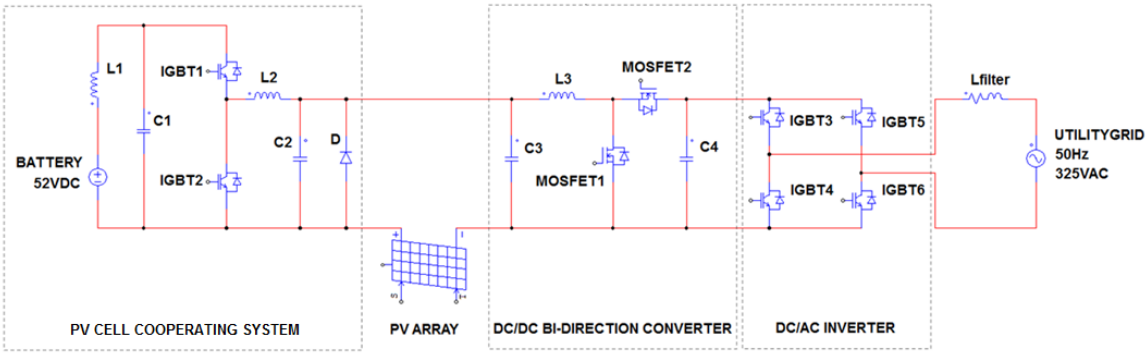

Figure. 4.8. Simulation circuit in PSIM program

Figure 4.9 illustrates the simulation results of the output current i_2 and the output voltage v_2 of the PV cell cooperating system in series connection mode. These results describe three operation modes of the PV cell emulating system.

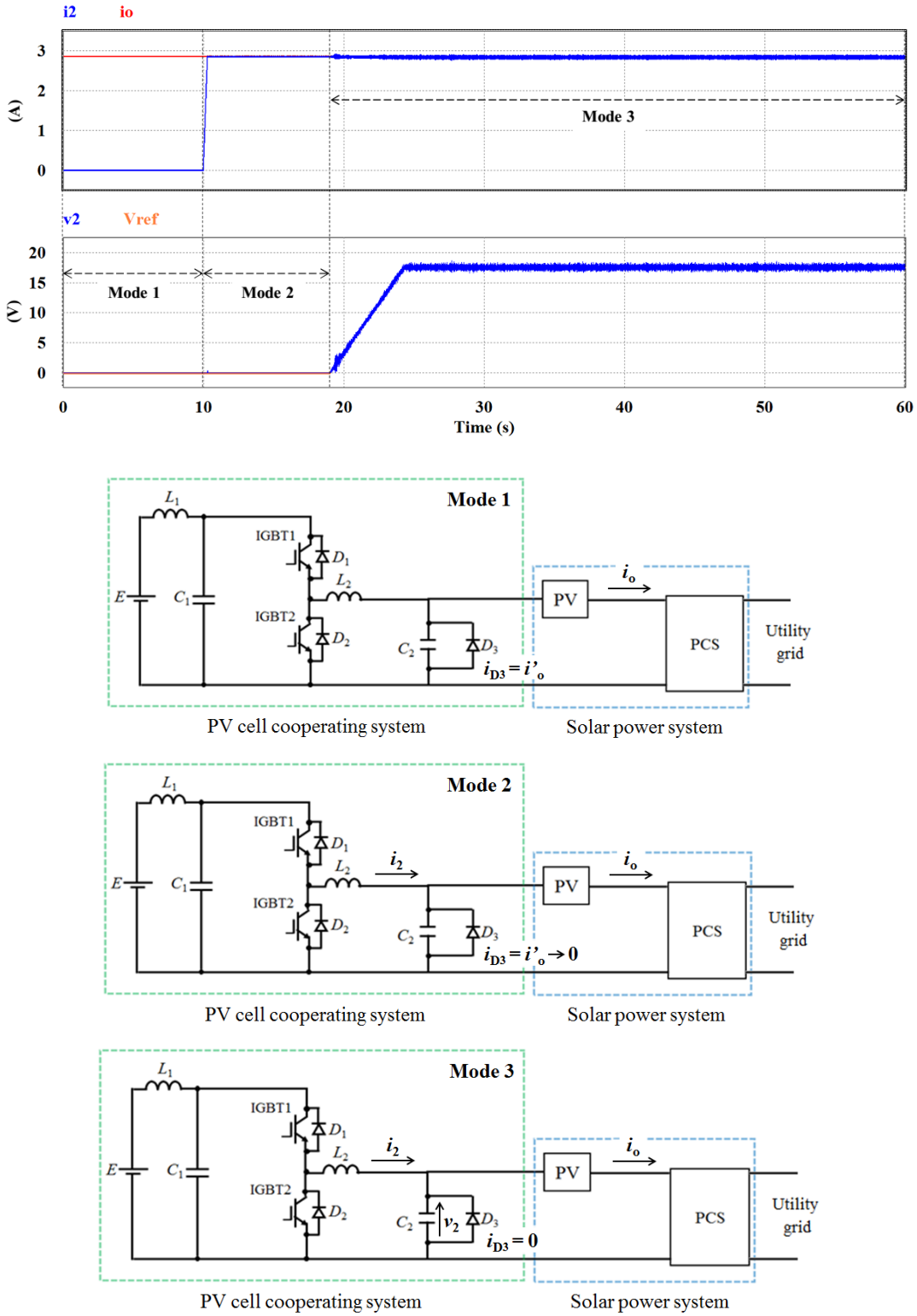

Figure 4.9. Operation modes of the PV cell cooperating system

In the operation mode 1, only the PV array generates the output current i_o and operates the grid-tied PCS which also performs the MPPT control. The PV cell

cooperating system does not work in this mode and the value of the current i_{D3} which flows to diode D3 equals the value of the output current i_o of the solar array.

In the operation mode 2, the value of the diode D3 current i_{D3} is controlled to reduce to zero while the PV cell cooperating system generates output current i_2 and starts to connect to PV array in series. The output current i_2 of the PV cell emulating system is regulated to match the PV array output current i_o in this mode.

In the operation mode 3, when the value of the diode D3 current i_{D3} becomes to be zero, the output voltage v_2 of the PV cell emulating system is controlled to follow the reference voltage value V_{ref} which is achieved by dividing the reference battery output power P_b by the output current i_o of the solar array. Hence, the PV cell cooperating system can connect to the PV array in series in the steady state and both the output power of the PV cell cooperating system and the output power of the PV array can be supplied to the grid-tied power conditioner.

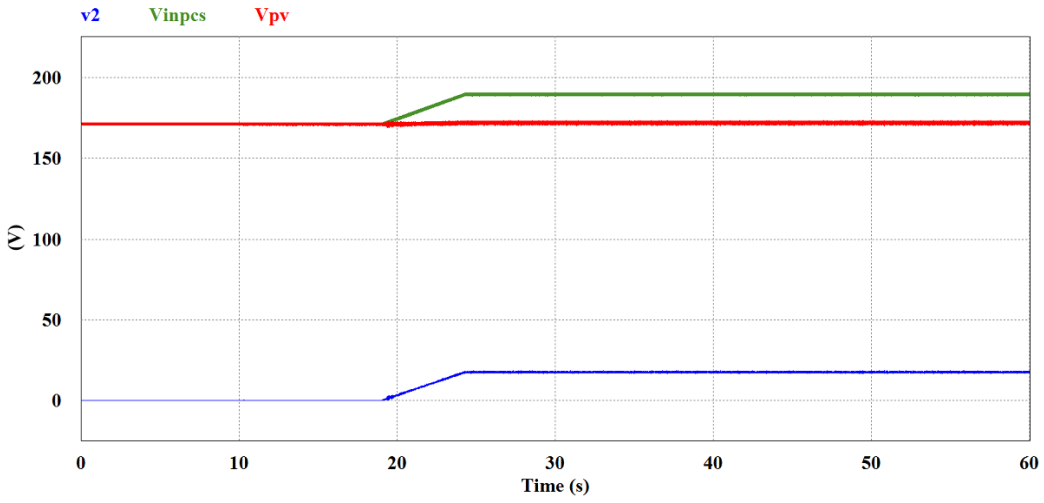

Figure 4.10. Input voltage of the PCS

Figure 4.10 and Figure 4.11 present the simulation results of the input voltage V_{inpcs} and the input power P_{inpcs} of the PCS. The results show that the input voltage V_{inpcs} of the PCS equals output voltage sum of the PV cell emulating system (v_2) and PV array (v_{pv}) after the PV cell cooperating system connects to solar panel in series mode from approximately 19th second. As a result, it causes the increasing of

the input power P_{inpcs} of the PCS.

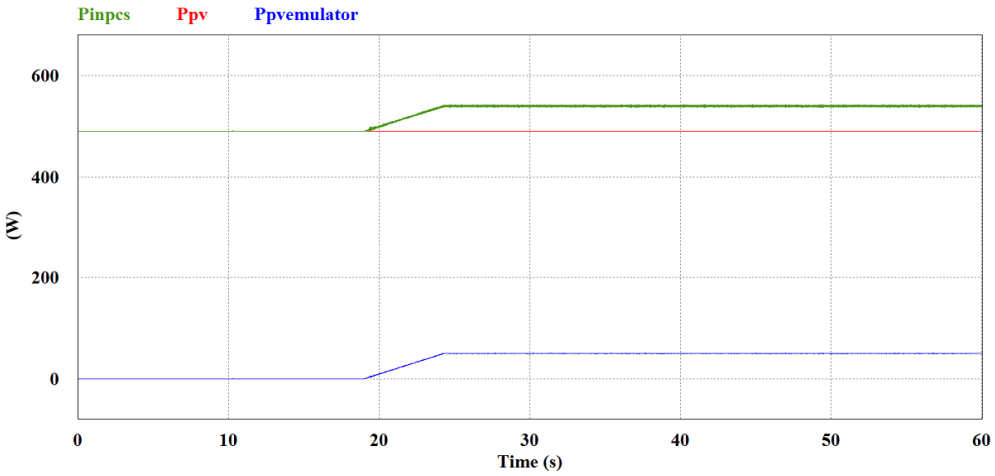

Figure 4.11. Input power of the PCS

4.4. Experimental results

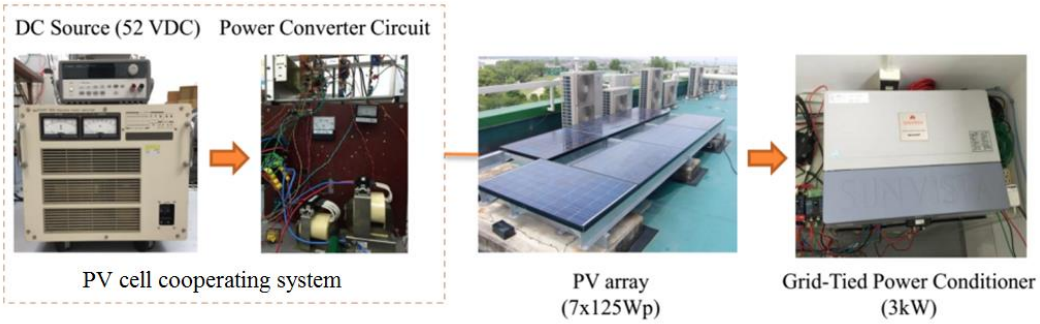

Figure 4.12. Configuration of experimental system

The experimental system of the grid-tied PV cell cooperating system in series connection mode is shown in Figure 4.12. Firstly, only the PV array including 7 solar panels 125Wp operates the grid-tied power conditioner SUNVISTA JH-S402 when receiving the sunlight. In the next stage, the PV cell emulating system, including DC source system and Power converter circuit, is regulated to connect to the solar array in series mode. The DC source system which comprises a DC power supply device and a power amplifier device is used to generate DC voltage of about 52 V and DC power of 50 W. A bi-directional chopper circuit is made as

the power converter circuit to decrease the DC source voltage into the appropriate value under the changed solar irradiation condition. The grid-tied power conditioner SUNVISTA JH-S402 performs the MPPT control and injects the power from the PV cell emulating system and the PV array into the utility grid. The Graphtec GL900-8 channel Data Acquisition Data logger measures the output voltage values and output current values of this system.

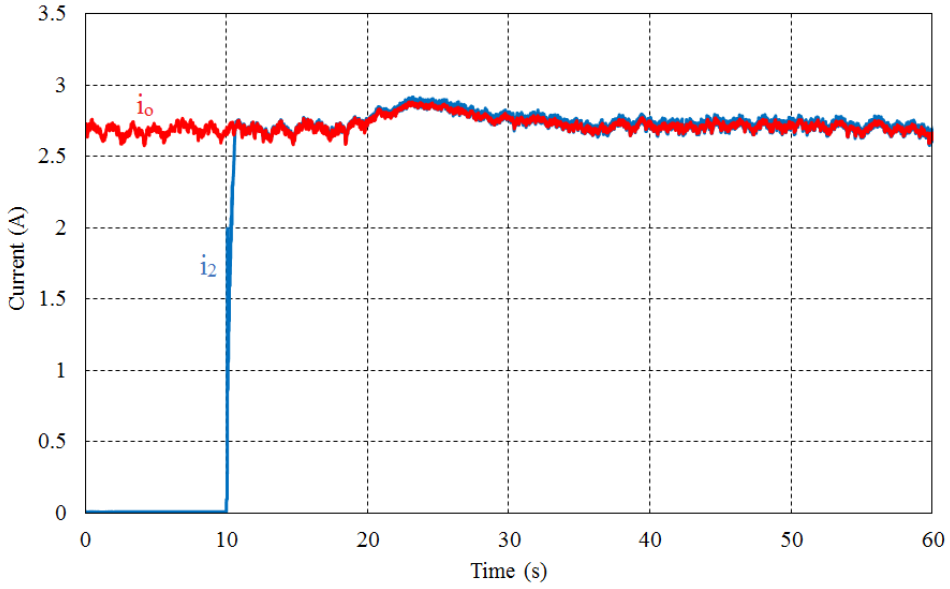

Figure 4.13. Output current of the PV cell cooperating system

Firstly, the grid-tied PV cell cooperating system in series connection mode is tested under stable solar irradiation condition. It can be seen in Figure 4.13, the output current i_2 of the PV cell emulating system is controlled to follow PV array output current i_o by the current control loop and the PV cell cooperating system starts to connect with the PV array in series after the PV array generates the output current i_o in the initial 10 seconds.

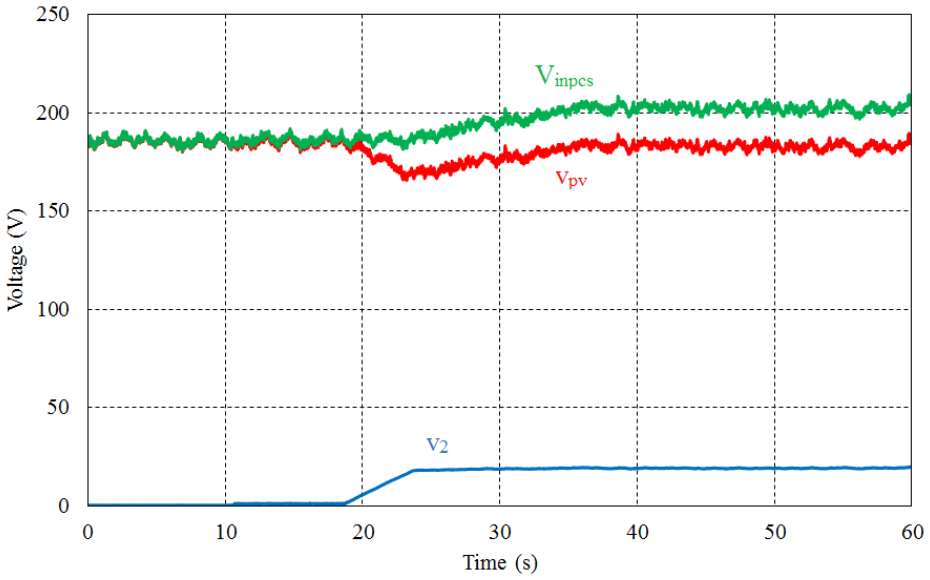

Figure 4.14. Input voltage of the PCS

As a result of the experimental test in Figure 4.14, after the PV cell cooperating system connects completely with the PV array in series from about 19th second, the voltage control loop regulates the output voltage v_2 of the PV cell cooperating system to match the reference voltage value V_{ref} which is obtained by dividing the reference battery output power P_b by the output current i_o of the PV array.

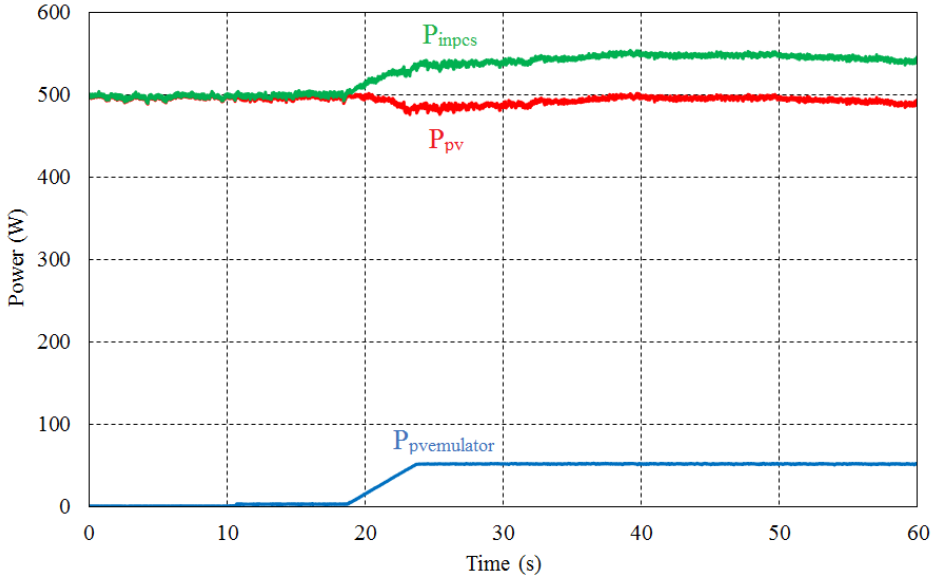

Figure 4.15. Input power of the PCS

It is clearly seen in Figure 4.15 that the input power P_{inpcs} of the PCS is increased because the input voltage V_{inpcs} of the PCS as shown in Figure 4.14 always equals output voltage sum of the PV cell cooperating system (v_2) and PV array (v_{pv}) when the PV cell cooperating system operates in the steady state. Thus, these results in accordance with proposed idea and the simulation results. Additionally, the results also display that the PV cell cooperating system does not affect the operation of PV array under stable solar irradiation condition when both systems work in the series connection mode in the steady state.

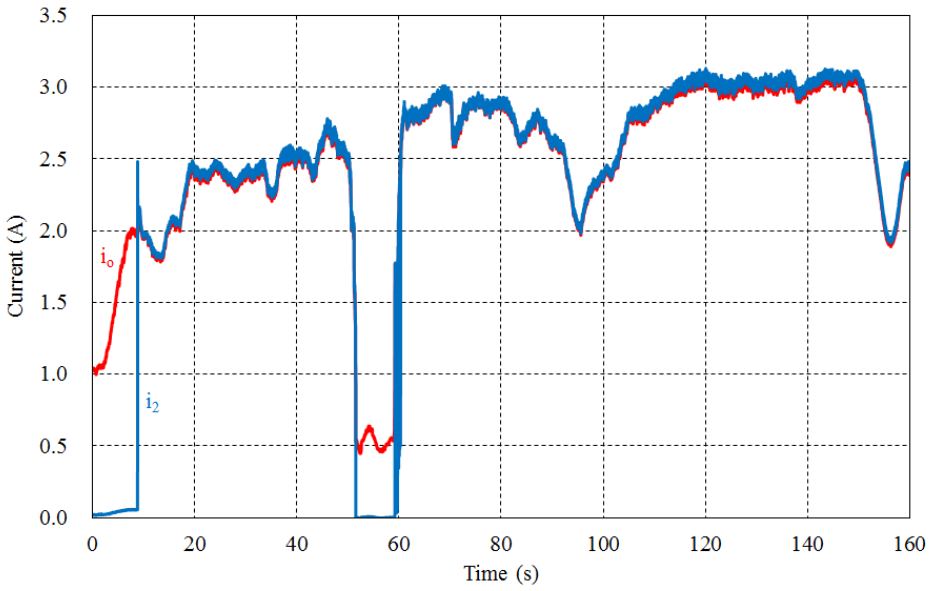

Figure 4.16. Output current of the PV cell cooperating system under changed solar irradiation condition

In the next experimental test of the grid-tied PV cell cooperating system in series connection mode under changed solar irradiation condition, the output current i_2 of the PV cell cooperating system in Figure 4.16 is controlled to match the PV array output current i_o by the current control loop after the PV array generates the output current in about initial 9 seconds. The electricity is supplied from the PV cell cooperating system under the changing of the solar irradiation up to about 52^{th} second. When the solar irradiation value becomes very low at the point of about 52^{th} second and the value of the PV array output current i_o is less than 1 (A), the operation of the PV cell cooperating system is stopped because the

duty ratio of the PV cell cooperating system is controlled to become zero. After about 7 seconds, the output current i_2 of the PV cell cooperating system continues to follow the PV array output current i_o when the solar irradiation increases again.

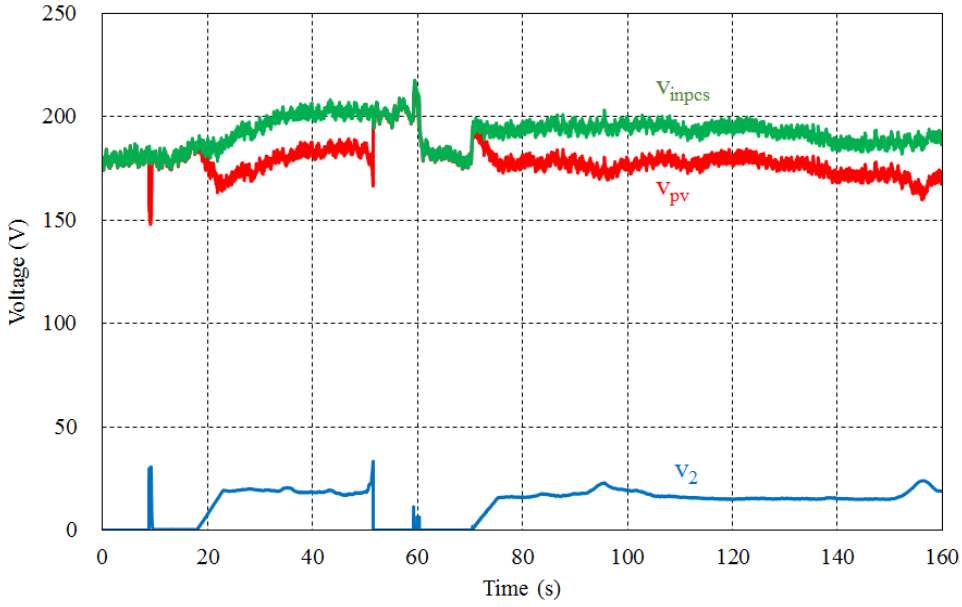

Figure 4.17. Input voltage of PCS under changed solar irradiation

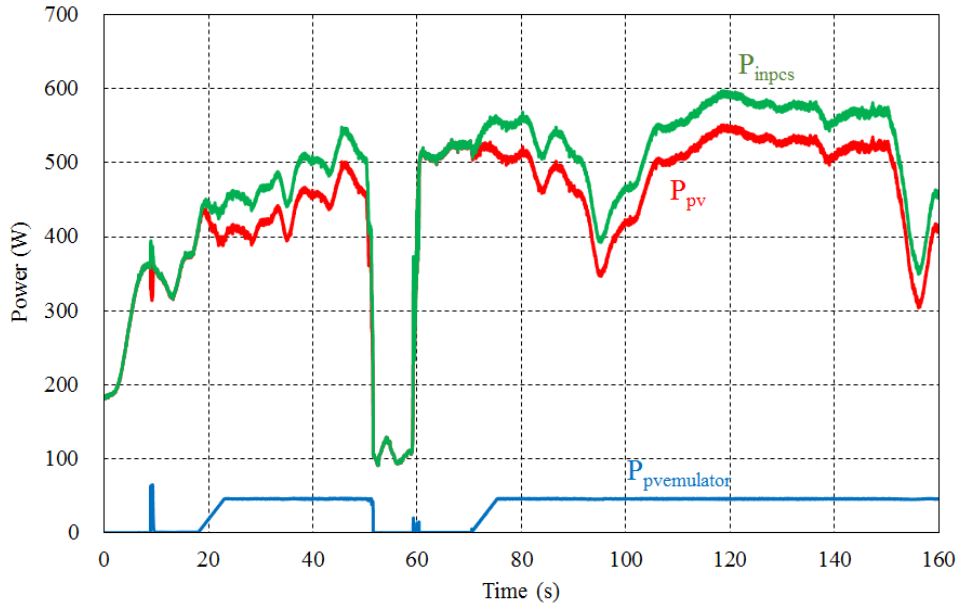

Figure 4.18. Input power of PCS under changed solar irradiation condition

The input voltage V_{inpcs} of the power conditioner in Figure 4.17 always equals output voltage sum of the PV cell cooperating system (v_2) and PV array (v_{pv}) with

the help of the voltage control loop after the PV cell emulating system is connected successfully to the PV array in series mode. By which, the PV cell cooperating system can generate the power of 50 W and the input power P_{inpcs} of the power conditioner as can be seen in Figure 4.18 is enhanced according to the changing of the solar irradiation except in the time from about 52^{th} second to about 59^{th} second because the PV cell cooperating system cannot work in this time period.

4.5. Conclusion

In this chapter, the study results verified that the utilization rate of the grid-tied PCS was enhanced because the PV cell cooperating system in series connection mode could run the grid-tied PCS of the solar power system in the daytime. Moreover, the results also indicated that the operation of the PV array in practice was not influenced by the PV cell cooperating system in series connection mode in the steady state.

However, when the solar irradiation value becomes very weak, the operation of the PV cell cooperating system was stopped because the duty ratio of the PV cell cooperating system was controlled to become zero.

Chapter 5

PV Cell Cooperating System in Parallel Connection Mode

5.1. Introduction

The installation of the solar power system develops very quickly all over the world, but solar power generation is dependent on sunlight to effectively collect energy from the sun. Thus, it decreases the utilization rate of the PCS in the grid-tied solar power system. The hybrid power system using the small wind turbine and solar array can increase the utilization rate of the power conditioner since the small scale wind power generating system can generate the power during the day and night time. However, the PCS of the solar power system cannot control optimally the small wind turbine because the output characteristics of the wind turbine and the solar array are different. We designed the novel method in the previous study in Chapter 4 to connect the small scale wind power generating system with the PCS of the grid-tied solar power system. So, the utilization rate of the PCS can increase by using the PV cell cooperating system in series connection mode. However, this enhanced operating efficiency of the PCS is not good in changing solar irradiation condition because the maximum input voltage of the PCS is restricted and the voltage of the PV alters slightly as can be seen in Figure 5.1.

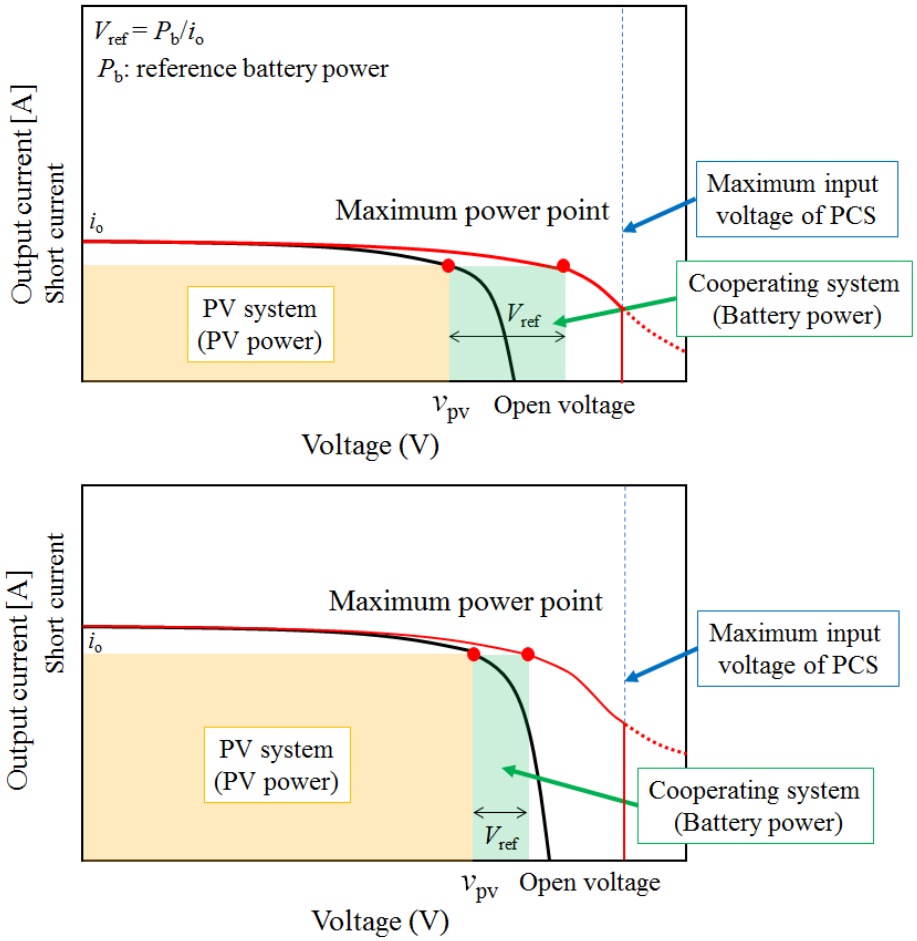

Figure 5.1. I - V characteristic in series connection mode in cloudy and rainy days

Therefore, we design a novel technical method of the PV cell cooperating system in Figure 5.2 which is connected in parallel with the solar panel to increase the operating efficiency of the PCS regardless the restricted maximum input voltage value of the PCS, especially in the bad weather days.

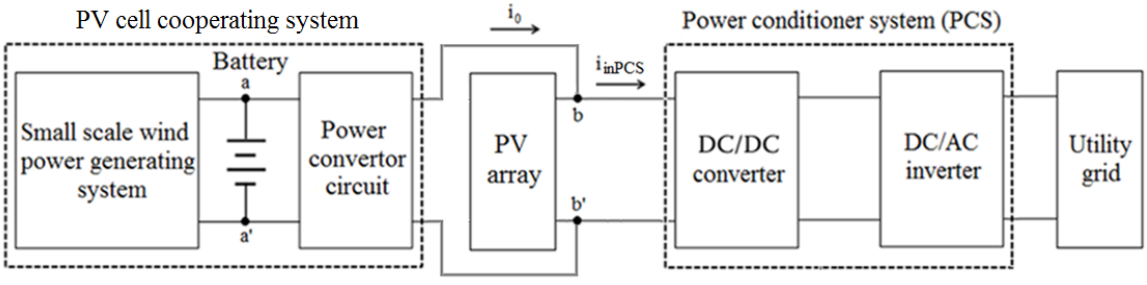

Figure 5.2. Grid-tied PV cell cooperating system in parallel connection mode

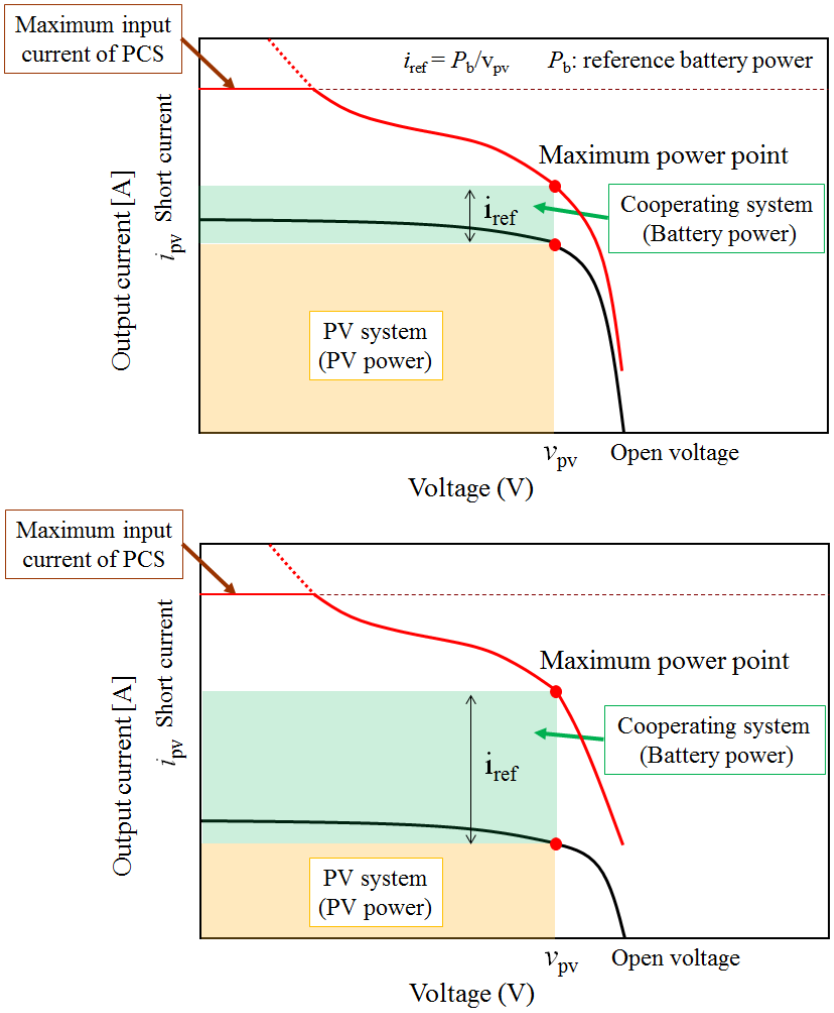

Figure 5.3. I - V characteristic in parallel connection mode in cloudy and rainy days

Figure 5.3 presents current - voltage characteristic of the PV cell cooperating system in parallel connection mode. The output voltage value of the PV cell cooperating system and the MPP voltage value of the solar panel must be identical because the PV cell cooperating system is connected to the solar panel in parallel. Thus, the input power of the PCS is increased because the input current i_{inPCS} of the PCS equals output current sum of the PV cell cooperating system and solar panel.

5.2. Control of PV cell cooperating system in parallel connection mode

Figure 5.4 presents the control method of the PV cell cooperating system in parallel connection mode. The output current of the PV cell cooperating system is regulated to follow the reference current value i_{ref} calculated by dividing the

reference battery output power P_b by the MPP voltage v_{pv} of the PV array with the support of a current control loop. The PI controller reduces the difference between the output current i_o of the PV cell cooperating system and the reference current i_{ref}. In parallel mode, the output voltage value v_0 of the PV cell cooperating system matches the MPP voltage value v_{pv} of the PV array. The output gate signals from the Pulse Width Modulation (PWM) adjust the switches of the boost DC/DC power converter.

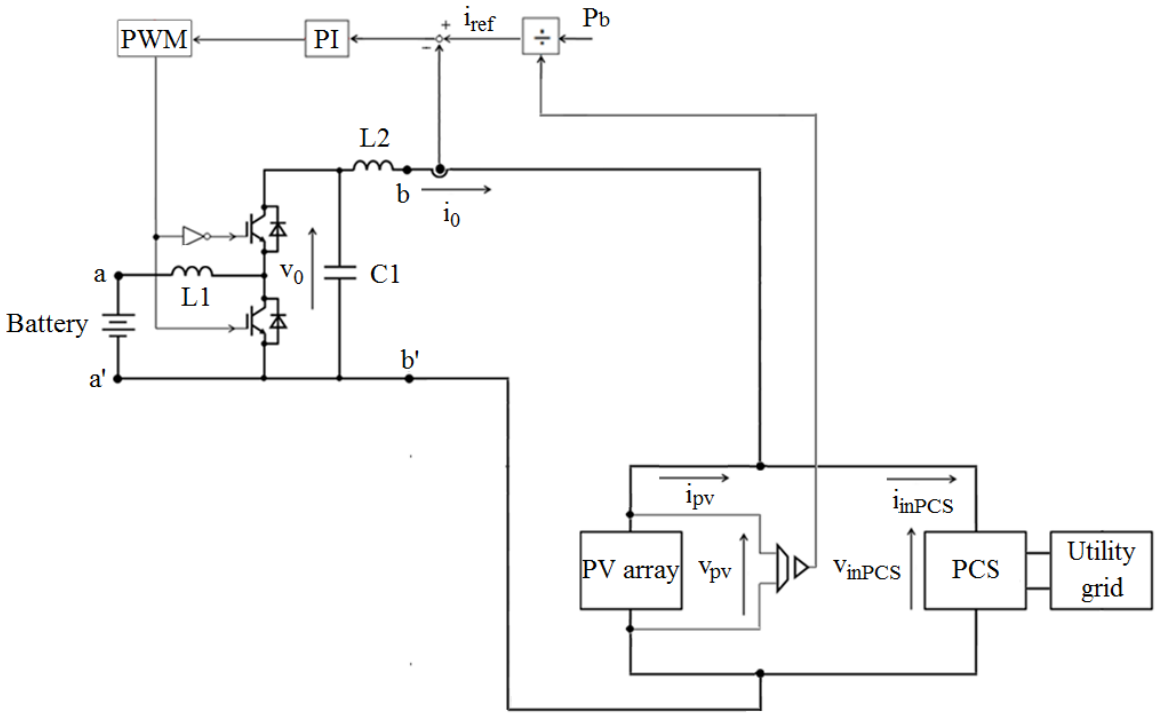

Fig 5.4. Control system of power converter circuit

5.3. Research result

Circuit of the grid-tied PV cell cooperating system in the parallel mode is shown in Figure 5.5. The PV cell cooperating system is connected to the solar array in parallel and both systems supply power to the bi-direction DC/DC converter in boost mode which is used to perform the maximum power point tracking (MPPT) by a current control method. The single phase grid voltage is of 230 Vrms and the input voltage of DC/DC converter is around 150 V. Before converting the DC voltage to AC voltage of 325 Vp (peak voltage) which is

equivalent to 230 Vrms, the DC voltage is increased up to around 380 V. The PV cell cooperating system is connected to the utility grid by a full-bridge inverter through an L-type filter. The four switches of grid-tied DC/AC inverter are controlled by the method that the instantaneous output current follows the reference current, as closely as possible.

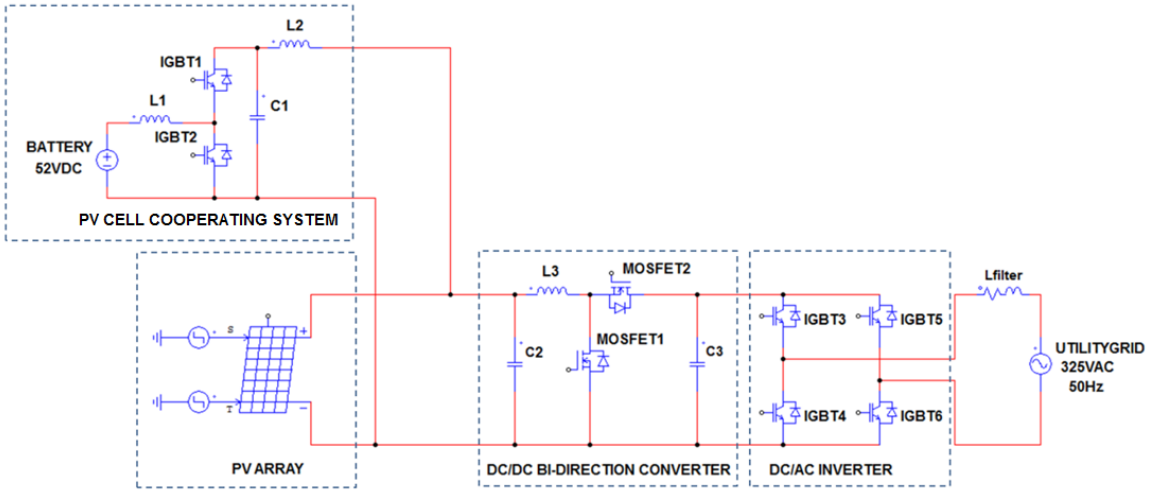

Figure 5.5. Circuit of the grid-tied PV cell cooperating system in the parallel mode

The operation of the grid-tied PV cell cooperating system in parallel connection mode is simulated by PSIM program and Table 5.1 shows system parameters for the simulation.

Table 5.1. System parameter for simulation

Parameter	Value
Power of PV system in solar radiation of 580 W/m^2	400 W
Power of battery	100 W
Inductor L1, L2, L3	10 mH, 2 mH, 2 mH
Capacitor C1, C2, C3	13.2 µF, 500 µF, 300 µF
Peak grid voltage	325 VAC
RMS grid voltage	230 VAC
Grid frequency	50 Hz
Filter inductor L	10 mH

Figure 5.6 illustrates the research results of the output current i_0 of the PV cell cooperating system in parallel connection mode. The PV cell cooperating system does not work in the first stage and only the solar panel generates output current i_{pv} with the help of the MPPT control system of the PCS. After about 14.8 seconds, the output current i_0 of the PV cell cooperating system is adjusted to match the reference current value i_{ref} calculated by dividing the reference battery output power P_b by the MPP voltage v_{pv} of the solar panel. The PV cell cooperating system is connected to solar panel in parallel mode in the steady state from about 18.7th second.

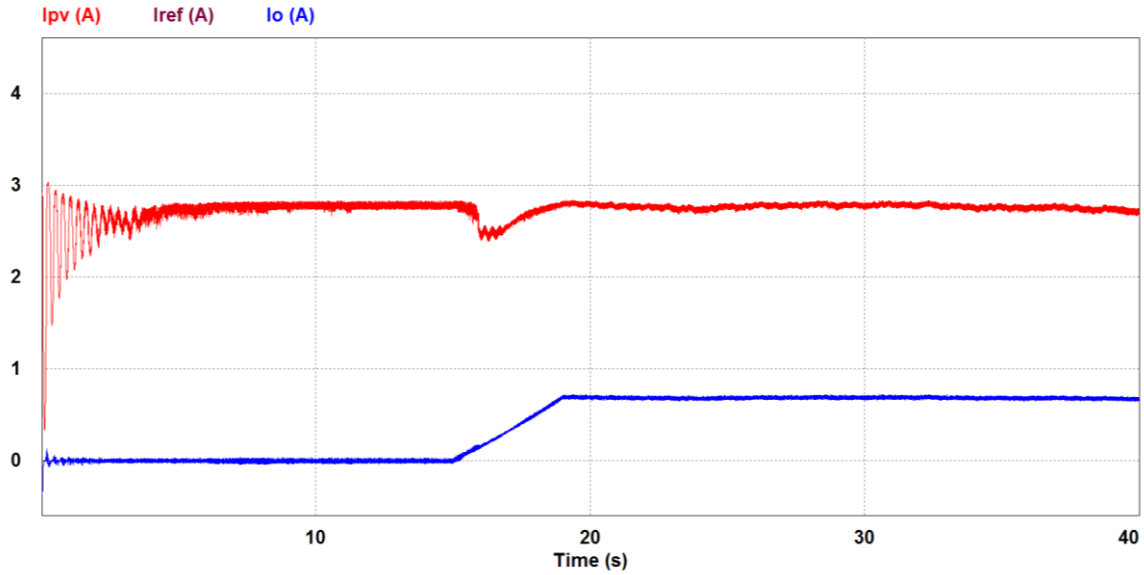

Figure 5.6. Output current of the PV cell cooperating system

In Figure 5.7, the PV cell cooperating system output voltage v_0 is regulated to equal the output voltage v_{pv} of the solar panel because the PV cell cooperating system connects to the solar array in parallel mode. Therefore, the power of both systems can be transmitted to the PCS.

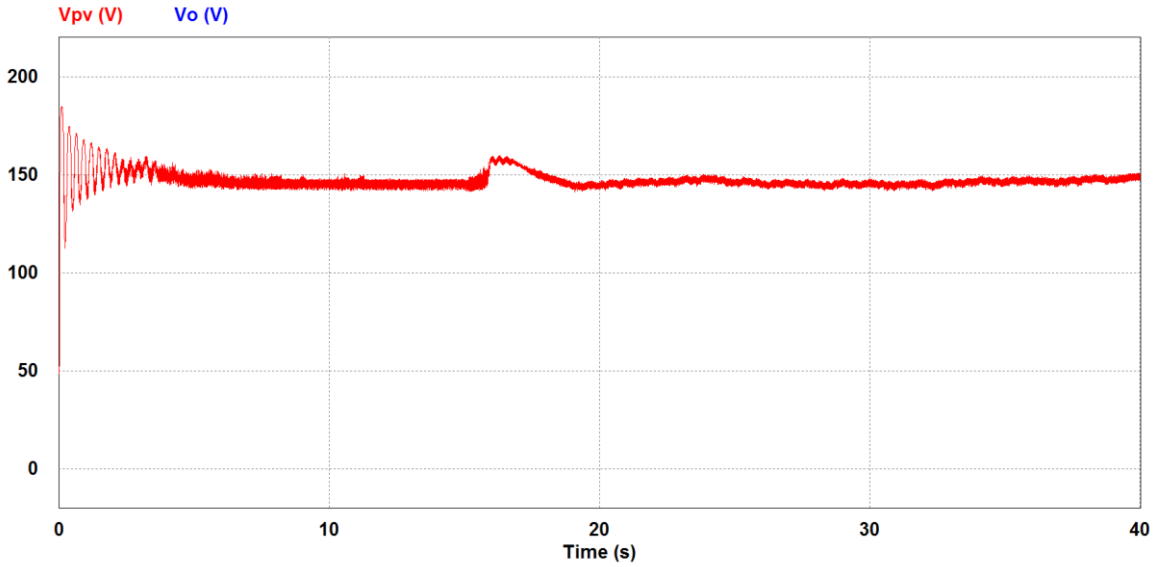

Figure 5.7. Output voltage of the PV cell cooperating system

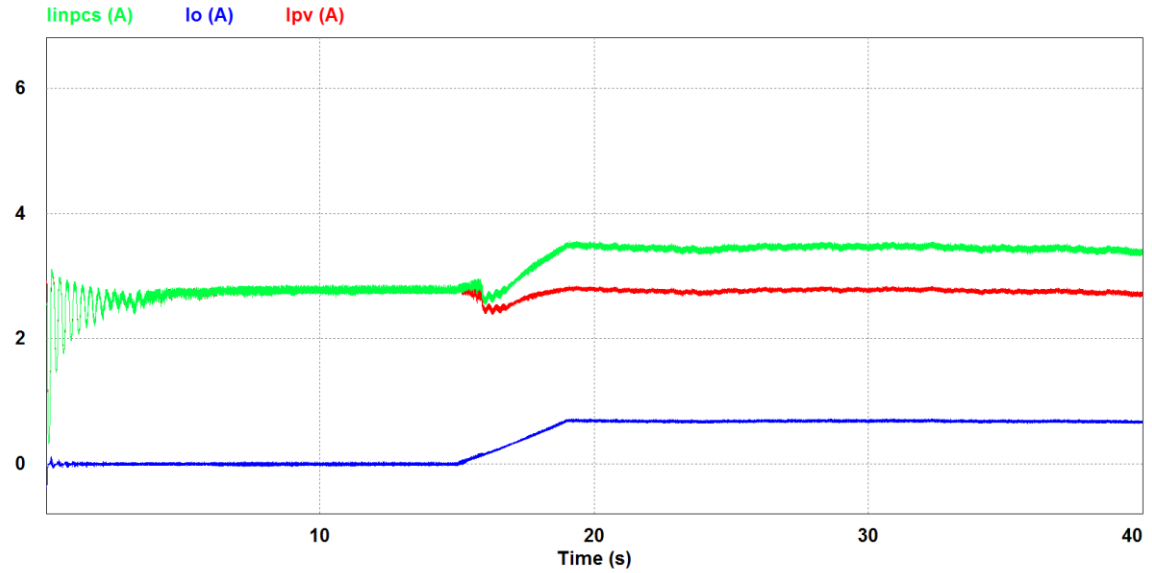

Figure 5.8. Input current of the PCS

Figure 5.8 and Figure 5.9 display the simulation results of input current I_{inpcs} and input power P_{inpcs} of the PCS in parallel connection mode. In the first stage, the PV array solely supplies power with the support of the MPPT control system and the PV cell cooperating system is connected to solar panel in parallel mode in the next stage. The input current i_{inPCS} of the PCS always equals output current sum of the PV cell cooperating system and the solar panel. Therefore, the PV cell

cooperating system output power is injected to the PCS with the output power of the solar panel and the input power P_{inPCS} of the PCS is increased.

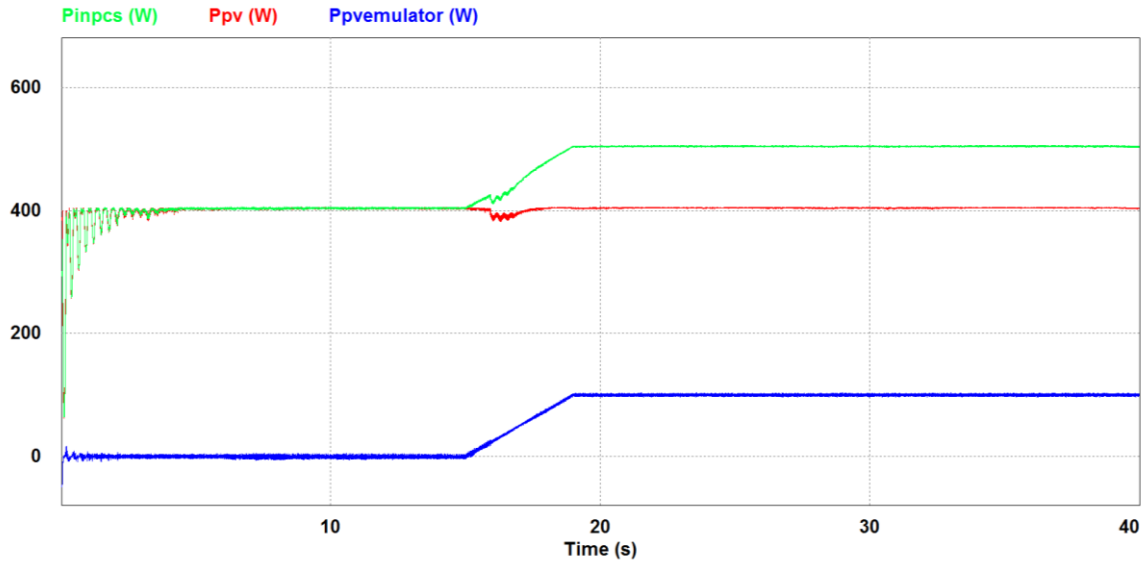

Figure 5.9. Input power of the PCS

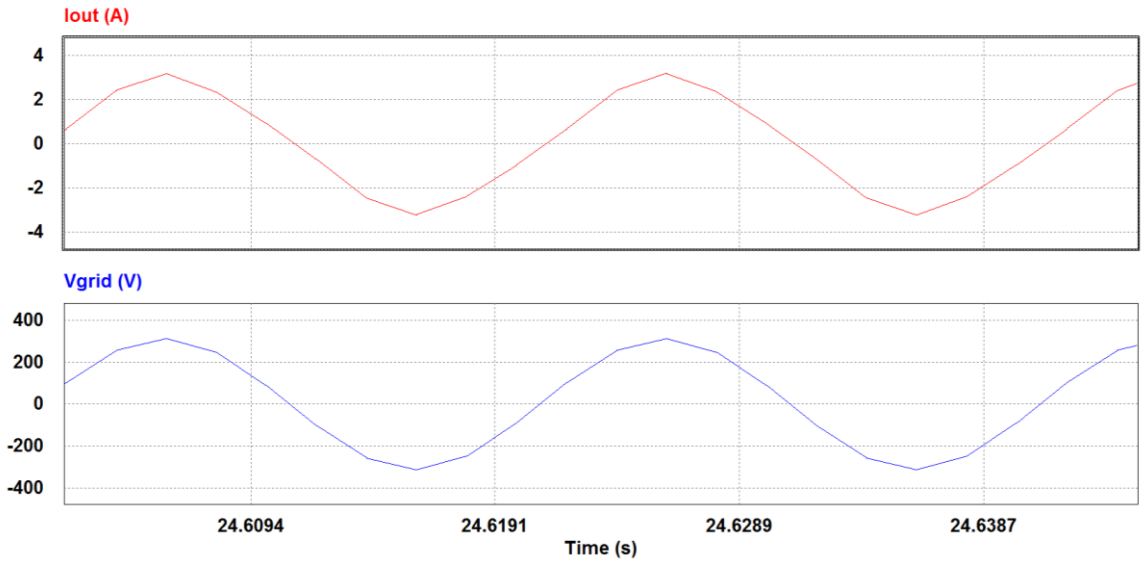

Figure 5.10. AC grid integration result

Figure 5.10 shows the output current of the DC/AC inverter of the PV cell cooperating system in parallel connection mode. The result presents that the output current I_{out} of the DC/AC inverter is sinusoidal and in phase with the grid voltage V_{grid}. Therefore, the active power of the PV cell cooperating system in parallel connection mode can be transmitted into the utility grid by using the grid-tied

control system.

5.4. Conclusion

This chapter presented the operation, the I - V characteristic, and the control system of the grid-tied PV cell cooperating system in parallel connection mode. The simulation results confirmed that this system can connect and transmit the electrical energy to the power grid. Moreover, the PV cell cooperating system which is connected in parallel with the solar panel can work well in the bad weather days, regardless the small altering output voltage value of the PV array and the restricted maximum input voltage value of the PCS. So, the operating efficiency of the PCS is better than the case in the series connection mode.

Chapter 6

Conclusions and Future Work

The focus of this thesis was on the novel design of the PV cell emulating system using the small scale wind turbine in order to increase the utilization rate of the PCS in the grid-tied solar power system.

Firstly, the research results presented that the PV cell emulating system in the stand alone mode could connect and transmit the power to the utility grid by using the grid-tied PCS in the case of the solar array could not receive sunlight.

Moreover, the PV cell cooperating system also connected to the solar array in the series and parallel connection mode in the case of the solar irradiation became weakly in the cloudy and rainy days. However, when the solar irradiation value became very weak, the operation of the PV cell cooperating system was stopped because the duty ratio of the PV cell cooperating system was controlled to become zero. The operating efficiency of the PCS when using the grid-tied PV cell cooperating system in parallel connection mode is better than the case in the series connection mode.

Therefore, the working efficiency of the PCS was improved because the PV cell cooperating system could use the remainder of the capacity of the PCS by day regardless of altering solar irradiation as well as in the case where the solar array could not receive the sunlight, especially the night time.

The future work in this thesis can be extended according to the proposed ideas

as follows:

- Research on the grid-tied PV cell emulating system in stand alone mode and PV cell cooperating system in series/parallel connection mode using fuel cell.

- Research on application of the novel model equation and the intelligent control methods for the control systems in the PV cell emulating system to improve the accuracy of the system.

Bibliography

[1] Jäger-Waldau, Arnulf, “Snapshot of Photovoltaics - March 2017,” Sustainability 9, no. 5: 783, 2017.

[2] European Photovoltaic Industry Association, "Global Market Outlook for Solar Power 2016-2020", 2016.

[3] International Energy Agency (IEA), “Technology roadmap: solar photovoltaic energy - 2014 edition,” 2014.

[4] Chih-Ming Hong, Chiung-Hsing Chen, “Intelligent control of a grid-connected wind-photovoltaic hybrid power systems,” Electrical Power and Energy Systems, Vol 55, pp. 554–561, 2014.

[5] Saravanan, S. & Babu, N. R., “Maximum power point tracking algorithms for photovoltaic system – A review,” Renewable and Sustainable Energy Reviews, Vol 57, pp. 192–204, 2016.

[6] Kerim Karabacaka, Numan Cetinb, “Artificial neural networks for controlling wind–PV power systems: A review,” Renewable and Sustainable Energy Reviews, Vol 29, pp. 804–827, 2014.

[7] Yasser E. Abu Eldahab, Naggar H. Saad, Abdalhalim Zekry, “Enhancing the maximum power point tracking techniques for photovoltaic systems,” Renewable and Sustainable Energy Reviews, Vol 40, pp. 505–514; 2014.

[8] Razman Ayop, Chee Wei Tan, “A comprehensive review on photovoltaic

emulator," Renewable and Sustainable Energy Reviews, Vol 80, pp. 430–452, 2017.

[9] A. Luque and S. Hegedus, "Handbook of Photovoltaic Science and Engineering," 2nd edition, John Wiley & Sons, Inc., 2011.

[10] Kishor, N., Villalva, M.G., Mohanty, S.R., and Ruppert, E, "Modeling of PV module with consideration of environmental factors," Proc. IEEE PES Innovative Smart Grid Technologies Conference Europe (ISGT Europe), 2010.

[11] Haitham Abu-Rub, Mariusz Malinowski, Kamal Al-Haddad, "Power Electronics for Renewable Energy Systems, Transportation, and Industrial Applications," IEEE Press and John Wiley & Sons Ltd, 2014.

[12] Julio López Seguel et al, "Methodology for the design of a stand-alone photovoltaic power supply," Ingeniare. Rev. chil. ing, vol. 21, no. 3, 2013.

[13] M.A. Eltawil, Z. Zhao, "Grid-connected photovoltaic power systems: Technical and potential problems - A review," Renewable and Sustainable Energy Reviews, vol. 14, no.1, pp. 112–129, 2010.

[14] GIZ, "NET-METERING REFERENCE GUIDE- How to avail solar roof tops and other renewables below 100 kW in the Philippines," 2013.

[15] Jacobsson, Staffan; Lauber, Volkmar, "The politics and policy of energy system transformation - explaining the German diffusion of renewable energy technology," Energy Policy, vol. 34, no. 3, pp. 256–276, 2006.

[16] Józef Paska et al, "Hybrid power systems – An effective way of utilising primary energy sources," Renewable Energy, vol 34, no 11, pp. 2414–2421, 2009.

[17] Y.S. Mohammed, M.W. Mustafa, N. Bashir, "Hybrid renewable energy systems for off-grid electric power: Review of substantial issues," Renewable and Sustainable Energy Reviews, vol 35, pp. 527-539, 2014.

[18] Diana Neves, Carlos A. Silva, Stephen Connors, "Design and implementation

of hybrid renewable energy systems on micro-communities: A review on case studies," Renewable and Sustainable Energy Reviews, vol 31, pp. 935–946, 2014.

[19] Subho Upadhyay, M.P. Sharma, "A review on configurations, control and sizing methodologies of hybrid energy systems," Renewable and Sustainable Energy Reviews, vol 38, pp. 47–63, 2014.

[20] Ned Mohan, Tore M. Undeland, William P. Robbins, "Power Electronics: Converters, Applications, and Design," 3rd edition, John Wiley & Sons, Inc., 2003.

[21] N. Husna A.W, Siraj S.F, M.Z. Ab Muin, "Modeling of DC-DC converter for solar energy system applications," Proc. IEEE Symposium on Computers & Informatics (ISCI), Malaysia, 2012.

[22] M.R. Islam et al, "Power Converters for Medium Voltage Networks," Springer, 2014.

[23] Eric Coates, Learnabout Electronics, 2017.

[24] Ahteshamul Haque, "Maximum Power Point Tracking (MPPT) Scheme for Solar Photovoltaic System," Energy Technology & Policy, vol. 1, no. 1, pp. 115–122, 2014.

[25] Mukund R. Patel, "Wind and Solar Power Systems: Design, Analysis, and Operation," 2nd Edition, CRC Press - Taylor & Francis Group, 2005.

[26] Jaw-Kuen Shiau, Min-Yi Lee, Yu-Chen Wei and Bo-Chih Chen, "Circuit Simulation for Solar Power Maximum Power Point Tracking with Different Buck-Boost Converter Topologies," Energies, vol. 7, pp. 5027–5046, 2014.

[27] S. Sivakumar, M. Jagabar Sathik, P.S. Manoj, G. Sundararajan, "An assessment on performance of DC–DC converters for renewable energy applications," Renewable and Sustainable Energy Reviews, vol. 58, pp. 1475–1485, 2016.

[28] S. Jalbrzykowski, T. Citko, "A bidirectional DC-DC converter for renewable

energy systems,” Bulletin of the Polish Academy of Sciences Technical Sciences, vol. 57, no. 4, 2009.

[29] Deepesh S Kanchan and Niranjan Hadagali, “Bidirectional DC/DC converter system for solar and fuel cell powered hybrid electric vehicle,” Proc. IEEE International Conference on Emerging Research Areas: Magnetics, Machines and Drives, pp. 1–6, India, 2014.

[30] Y. Hu, J. Tatler, and Z. Chen, “A bidirectional dc/dc power electronic converter for an energy storage devices in an autonomous power system,” Proc. Power Electron. Motion Conf., pp. 171–176, 2004.

[31] S. Kolsi, H. Samet, M. Ben, “Amar Design Analysis of DC-DC Converters Connected to a Photovoltaic Generator and Controlled by MPPT for Optimal Energy Transfer throughout a Clear Day,” Journal of Power and Energy Engineering, vol. 2, pp. 27–34, 2014.

[32] Yang H., Shang M., Liu J, “The Simulation of the Principle of MPPT Control of PV Systems Based on BOOST Circuit,” Proc. Electrical, Information Engineering and Mechatronics, pp. 2127–2135, China, 2011.

[33] Solanki, Chetan Singh, “SOLAR PHOTOVOLTAICS - Fundamentals, Technologies and Applications,” PHI Learning Pvt. Ltd, 2015.

[34] Fernando Lessa Tofoli, Dênis de Castro Pereira, and Wesley Josias de Paula, “Comparative Study of Maximum Power Point Tracking Techniques for Photovoltaic Systems,” International Journal of Photoenergy, pp. 1–10, 2015.

[35] Nicola Femia, Giovanni Petrone, Giovanni Spagnuolo, Massimo Vitelli, “Power Electronics and Control Techniques for Maximum Energy Harvesting in Photovoltaic Systems,” CRC Press Taylor & Francis Group, 2013.

[36] Remus Teodorescu, Marco Liserreand Pedro Rodríguez, “Grid Converters for Photovoltaic and Wind Power Systems,” John Wiley & Sons Ltd, 2011.

[37] Ioulia T. Papaioannou, Minas C. Alexiadis, Charis S. Demoulias, Dimitris P. Labridis, and Petros S. Dokopoulos, “Modelling and Field Measurements of Photovoltaic Units Connected to LV Grid. Study of Penetration Scenarios,” IEEE Trans. Power Delivery, pp. 979–987, 2011.

[38] Ali Algaddafi, Saud A. Altuwayjiri, Oday A. Ahmed, and Ibrahim Daho, “An Optimal Current Controller Design for a Grid Connected Inverter to Improve Power Quality and Test Commercial PV Inverters,” The Scientific World Journal, vol 2017, pp. 1–12, 2017.

[39] Atiqah Hamizah Mohd Nordin, Ahmad Maliki Omar, Hedzlin Zainuddin, “Modeling and Simulation of Grid Inverter in Grid Connected Photovoltaic System,” International Journal of Renewable Energy Research, vol. 4, no. 4, pp. 949–957, 2014.

[40] Mihail Antchev, Ivailo Pandiev, Mariya Petkova, Eltimir Stoimenov, Angelina Tomova, and Hristo Antchev, “PLL for Single Phase Grid Connected Inverters,” International Journal of Electrical Engineering and Technology, pp. 56–77, Oct. 2013.

[41] Masoud Karimi-Ghartemani, “Enhanced Phase Lock Loop Structures for Power and Energy Applications,” IEEE Press and John Wiley & Sons Ltd, p. 3–12, 2014.

[42] S.M. Silva, B.M. Lopes, B.J.C. Filho, R.P. Campana and W.C. Bosventura, “Performance evaluation of PLL algorithms for single-phase grid-connected systems,” Proc. IEEE 39th IAS Annual Meeting. Conference Record of the Industry Applications Conference, pp. 2259–2263, 2004.

[43] Krismadinata, Nasrudin Abd Rahim and Jeyraj Selvaraj, “Implementation of Hysteresis Current Control for Single-Phase Grid Connected Inverter,” Proc. IEEE 7th International Conference on Power Electronics and Drive Systems, Thailand, 2007.

[44] Evren Isen, “Modelling and Simulation of Hysteresis Current Controlled Single-Phase Grid-Connected Inverter,” Proc. 17th International Conference on Electrical and Power Engineering, Holland, pp. 322–326, 2015.

[45] P.A. Dahono, I. Krisbiantoro, “A hysteresis current controller for single-phase full-bridge inverters,” Proc. 4th IEEE International Conference on Power Electronics and Drive Systems, Indonesia, 2001.

[46] X. Zong, P. W. Lehn, “Reactive Power Control of Single Phase Grid-tied Voltage Sourced Inverters for Residential PV Application,” in Proc. 38th Annual Conference of the IEEE Industrial Electronics Society (IECON), Montreal, Canada, pp. 696–701, 2012.

[47] M.A. Eltawil, Z. Zhao, “Grid-connected photovoltaic power systems: Technical and potential problems - A review,” Renewable and Sustainable Energy Reviews, vol. 14, no.1, pp. 112–129, 2010.

[48] F. Freijedo et al, “Grid synchronization methods for power converters,” in Proc. 35th Annual Conference of IEEE Industrial Electronics (IECON), Porto, Portugal, pp. 522–529,2009 .

[49] M. G. Villalva, J. R. Gazoli, E. Ruppert F, “Comprehensive approach to modeling and simulation of photovoltaic arrays,” IEEE Transactions on Power Electronics, vol. 25, no. 5, pp. 1198-1208, 2009.

[50] Bendib, B., Belmili, H. & Krim, F, “A survey of the most used MPPT methods: Conventional and advanced algorithms applied for photovoltaic systems,” Renewable and Sustainable Energy Reviews, vol. 45, pp. 637–648, 2015.

[51] W. De Soto, S. A. Klein, and W. A. Beckman, “Improvement and validation of a model for photovoltaic array performance,” Solar Energy, vol. 80, no. 1, pp. 78–88, 2006.

[52] A.O. Di Tommaso, F. Genduso, R. Miceli, “Analytical investigation and control system set-up of medium scale PV plants for power flow management,” Energies, 5 (11), pp. 4399-4416, 2012.

[53] R. J. Wai, and W. H. Wang, “Grid-Connected Photovoltaic Generation System,” IEEE Transactions on Circuits and Systems, vol. 55, no. 3, pp. 953-964, 2008.

[54] Xing Ju, Chao Xu, Yangqing Hu, Xue Han, Gaosheng Wei, Xiaoze Du, “A review on the development of photovoltaic/concentrated solar power (PV-CSP) hybrid systems,” Solar Energy Materials & Solar Cells, vol. 161, pp. 305–327, 2016.

[55] Simon Ang, Alejandro Oliva. “Power Switching Converters”, CRC Press Taylor & Francis Group, p. 199–318, 2005.

[55] Yan Jia, Ryosuke Shibata, Naoki Yamamura, Muneaki Ishida, “A Control Method of Prolonging the Service Life of Battery in Stand-alone Renewable Energy System using Electric Double Layer Capacitor (EDLC),” Proc. IEEE International Conference on Power Electronics and Drives Systems, Malaysia, 2005.

[56] Yan Jia, Ryosuke Shibata, Naoki Yamamura, Muneaki Ishida, “A Study on Electric Power Smoothing System for Lead-acid Battery of Stand-alone Natural Energy Power System Using EDLC,” IEEJ Transactions on Industry Applications, vol. 127, no. 12, pp.1181–1189, 2007.

[57] S. Masashi, N. Yamamura, and M. Ishida, “Development of Photovoltaic Cell Emulator using the Small Scale Wind Turbine,” Proc. IEEE, 15th International Conference on Electrical Machines and Systems (ICEMS), Sapporo, Japan, Oct. pp. 1–4, 2012.

[58] Vu Minh Phap, N. Yamamura, M. Ishida, J. Hirai, and K. Nakatani, “Development of Novel Connection Control Method for Small Scale Solar -Wind

Hybrid Power Plant," International Journal of Engineering Research, vol. 5, no. 8, pp. 730-734, 2016.

[59] Vu Minh Phap, N. Yamamura, M. Ishida, J. Hirai, K. Yubai and Nguyen Thuy Nga, "Modeling and Experimental Test of Grid-Tied Photovoltaic Cell Emulating System in the Stand-alone Mode," Journal of Electrical Systems, vol. 13, no. 2, pp. 387-397, 2017.

[60] Kirian Guiller, Vu Minh Phap, N. Yamamura, M. Ishida, J. Hirai, "Study on new control system design of PV cell emulating system in the stand alone mode," Proceeding in 2017 International Conference on Engineering, Science, and Application (ICESA), vol.1, no.1, pp. 153-161, 2017.

[61] Vu Minh Phap, N. Yamamura, M. Ishida, J. Hirai, and N. T. Nga, "Design of Novel Grid-tied Solar - Wind Hybrid Power Plant Using Photovoltaic Cell Emulating System," Proceeding in IEEE 4th International Conference on Sustainable Energy Technologies (ICSET), Hanoi, Vietnam, pp. 168-171, 2016.

[62] Vu Minh Phap, N. Yamamura, M. Ishida, and N. T. Nga, "Impact of Solar Irradiation on PV Cell Emulating System in Series Connection Mode," Proceeding in IEEE International Conference of High Voltage and Power System (ICHVEPS), Bali, Indonesia, pp. 282-285, 2017.

List of Publications

I. Journal

1. Vu Minh Phap, N. Yamamura, M. Ishida, J. Hirai, and K. Nakatani, "Development of Novel Connection Control Method for Small Scale Solar -Wind Hybrid Power Plant," *International Journal of Engineering Research*, vol. 5, no. 8, pp. 730-734, 2016.

2. Vu Minh Phap, N. Yamamura, M. Ishida, J. Hirai, K. Yubai and Nguyen Thuy Nga, "Modeling and Experimental Test of Grid-Tied Photovoltaic Cell Emulating System in the Stand-alone Mode," *Journal of Electrical Systems*, vol. 13, no. 2, pp. 387-397, 2017.

3. Vu Minh Phap, N. Yamamura, M. Ishida, K. Nakatani, and Nguyen Thuy Nga, "Experimental Study on Photovoltaic Cell Emulating System in Series Connection Mode," *Journal of Electrical Systems*. (Accepted).

II. International conference proceedings

1. Vu Minh Phap, N. Yamamura, M. Ishida, J. Hirai, and K. Nakatani, "Development of Novel Connection Control Method for Small Scale Solar -Wind Hybrid Power Plant," *in Proc. Seoul International Conference on Applied Science and Engineering (SICASE)*, Seoul, Korea, 2016, pp. 43-53.

2. Vu Minh Phap, N. Yamamura, M. Ishida, J. Hirai, and N. T. Nga, "Design of Novel Grid-tied Solar - Wind Hybrid Power Plant Using Photovoltaic Cell Emulating System," *in Proc. IEEE, 4th International Conference on Sustainable Energy Technologies (ICSET)*, Hanoi, Vietnam, 2016, pp. 168-171.

3. Kirian Guiller, Vu Minh Phap, N. Yamamura, M. Ishida, J. Hirai, "Study on new control system design of PV cell emulating system in the stand alone mode," *in Proc. International Conference on Engineering, Science, and Application (ICESA)*, vol.1, no.1, Tokyo, Japan, 2017, pp. 153-161.

4. Vu Minh Phap, N. Yamamura, M. Ishida, and N. T. Nga, "Impact of Solar Irradiation on PV Cell Emulating System in Series Connection Mode," *in Proc. IEEE, International Conference of High Voltage and Power System (ICHVEPS)*, Bali, Indonesia, 2017, pp. 282-285.

5. Vu Minh Phap, N. Yamamura, M. Ishida, I. Mizoguchi, T. Yamashita and N. T. Nga, "Efficiency Enhancement of PV Cell Emulating System in Connection Mode," *in Proc. IEEE, International Conference on Industrial Technology (ICIT)*, Lyon, France, 2018.

III. Other proceedings (International Workshop, National Conference, International Symposium)

1. Vu Minh Phap, N. Yamamura, M. Ishida, J. Hirai, "Simulation of MPPT control system with DC/DC bidirection converter in boost mode for PV system," *in Proc. International scientific workshop: Clean Energy in Vietnam after COP21*, Hanoi, Vietnam, 2015.

2. Vu Minh Phap, N. Yamamura, M. Ishida, J. Hirai, "Single Phase Grid Connected Photovoltaic System Using Maximum Power Point Tracking Technique," *in Proc. International Symposium for Sustainability by Engineering at Mie University*, Tsu, Mie, Japan, 2015.

3. Mizoguchi Isamu, Vu Minh Phap, Yamamura Naoki, Ishida Muneaki, "Development of the small scale wind power generating device connecting to the solar power generation system in parallel," *in Proc. Japan Toukaishibu Conference*, Nagoya, Japan, 2017.

4. Isamu Mizoguchi, Naoki Yamamura, Muneaki Ishida, Vu Minh Phap, "Experimental investigation on photovoltaic cell emulating systemin series

connection mode," *in Proc. 9th International Workshop on Regional Innovation Studies (IWRIS2017)*, Mie, Japan, 2017.